MAPPING WETLANDS IN NOVA SCOTIA WITH MULTI-BEAM RADARSAT-2 POLARIMETRIC SAR, OPTICAL SATELLITE IMAGERY, AND ELEVATION DATA

by

Raymond Jahncke

Submitted in partial fulfillment of the requirements
for the degree of Master of Environmental Studies

at

Dalhousie University
Halifax, Nova Scotia
April 2016

Table of Contents

List of Tables

List of Figures

Abstract

Nova Scotia introduced a new wetland policy in 2011 which included a goal to have no net loss of wetlands. In order to meet this goal, the Nova Scotia government has committed to updating the provincial wetland inventory. The objective of this study will be to assess the accuracy of wetland mapping using remote sensing processes based on RADARSAT-2 polarimetric SAR images, optical imagery, and elevation data.

RADARSAT-2 polarimetric SAR images were acquired between 2010 and 2013 over an area southwest of Halifax. Two sources of optical imagery (QuickBird and Landsat 8) and two sources of terrain information (lidar and the provincial government contours) were combined in various arrangements with the radar. A non-parametric supervised Random Forests classifier was applied to the different data combinations. An accuracy assessment showed that using RADARSAT-2 combined with either source of data improved the accuracy of wetland identification over the existing inventory.

Keywords: wetland mapping, wetlands, RADARSAT-2, lidar, QuickBird, Landsat 8, polarimetric SAR

List of Abbreviations Used

AMSL	above mean sea level
CHM	canopy height model
CRV	curvature
CTI	compound topographic index
DEM	digital elevation model (e.g. elevation of ground)
DSM	digital surface model (e.g. elevation of vegetation canopy)
ELC	Ecological Land Classification
ESRI	Environmental Systems Research Institute
FAC	facultative – vegetation can be found either in wetland or upland.
FACU	facultative upland - usually found in upland area, but sometimes found in wetlands.
FACW	facultative wetland – plants are usually found in wetlands, but sometimes found in upland.
GPS	global positioning system
HH, HV, VH, VV	polarimetric transmit H and V on alternate pulses / receive H and V on any pulse
IDW	inverse distance weighting
IRBM	Integrated River Basin Management
lidar	light detection and ranging
MLC	maximum likelihood classification
MMU	minimum mappable unit
NIR	near infrared
NSDNR	Nova Scotia Department of Natural Resources
OBIA	object based image analysis
OBL	obligate - plants are almost always in wetlands.
OWES	Ontario Wetland Evaluation System
PolSAR	polarimetric synthetic aperture radar
radar	radio detection and ranging
RF	Random Forests
SAR	synthetic aperture radar
SLP	slope
TOA	top of atmosphere
TPI	topographic position index
UPL	upland – plants which are almost always in upland areas.

Glossary

DNR map   wetland map that is currently in use by the government of Nova Scotia

lidar DEM   digital elevation model created from lidar

NS DEM   Nova Scotia Topographic Database digital elevation model

Acknowledgements

Co-supervisors: Peter Bush and Peter Duinker

Committee members: Brigitte Leblon, Randy Milton, and Danika van Proosdij

Chapter 1.   Introduction

1.1   Problem Statement

In 2011, Nova Scotia released a wetland conservation policy implemented in part to ensure no net loss of wetlands (i.e. equal offsetting of loss using reclamation or restoration). It is a critical policy that aims to protect an essential feature of the landscape. According to the Environmental Goals and Sustainability Prosperity Act (2007) (Bill No. 146), this program aims to prevent any loss in wetland area *and* function. Indeed, as in other parts of the world, wetlands are key elements of long-term monitoring and natural resource management, as described by Mitsch and Gosselink (2007):

> Wetlands, landscape features found in almost all parts of the world, are known as 'the kidneys of the landscape' and 'ecological supermarkets' to bring attention to the important values they provide… Wetlands have been destroyed at alarming rates throughout the developed and developing worlds. Now, as their many values are being recognized, wetland conservation and protection have become the norm in many parts of the world… Wetland management, as the applied side of wetland science, requires an understanding of the scientific aspects of wetlands balanced with legal, institutional, and economic realities (p. 3).

Historically, wetlands were mapped by field crews on foot or in boats. Wetlands can be mapped in the field using *in situ* techniques to measure vegetation, hydrology, and soils. These methods are comprehensive, but the high associated cost generally restricts their use to local mapping.

The Nova Scotia Department of Natural Resources (NSDNR) completed a province-wide wetland inventory in 2004. This inventory was produced by digitizing aerial photographs from the 1980s and 1990s, and provides the most recent estimates for the number, location and class of wetlands in the province that are greater than or equal to ½ hectare (Nova Scotia Environment 2009). In addition to the area constraint of the minimum mappable unit (mmu), no forested polygons on site class 3 or higher could be classified as wetland. The wetland inventory was part of the seamless landcover mapping for the forest resource inventory, a

geospatial dataset primarily designed to guide timber harvesting and land management activities within the province. However, a number of authors have suggested that photo-interpretation of aerial photographs is unreliable for the identification, delineation, and classification of wetlands (Jacobson et al. 1987; Sader et al. 1995; Hogg and Todd 2007). Furthermore, forested regions are especially problematic because the photo-interpretation of aerial photography is prone to errors in areas of shadow and dense tree cover (Hogg and Todd 2007).

While the NSDNR has been adapting its inventory for integration into the Canadian National Wetland Inventory (the national effort to map wetlands using satellite remote sensing) (Nova Scotia Department of Natural Resources 2011), there are still some wetlands that have not yet been identified in the new NSDNR wetland inventory. These wetlands pose two significant problems: 1) something that is not known cannot be managed, and 2) an underestimation of wetland area will have an impact on implementation of the 2011 Nova Scotia wetland policy. With increasing pressures on wetlands from development, resource extraction, and the effects of climate change, having an accurate and comprehensive province-wide wetland inventory in Nova Scotia is imperative, as these inventories can facilitate continual monitoring of ecosystem health. Thus, it is important to explore new methods which can help improve the wetland inventory in Nova Scotia. An ideal mapping method should be able to identify the wetland type (e.g. marsh, fen, bog, or swamp), location, and edges (i.e. transition area).

As reviewed in Chapter 2, one of the available mapping methods is based on radar and optical satellite remote sensing. Satellite imagery offers the advantages of extensive regional coverage, zero disturbances of the area to be mapped, as well as a method for acquiring data in less accessible areas on a regular and cost effective basis. It has therefore become a good operational tool for large wetland mapping projects, both in terms of seasonal monitoring and in terms of defining a baseline for long-term monitoring (Mitsch and Gosselink 2007). Optical satellite images like those acquired by Landsat or SPOT satellites can be used, but image acquisition is restricted to cloud-free daytime conditions, a limitation that can be overcome by using Synthetic Aperture Radar (SAR) images. SAR are active sensors that generate their own

energy at generally longer microwave wavelengths, and thus collect imagery independent of atmospheric conditions. Furthermore, microwave radiation is sensitive to surface morphology, surface roughness, soil moisture and water levels, which are all useful properties for discriminating wetland types.

1.2   Thesis goal, objectives and hypotheses

The goal of this thesis is to help improve the knowledge base of wetland mapping using remote sensing and GIS, which could benefit the operational needs of regional wetland mapping projects in Nova Scotia. To meet this goal a study area was chosen, and several objectives need to be met which will be addressed using the following research questions:

1) How well can wetland be delineated from upland with a combination of polarimetric synthetic aperture radar (PolSAR), optical imagery, and elevation data?
2) How well can each wetland type (marsh, fen, bog, and swamp) be mapped when using a combination of PolSAR, optical imagery, and elevation data?
3) Which PolSAR, optical imagery, and elevation variables are the most influential to improve wetland classification?
4) Compared to high resolution data, how well can medium resolution data map the various wetland types?

Several methods and techniques were used to answer the research questions:

- Models were designed and implemented to classify elevation derivatives to identify potential wetland areas.
- The efficacy of pre-existing algorithms used in the classification of vegetation and soil moisture using PolSAR and optical imagery was investigated.
- Classification accuracy was calculated quantitatively with confusion matrices using in situ field data, and qualitatively using visual interpretation.
- Classification from various input data combinations and the two different resolutions were compared and discussed.

I approached each one of the three wetland-defining criteria (wetland hydrology, hydric soil, and hydrophytic vegetation) with the data acquired (PolSAR, optical imagery, and

elevation). The three types of remote sensing data were considered for their unique qualities that could address the different landcover characteristics. By combining the data and applying suitable modeling methods, my hypotheses are: (a) polSAR images will improve wetland mapping compared to optical images, (b) medium scale optical and DEM data will have satisfactory mapping accuracies, (c) using images acquired with various beam modes and when water levels are different can improve mapping accuracy, and (d) using the Random Forests (RF) classifier instead of the maximum likelihood classifier will produce higher accuracies.

This thesis is presented with six chapters, of which chapters four and five are presented in manuscript form. Chapter one discusses the purpose and approach of the study, and chapter two provides a review of wetland type characterization and wetland mapping using optical and SAR imagery. Chapter three describes research methods. Chapter four focuses on the use of PolSAR, lidar and high resolution optical imagery (QuickBird). Chapter five emphasizes the use of PolSAR, the Nova Scotia Topographic Database elevation, and medium resolution optical imagery (Landsat 8) as a way to improve wetland mapping at a provincial scale with existing medium scale datasets. Chapter six draws conclusions from the study as a whole and specifically compares the two methods to provide information for further research or as input to any functional application put into practice.

1.3   References

Hogg, A., and Todd, K. 2007. "Automated discrimination of upland and wetland using terrain derivatives." *Canadian Journal of Remote Sensing*, Vol. 33, pp. S68-S83.

Jacobson, J. E., Ritter, R. A. and Koeln, G. T. 1987. "Accuracy of Thematic Mapper derived wetlands as based on National Wetland Inventory data." *American Society Photogrammetry and Remote Sensing Technical Papers*, 1987 ASPRS-ACSM Fall Convention, Reno, NV. pp. 109-118.

Mitsch, W. J., and Gosselink, J. G. 2007. *Wetlands*. Hoboken, New Jersey, USA: John Wiley & Sons, Inc.

Nova Scotia Department of Natural Resources. 2011. "Ecosystems and Habitats Program Overview." Retrieved from http://novascotia.ca/natr/wildlife/habitats/wetlands.asp

Nova Scotia Environment. 2009. "Nova Scotia Wetland Conservation Policy (Draft for Consultation)." pp. 1-24. Retrieved from http://www.gov.ns.ca/nse/wetland/docs/Nova.Scotia.Wetland.Conservation.Policy.pdf

Nova Scotia Legislature. 2007. "Environmental Goals and Sustainable Prosperity Act, Bill No. 146." Retrieved from http://nslegislature.ca/legc/PDFs/annual%20statutes/2007%20Spring/c007.pdf

Sader, A., Ahl, D., and Liou, W. 1995. "Accuracy of Landsat-TM and GIS rule-based methods for forest wetland classification in Maine." *Remote Sensing of Environment,* Vol. 53, pp. 133-144.

Chapter 2.   Background

2.1   Wetlands Definition and Description

Wetlands play a central role in basin hydrology, acting as water storage reservoirs as well as significantly influencing water quality and sediment (Brooks, Ffolliott and Magner 2013). Wetlands are critically important ecological systems that are comparable to tropical rain forests in terms of biodiversity. They improve water quality by providing natural filtration mechanisms and by controlling the rate of runoff. Wetlands also provide social benefits for people and unique habitat for a multitude of plant and animal species. The economic value of wetlands may appear to be less clear at first; however, when factors such as waterflow regulation, erosion control, and recreational benefits are considered, their substantial monetary value becomes more obvious. For these reasons, accurate assessment of wetland classification is essential for long-term monitoring, urban planning, and natural resource management applications (Mitsch and Gosselink 2007). With proper stakeholder involvement, a watershed plan that provides clear and comprehensive strategies to address environmental and management issues can be created (Prince Edward Island Environment, Energy and Forestry nd).

Before the mapping process begins, it is necessary to establish appropriate definitions. Such standardization which corresponds to the Canadian context, helps remove potential confusion or ambiguity. Environment Canada (2011) defines a wetland as: "land where the water table is at, near or above the surface or which is saturated for a long enough period to promote such features as wet-altered soils and water tolerant vegetation".

The Nova Scotia Wetland Inventory is adapting to the following wetland classes described in the Canadian Wetland Classification System: bog, fen, swamp, shallow water marsh, and deep marsh (Nova Scotia Department of Natural Resources 2011) such as those in Figure 2.1. The Canadian Wetland Classification System defines these wetland classes (Warner and Rubec 1997) as follows: (1) Bogs are peat landforms with a raised or level surface and that may or may not be treed. As a result of the topography, bogs are not significantly affected by runoff water or groundflow. Sphagnum moss and ericaceous shrubs are the common

6

vegetation in bogs. Accordingly, terrain and vegetative characteristics that can be identified using remote sensing techniques are useful for class separation of bogs. (2) Fens are also peatlands, but unlike bogs, ground and surface water movement is normal, and exposed water can form characteristic patterns alternating with vegetation that are especially visible from a bird's-eye view. Those patterns and vegetation like sedges and brown moss are useful in fen delineation. (3) Swamps comprise wetlands dominated by trees (typically > 30% cover) that are influenced by minerotrophic groundwater. Swamps can be found on either mineral or peat soils and are typically considered the driest wetland type. Dry swamps on mineral soil can transition into upland forest and wet swamps can transition to treed fen that is wetter and has less tree canopy. (4) Marshes have shallow water levels that can fluctuate daily and expose the soil. They can receive water from a number of sources, including streams, surface flow, groundwater, and precipitation. (5) Shallow-water wetlands have water depths up to two metres that are typically stable, but soil may occasionally become exposed. Shallow-water wetlands may be identified by remote sensing if emergent vegetation is present to distinguish these features from deep water bodies. These diverge in naming convention and are not to be confused with deep-water marsh but are also referred to as aquatic beds or open-water wetlands.

Figure 2.1: Photographs of typical wetland classes found in the study area.

Wetlands are complex ecological systems that can only form in the presence of favourable hydrological, geomorphological, and biological conditions, and in Canada are characterized according to soil, water, and vegetation (Warner and Rubec 1997). Using specific data to provide information on each of these conditions should enhance the reliability of classification by avoiding limitations any single data source would have (Figure 2.2).
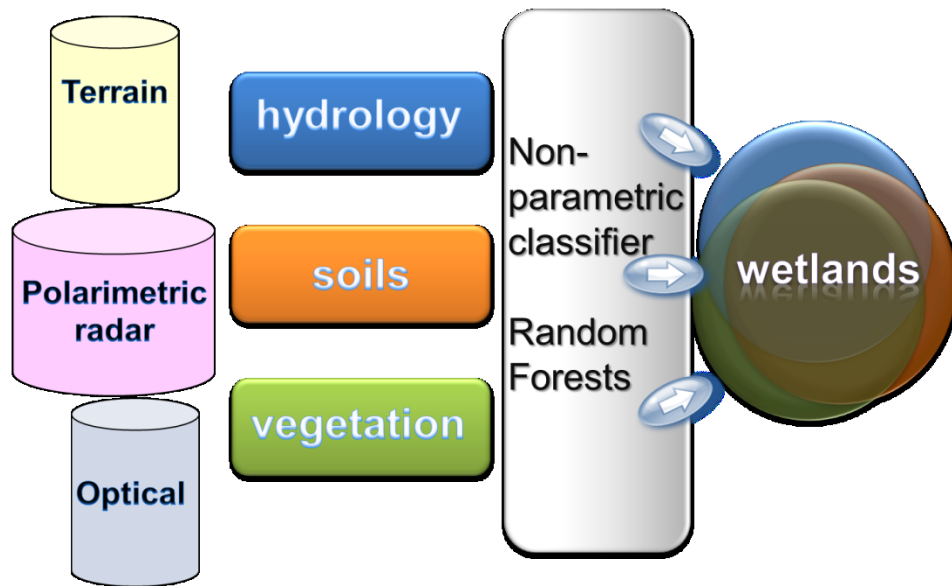
Figure 2.2: Different input data sources may provide information on different wetland characteristics.

Certain wetland classes are more difficult to determine. For example, distinctive features of bogs and fens (including morphology, physiognomy, floristics, and nutrient status) may be confused, as these wetlands can develop in the same way (Canada Committee on Ecological [Biophysical] Land Classification 1988). However, bogs primarily receive nutrients through precipitation and are thus oligotrophic. Conversely, fens obtain more nutrients through both precipitation and flow from surrounding upland soils, and so can support vegetation not seen in a bog. When this is the case, these two wetland classes can be distinguished using remote sensing. Similarly, marsh and some open fen can appear to be a uniform treeless expanse. However, a marsh experiences minerotrophic conditions which results in a different vegetation community (Warner and Rubec 1997). Unlike a fen which has a more stable water table, a marsh is dominated by fluctuating water and is usually situated in deeper lowlands.

Considering which factors affect wetland formation and recognizing these factors can aid in the proper identification of wetlands. Figure 2.3 illustrates (1) how different wetland classes exhibit variation in hydrology and nutrients, and (2) the gradational changes that occur between wetland classes showing that these transitions are not always distinct.
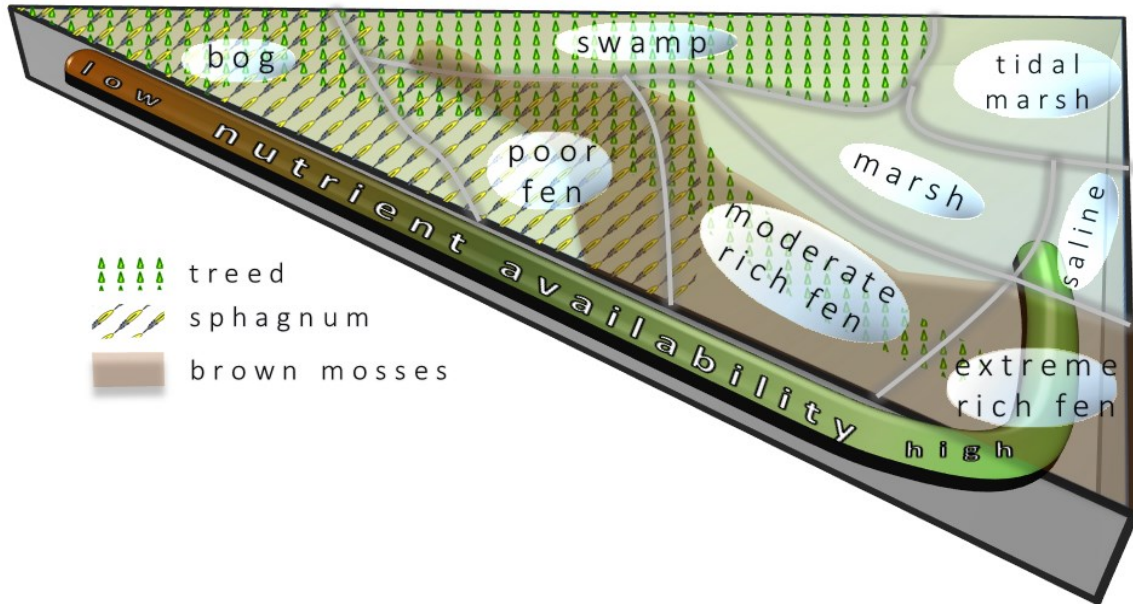
Figure 2.3: Proximity of wetland class characteristics, showing an underlying ecological process. Adapted from Vitt (1994) with permission.

To show the transition from class to class with the vertical profile of wetlands extracted from lidar, Figure 2.4 shows (from left to right) an upland forest (light green trees/brown ground) transitioning into a small treed bog and then into a large raised bog (blue) with low vegetation (dark green). The bog edge slopes down on the right into a lag with open water where the taller vegetation starts again. Up the hill leads to another bog comprised of open and treed areas.

Figure 2.4: Profile of transitioning wetland classes, with terrain and vegetation height extracted from lidar points.

Although the classifications are quite distinct, in practice wetlands often comprise a mixture of various classes (Canada Committee on Ecological [Biophysical] Land Classification 1988). For example, the perimeters of marshes often occur in a transitional zone between open

water and swamp. Consistent combinations can be accommodated in a classification; however, such combinations have the potential to confuse remotely sensed methods. Furthermore, even when evaluators and mappers adhere to criteria as well as they can, the wetland class may still be unclear. Wetland classification is further complicated by: (1) subjective interpretations, and (2) environmental characteristics that vary temporally. Nonetheless, rigorous sampling techniques and skills of generalization can allow credible delineation to be achieved.

2.2   Disturbance and Effect on Wetland Mapping

The term 'hydrogeomorphology' encompasses climate, geomorphology, and hydrology. Hydrology modifies a wetland's physical-chemical environment and also contributes to the transport of sediment and nutrients (except in bogs). Furthermore, changes in physiochemical conditions directly affect vegetation, and vegetation then exerts biotic controls on wetland hydrology (e.g. sediments can be trapped or bound by vegetation which then helps regulate erosion and disrupt flow) (Mitsch and Gosselink 2007). One example is peat accumulation causing vertical growth in bogs, plus fluctuations in water levels as vegetation patterns change (Mitsch and Gosselink 2007). Changes to the hydrogeomorphology have the potential to directly alter wetlands and this effect on mapping has to be considered. In the case of Nova Scotia today, agriculture, urban development, resource extraction and natural events (e.g. beaver dam construction, fire, insects, etc.) can lead to significant changes in hydrology. If the change is persistent, new wetlands can form and existing wetlands can be highly altered or be destroyed, sometimes rather quickly. These types of events further support wetland mapping as a continuous ongoing program to capture important alterations in the landscape.

It is expected that disturbances will affect land cover mapping, so may confuse the classification process in the short term. Fire has been a major natural disturbance agent in the forests of Nova Scotia since European settlement (Neily et al. 2008). Fire can modify soil and the structure of the vegetation, and this can change the hydrologic processes of the watershed leading to long term impacts (Brooks, Ffolliott and Magner 2013). Especially in the case of dry conditions, where fire is more severe, peat can be destroyed and the impact much more damaging (Brooks, Ffolliott and Magner 2013). Nonetheless, the effect of fire disturbance is not as long-lasting compared to urban development and probably would not cause permanent

damage; albeit, there is still a recovery period to consider with resulting changes to hydrology and wetlands (Brooks, Ffolliott and Magner 2013). Disturbance from urban development has an essentially permanent impact on the hydrology and wetlands, even with lower impact methods in management and practices to minimize harmful effects of development (Brooks, Ffolliott and Magner 2013). A change in wetland area and function is inevitable, and mapping and monitoring will help to reduce future issues such as flooding and water quality.

2.3   Wetland Identification in the Field

Wetland identification is the term which describes the techniques used to establish the class of a wetland and to distinguish it from upland features. For the identification, three criteria are generally used which are: hydrology, hydrophytic vegetation species, and hydric soils. The descriptions of these criteria are below.

Wetland hydrology refers to "all hydrological characteristics of areas that are periodically inundated or have soils saturated to the surface at some time during the growing season. Areas with evident characteristics of wetland hydrology (like Figure 2.5) are those where the presence of water has an overriding influence on characteristics of vegetation and soils due to anaerobic and reducing conditions respectively" (Environmental Laboratory 1987, p. 28).

Figure 2.5: Hummocky terrain and water visible indicating wet hydrologic conditions.

Hydrology is often the least exact indicator for wetlands, although it is necessary to establish that soil water saturation occurs sometime during the growing season (Environmental Laboratory 1987). A list of indicators includes (Illinois Department of Natural Resources 2011):

- soft, mushy, waterlogged ground;
- water marks on trees or other erect objects;
- thin layers of sediment deposited on leaves or other objects;
- drift lines - small piles of debris lodged in trees or piled against other objects and oriented in the direction of water movement through an area;
- visible mud or dried mud cracks in low-lying places

Hydrophytic vegetation is determined by "the sum total of macrophytic plant life that occurs in areas where the frequency and duration of inundation or soil saturation produce permanently or periodically saturated soils of sufficient duration to exert a controlling influence on the plant species present" (Environmental Laboratory 1987, p. 12). Hydrophytic vegetation, such as the Northern Pitcher Plant (*Sarracenia purpurea L.*) in Figure 2.6, is adapted to successfully colonize wetland areas. Hydrophytic plants can grow successfully in areas that are permanently or temporarily inundated with water, or in soils that have been affected by that water. Following a standard vegetation inventory, species composition is recorded and applied to a methodology designed to categorize the sample area as wetland or not (i.e. the presence of an individual hydrophytic plant does not necessarily indicate a wetland). To assist in the classification, groups have been defined that categorize where plants are usually found based on their adaptation to the moisture regime (Table 2.1). A thorough and more detailed spreadsheet is maintained by the Nova Scotia Department of Environment website that lists plants by name (https://www.novascotia.ca/nse/wetland/indicator.plant.list.asp).

Figure 2.6: Northern Pitcher plant – an example of obligate hydrophytic vegetation.

Table 2.1: Groupings to describe where plants are typically found.

Category	Description
Obligate (OBL)	plants are almost always (greater than 99%) in wetlands
Facultative Wetland (FACW)	usually found in wetlands (67-99%); sometimes found in upland (1-33%)
Facultative (FAC)	vegetation can be found either in wetland or upland (34-66%)
Facultative Upland (FACU)	usually found in upland (67-99%); sometimes found in wetlands (1-33%)
Upland (UPL)	plants which are almost always in upland areas (greater than 99%)

Hydric soil identification includes measuring consistency and colour against standard measurements. Common characteristics to aid detection are smell (rotten egg from hydrogen sulfide), predominance of decomposed vegetation (peat or muck), and the appearance of mottling or streaking that is usually reddish or dark in colour (e.g. Figure 2.7). The lack of indicators listed above does not always mean a soil is not hydric (Illinois Department of Natural Resources 2011). With some soil types, it can also be helpful to use solutions (Alpha-alpha-Dipyridyl) to produce a chemical reaction which can confirm the presence of ferrous iron in soil and indicate reducing conditions (United States Natural Resources Conservation Service 2012).

Figure 2.7: Distinctive colouring and material of hydric soil.

Hydric soils fall into two broad categories of organic and mineral. Organic hydric soils are commonly known as peat and muck, and develop in conditions of almost permanent water saturation (Environmental Laboratory 1987). Mineral hydric soils are periodically saturated so that chemical and physical soil properties associated with a reducing environment have time to develop (Environmental Laboratory 1987). They usually exhibit the tell-tale colouring and mottling appearance, as mentioned above, or have a dark layer over gray or mottled subsurface horizons. However, care must be taken in certain sandy soils and soils with acidic conditions which can confuse the assessment. For these locations, other indicators must supersede in the assessment.

2.4   Remote Sensing and GIS for Wetland Identification

In context of modern resource management, remote sensing is the science of analysing spatial information from the earth's surface that is received with sensor equipment (Lillesand and Kiefer 1994). The digital image is stored on a computer (as an array of pixels) and is available for various types of analysis. It is often used in land and resource management and usually it must be interpreted to extract information for a particular use such as landcover mapping. Combining additional information sources in remote sensing can increase the success of landcover classification in a synergistic manner. Together, context may be established more

easily than each data input on their own. King (2002) described this type of context with an example of aerial photograph interpretation, where the use of pattern, landscape position and association is common and expected. Calling it a bottom-up approach, King (2002) recommended using that classical mapping approach with the software processing to increase the information obtained.

Remote sensing data can be collected using active or passive technology. Active sensors, like radar, provide their own energy, which is then measured after scattering from an object. The energy received by the sensor will show a unique spectral signature that is typical of the interaction of energy and a particular feature. Passive sensors are sensors that measure reflected, or re-emitted energy, which usually originates from the sun. It will also have a unique set of responses, and this ability to differentiate based on the spectral signature is the basis for automated image classification (Lillesand and Kiefer 1994). QuickBird and Landsat 8 sensors both rely on energy reflected from the sun.

While some radiation from the sun is absorbed or scattered in the atmosphere, the rest that reaches the earth surface interacts in one of three ways: absorption, transmission or reflection. The proportion depends on both the wavelength of the energy and the composition of the feature, and by measuring the unique set of responses for multiple wavelengths, a signature that is characteristic of a particular feature can be established (Canada Centre for Remote Sensing nd). Processing of remotely sensed images involves the statistical analysis of reflectance (in the case of optical imagery) or scattering characteristics (as in the case of radar). There are advantages to both optical and radar imagery. Radar has a longer wavelength and because of that has advantages when measuring soil moisture as well as transmission through cloud or minor precipitation. This means that revisit time is improved so changes in wetlands over the year can be observed more easily, which in turn can aid the classification process. Conversely, because optical imagery satellites are not as bulky as radar platforms, it is technically easier to have higher-resolution sensors (Canada Centre for Remote Sensing nd). This allows satellites such as QuickBird to have superior spatial resolving capability.

Resolution is an important concept in remote sensing and will often determine the intended use of a particular sensor. There are four types of resolution in remote sensing:

temporal, spatial, spectral and radiometric (Lillesand and Kiefer 1994). Temporal refers to the repeat rate of the images – this is useful for change detection over seasons or longer periods of time. Spatial resolution refers to the dimensions of each pixel as data are collected, and determines the limits of feature size that can be detected and the precision of the edges. Spectral resolution is the precision of wavelength breadth that can be measured. Different features can often only be detected based on subtle differences in how they interact with the energy that is reflected. Vegetation condition is an example, as it shows a marked difference between the red band and the near infrared band. Finally, radiometric resolution is the difference in steps of exposure that can be measured, so that the gradient between energy differences is smoother or coarser (Lillesand and Kiefer 1994).

Wetland changes, such as that measured over seasons, can be very good indicators of wetland characteristics. An example is how non-persistent emergent vegetation appears at the beginning of the growing season in open water and increasingly expands its territory over time. Another is changing soil moisture content from season to season. For this reason it is important that imagery be available at multiple stages in the growing season. Some, like RADARSAT-2, have a higher capacity for this repeat cycle. Often the spring/summer (wetter/drier) comparison will indicate the position of a wetland for this reason. This pattern of changing water level is called the *hydroperiod* and is analogous to the wetland's unique hydrologic signature (Mitsch and Gosselink 2007). Multi-temporal data will provide a crucial additional component to determining where wetlands are located (Brisco 2015). Because of the variation in wetland characteristics throughout the year (due to changes in vegetation and water/soil moisture levels) spring, summer and fall imagery are important to consider for data inputs.

A multi-sensor/multi-temporal approach can be used to decrease errors of omission and commission by confirming the existence of the features in the landscape in a way that one dataset cannot on its own. To address the hypothesis that a multi-sensor/multi-temporal approach will be better, various datasets of differing types and resolutions will be used to help define the wetland hydrology, hydric soil, and hydrophytic vegetation, so that wetland class can be determined. A search of the literature indicating input variables (e.g. terrain, optical, single

polarimetric, multi-polarimetric), type of classifier (e.g. maximum-likelihood or RF), and classification accuracy, is displayed in Table 2.2 (See Appendix B for more detail).

Table 2.2: Literature results on studies using dual-polarized, polSAR (fully polarized), optical imagery, and elevation, for wetland mapping.

classifier	SAR	aerial photo	optical satellite	DEM	Soils	main surrounding landscape	class detail (*)	overall accuracy	author
RF	C dualPol L dualPol	✗	✓	✓	✗	forest	2	94.30%	LaRocque et al. 2015
RF	C polSAR L dualPol	✓	✓	✓	✓	forest	3	69.00%	Corcoran et al. 2013
MLC	C polSAR	✗	✗	✗	✗	agriculture	1	64.65%	Brisco et al. 2011
RF	C polSAR	✓	✗	✓	✗	forest	3	63.00%	Corcoran et al. 2011
RF	C polSAR	✗	✗	✓	✗	agriculture	2	88.00%	Millard and Richardson 2013
RF	S polSAR X polSAR	✓	✓	✓	✗	coastal	1	78.20%	van Beijma et al. 2014

(*) class detail was categorized to:
1. more detail – i.e. vegetation species,
2. moderate detail - such as specific wetland classes, and
3. less detail with broader wetland classes.

2.4.1   Inputs to Wetland Mapping - Digital Elevation Model

Wetlands are complex ecological systems and only form when processes of hydrology, geomorphology and biology work collectively to create the necessary conditions (Lynch-Stewart et al. 1996). Water source (precipitation, groundwater discharge, and lateral surface flow) is important for determining different types of wetlands (Brinson 1993). Generally speaking, marshes are the wettest, bogs and fens intermediate, and swamps (treed wetlands) are the driest. For this reason, wetlands specifically are influenced by hydrogeomorphic criteria. For example, where and how water will flow, like in the examples shown in Figure 2.8, can be modeled on various derivatives in the DEM. Topography affects the way water flows across or into a wetland. Wetlands can form in a variety of landscapes; however, in all settings, terrain morphology will influence where surplus water will move and collect, and so plays a major role in determining where wetlands will form (Canada Committee on Ecological (Biophysical) Land Classification 1988). Laser scanning, or lidar, provides an accurate and dense series of points measuring elevation of ground and vegetation (so a canopy height model is possible too). Slope

and other outputs can be derived from the digital elevation model (DEM) that will provide information on topography for calculating water movement. Other data sources like those produced using coarser photogrammetric methods can also be used for terrain analysis, where, depending on the sensitivity of the data, are able to infer different types of landcover.
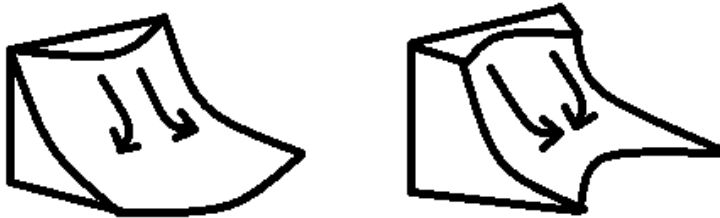
Figure 2.8: Schematic showing examples of landform shape influencing water flow. (adapted from Pennock, Zeborth, & DeJong 1987).

Topography relates to the way water flows across or into a wetland. Wetlands can form in a variety of landscapes, but morphology helps direct the distribution of surplus water and consequently the location of wetlands (Canada Committee on Ecological (Biophysical) Land Classification 1988). Nova Scotia has elevation information produced using photogrammetric data capture and stored in GIS as points, contours and break lines. These sources are common and rely on stereoscopic interpretation of air photographs using a stereoplotter (Wilson and Gallant 2000). This data must be interpolated to form a continuous surface in order to be easily used in terrain analysis. Likewise, lidar is another source of elevation data. Lidar results in a highly accurate and precise DEM that would presumably provide a superior source of information. The Nova Scotia digital elevation model will be referred to as the "NS DEM", and the DEM created from lidar will be denoted as "lidar DEM".

In the case of elevation, absolute accuracy refers to a value based on an established vertical datum. The elevation points for the province are not particularly accurate in that absolute sense, and the error is not consistent. However, concerning the creation of derivative products such as slope, the scale of the NS DEM may still be suitable to aid wetland modeling. This scale is referred to as the *topo scale*, where the surface morphology that affects catchment hydrology can be measured (Wilson and Gallant 2000). A lidar DEM, and the provincial DEM, are both at a scale suitably characterized as *topo scale*.

Errors in DEMs have been shown to be clearly correlated with terrain slope (Castrignano, Buttafuoco, Comolli, and Ballabio 2006). They found that the most significant errors occurred in the steepest part of their study area. However, wetlands are generally found in areas of low slope so the errors associated with steep areas would be minimized. Equally important, the minimum slope that can be calculated accurately is presumably greater than the lower limit of reliable measurements.

2.4.2   Inputs to Wetland Mapping - Optical Imagery

Optical imagery measures the spectral response of reflected energy from features on the earth's surface which can be analysed using software to map features such as wetlands. If the spectral signatures are adequately resolved, different land cover classes can be inferred. That ability to differentiate based on the spectral signature is the basis for automated image classification (Lillesand and Kiefer 1994). Different features can often only be detected based on subtle differences in how they interact with the energy that is reflected. Vegetation condition is an example, as it shows a marked difference between the red band and the near infrared band. Both QuickBird and Landsat 8 are optical systems relying on passive sun energy reflected from the earth's surface, so they are unlike radar (e.g. PolSAR from RADARSAT-2) which produces its own energy source (an active sensor). The wavelengths in which optical sensors operate are smaller and work by differentiating objects based on their chemical (e.g. chlorophyll) or microscale features. In contrast, radar wavelengths are affected by the physical structure that we see as the shape or texture of objects established (Canada Centre for Remote Sensing nd). In several studies, optical imagery was found to be suitable for mapping wetlands, particularly in the case of open wetlands with low vegetation (Pietroniro and Leconte 2005; Harris et al. 2005, 2006; Meingast et al. 2014). Ozesmi and Bauer (2002), in their review, showed that most of the previous wetland mapping studies used optical imagery, but that the addition of radar would be useful.

2.4.3   Inputs to Wetland Mapping - SAR

SAR imagery pixel values represent backscatter, or power, that is received by the sensor after the microwave energy is emitted and interacts with the scatterer or target. Different targets will, then, appear brighter or darker depending on their physical features. SAR operates

by sending and receiving signals at an angle, and the use of various angles result in different information received from the scattering surface. Individual SAR platforms also allow for the collection of distinct wavelengths that will have unique results over the same area. Because of the numerous arrangements possible in SAR, it is important to test distinct incidence angles, as in Figure 2.9, plus different wavelengths to try and extract more information.
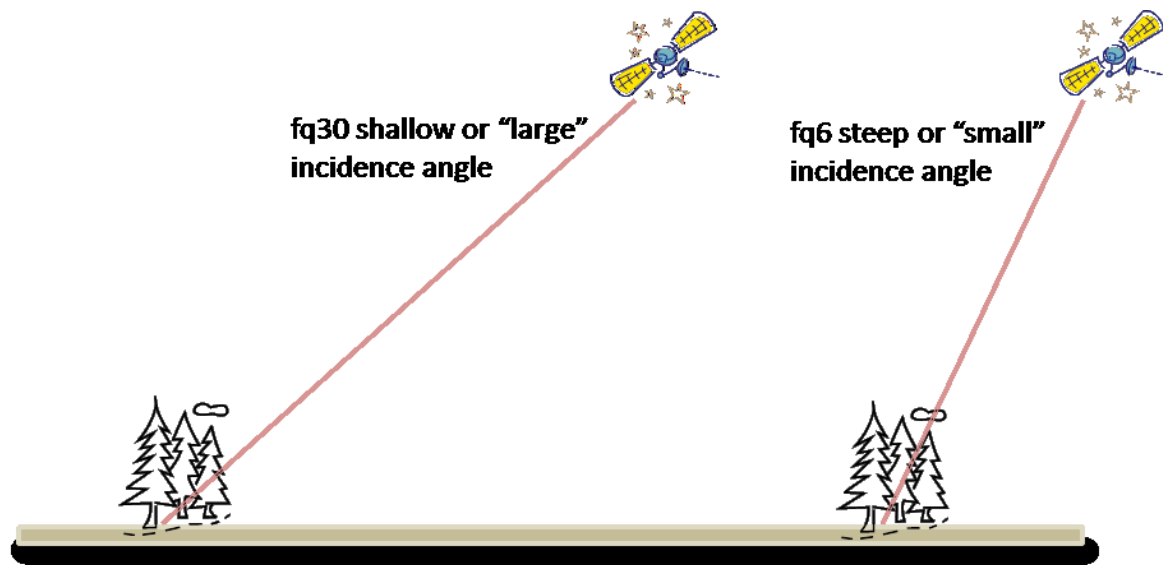
Figure 2.9: RADARSAT-2 may be acquired at different incidence angles.

While most of the previous wetland mapping studies have used optical satellite images (see the review of Ozesmi and Bauer 2002), single polarized SAR has been tested in Canada for mapping wetlands as part of the Canadian Wetland Inventory (Li and Chen 2005; Grenier et al. 2007; Fournier et al. 2007). High sensitivity to surface water and soil moisture, because of its high dielectric constant, can make radar an efficient tool for determining hydrology (Kasischke et al. 1997a; Rao et al. 1999). Single polarization SAR is important for measuring wetland water extent for landcover classifications. For example, some wetland types experience seasonal flooding so not only is soil moisture an important parameter, but the existence of standing water as well. Standing water is often observable as a double-bounce signature as a result of the wave energy reaction with the water and vegetation (Brisco et al. 2008).

There are, however, limitations to the HH single polarization available from satellites such as RADARSAT-1 that would make visible near infrared imagery a required complement

(Touzi et al. 2007). Furthermore, wetland classification can be improved through the use of multiple polarizations in place of single polarized imagery (Ozesmi and Bauer 2002; Wang et al. 1998). However, most recently, radar polarimetric SAR (polSAR) images have been tested. The launch of fully polarimetric SAR X, C and L-band sensors (TerraSAR-X and RADARSAT-2 in 2007, and PALSAR in 2006) provides data that allow a complete description of the scattering properties because it provides the full scattering matrix. Radar polarimetry is an important area of research for extracting bio-geophysical parameters for targets on the earth's surface (Touzi et al. 2009). Fully polarimetric systems, like RADARSAT-2, lead to new insights in wetland studies as they could measure backscatter phase as well as magnitude (Pope et al. 1997). Polarimetric data have already been shown to be highly effective for wetland mapping (Touzi et al. 2007).

Such an advantage from polSAR offers an opportunity to develop improved tools for mapping wetlands. A number of additional procedures are available to remote sensing analysts using software that takes advantage of the full potential of polarized SAR data (Woodhouse 2006), and these include tools for polarization synthesis, and for creation of polarimetric variables and polarimetric decomposition parameters. When orthogonal pairs are combined, the complete scattering properties can be determined, and these scattering properties are analyzed, using various statistical means and algorithms, into a comprehensible product, graph or classification map.

The Cloude-Pottier decomposition is one such approach to use in classification techniques. The Cloude-Pottier decomposition is roll-invariant and has been a commonly used method; the alpha angle (α) parameter combined with entropy (H) is the most popular approach (Touzi et al. 2007). Even though the Cloude-Pottier H/α has been widely validated (Touzi et al. 2007), subsequent research has shown that the Cloude-Pottier H/α only performs as well as single polarization HH data for wetland discrimination. This means that it is not possible to discriminate between certain wetland classes (Touzi et al. 2009). To address some issues with the Cloude-Pottier H/α, Touzi et al. (2007) examined PolSAR, as applied to wetlands in a temperate climate, to break down the average scattering mechanisms to associate a physical mechanism to each component. Phase difference between HH and VV polarizations

has provided the most successful results (Touzi et al. 2009). Another available decomposition, namely the Touzi decomposition, uses the complex entity of the symmetric scattering type to describe the target scattering type while the symmetric nature of target scattering is assessed by Huynen's target helicity (Touzi et al. 2009). Comparisons were made between the Cloude-Pottier H/α and the Touzi incoherent target decomposition methods and they demonstrate the requirement for phase and magnitude of the symmetric scattering type (Touzi et al. 2009).

As an example of recent work using polSAR and associated tools, classification inside of the Mer Bleue wetland (a large, contiguous wetland near Ottawa consisting of marsh, treed bog, shrub bog, and fen classes) has been improved by the phase of the symmetric scattering type, and a clear separation of dominant wetland classes was possible (Touzi et al. 2007). The ability of the scattering phase to successfully distinguish wetland classes has been hypothetically attributed to the interactions with the type of sub-surface water flow (Touzi et al. 2009). As mentioned previously, wetland development is related to the physical nature of the hydrology and soils. Therefore, it can be expected that different wetland types are a result of different hydrological and soil conditions; and the sub-surface capabilities of radar are an ideal mechanism for this application.

2.5 Challenge of using Remote Sensing and GIS for Wetland Identification

One objective of interpreting the earth's surface remotely is to achieve the most accurate representation of the land cover. However, remote sensing involves processing and interpreting geospatial data that is subject to personal conceptualisations (Comber 2005), meaning that the user of the classification information must be aware of how it was created and for what purpose, so that they can use their best judgement for its suitability. Though researchers familiar with the input data will know and accept the error attributed to the model, care must be taken when using this information in other future applications for which it was not originally intended. Thus, new projects may be the preferred approach from an operational point of view. Indeed, the categorisation of wetland types can be complicated. For example, many plant species typically found in wetlands can also be found in uplands. The opposite is true as well, and for these reasons the wetland evaluator must incorporate estimates of vegetation cover in the process of wetland delineation. In addition, wetlands do not need to

exhibit high water levels continually; thus, for example, a "dry" forest may in fact be accurately delineated as a wetland (Mitsch and Gosselink 2007). Despite the uncertainty of difficult interpretations, a land cover information database can still be used successfully provided certain criteria of understanding are met. For example, comprehensively documenting the classification process is necessary, and part of that process involves an assessment of accuracy. Thematic accuracy assessments are a commonly used quantitative approach whose goal is to identify and measure map errors (Congalton 2009). The details about the mapping process with accuracy should allow the user to be able to decide if that the information is usable for their purpose.

Various image analysis techniques are often used in land and resource management, and resulting classifications can assist researchers to detect ecological changes over time. A comprehensive understanding of methodological principles as well as knowledge pertaining to appropriate data use are required to ensure that maximum information can be extracted from remotely sensed sources.

2.6 References:

Brinson, M.M. 1993. "Changes in the Functioning of Wetlands Along Environmental Gradients." *Wetlands.* Vol. 13, No. 2, pp. 65-74.

Brisco, B., Kapfer, M., Hirose T., Tedford, B., and Liu, J. 2011. "Evaluation of C-band polarization diversity and polarimetry for wetland mapping." *Canadian Journal of Remote Sensing*, Vol. 37, pp. 82-92.

Brisco, B. 2015. "Mapping and monitoring surface water and wetlands with synthetic aperture radar." In R. Tiner, M. Lang, and V. Klemas (Eds.), *Remote Sensing of Wetlands: Applications and Advances* (pp. 119-136). Boca Raton, FL, USA: CRC Press.

Brisco, B., Touzi, R., van der Sanden, J. J., Charbonneau, F., Pultz, T. J. and D'Iorio, M. 2008. "Water resource applications with RADARSAT-2 – a preview." *International Journal of Digital Earth*, Vol. 1, No. 1, pp. 130-147.

Brooks, K., Ffolliott, P., and Magner, J. 2013. *Hydrology and the management of watersheds (4th ed.)*. Ames, Iowa, USA: Wiley-Blackwell.

Canada Centre for Remote Sensing. nd. "Fundamentals of Remote Sensing: A Canada Centre for Remote Sensing Remote Sensing Tutorial." Retrieved from http://www.nrcan.gc.ca/sites/www.nrcan.gc.ca/files/earthsciences/pdf/resource/tutor/fundam/pdf/fundamentals_e.pdf.

Canada Committee on Ecological (Biophysical) Land Classification. 1988. "Wetlands of Canada." Ottawa: Sustainable Development Branch, Canadian Wildlife Service, Conservation and Protection, Environment Canada. pp. 1-61.

Castrignano, A., Buttafuoco, G., Comolli, R., and Ballabio, C. 2006. "Accuracy assessment of digital elevation model using stochastic simulation." *Proceedings of the 7th International Symposium on Spatial Accuracy Assessment in Natural Resources and Environmental Sciences.* pp. 490–498.

Comber, A., Fisher, P., and Wadsworth, R. 2005. "What is land cover?" *Environment & Planning B: Planning & Design*, Vol. 32, No. 2, pp. 199-209.

Congalton, R. G., and Green, K. 2009. "Assessing the accuracy of remotely sensed data: Principles and practices." Boca Raton, FL, USA: CRC Press/Taylor & Francis.

Corcoran, J. M., Knight, J. F., Brisco, B., Kaya, S., Cull, A., and Murnagahn, K. 2011. "The integration of optical, topographic, and radar data for wetland mapping in Northern Minnesota." *Canadian Journal of Remote Sensing*, Vol. 37, No. 5, pp. 564-582.

Corcoran, J. M., Knight, J. F., and Gallant, A. L. 2013. "Influence of multi-source and multi-temporal remotely sensed and ancillary data on the accuracy of Random Forest classification of wetlands in Northern Minnesota." *Remote Sensing*, Vol. 5, No. 7, pp. 3212-3238.

Environment Canada. 2011. "Glossary". Retrieved from http://www.ec.gc.ca/default.asp?lang=En&n=7EBE5C5A-1#glossaryw

Environmental Laboratory. 1987. "Corps of Engineers wetlands delineation manual" Technical Report Y-87-1. U.S. Army Engineer Waterways Experiment Station, Vicksburg, MS.

Fournier, R., Grenier, A, M., Lavoie, A., and Hélie, R. 2007. "Towards a strategy to implement the Canadian Wetland Inventory using satellite remote sensing." *Canadian Journal of Remote Sensing*, Vol. 33, Supp. 1, pp. S1–S16.

Grenier, M., Demers, A.-M., Labrecque, S., Benoit, M., Fournier, R. A., and Drolet, B. 2007. "An object-based method to map wetland using RADARSAT-1 and Landsat ETM images: Test case on two sites in Quebec, Canada." *Canadian Journal of Remote Sensing*, Vol. 33, Supp. 1, pp. S2-S45.

Harris, A., Bryant, R. G., and Baird, A. J. 2005. "Detecting water stress in Sphagnum spp." *Remote Sensing of Environment*, Vol. 97, No. 3, pp. 371–381.

Harris, A., Bryant, R. G., and Baird, A. J. 2006. "Mapping the effects of water stress on Sphagnum: Preliminary observations using airborne remote sensing." *Remote Sensing of Environment*, Vol. 100, No. 3, pp. 363-378.

Illinois Department of Natural Resources. 2011. "*Hydrophytic Vegetation.*" Retrieved from http://dnr.state.il.us/wetlands/ch1e.htm

Kasischke, E.S. and Bourgeau-Chavez, L.L. 1997. "Monitoring South Florida Wetlands Using ERS-1 SAR Imagery." *Photogrammetric Engineering & Remote Sensing.* Vol. 63, No. 3, pp. 281-291.

King, R.B. 2002. "Land cover mapping principles: a return to interpretation fundamentals." *International Journal of Remote Sensing.* Vol. 23, No. 18, pp. 3525-3545.

LaRocque, A., Leblon, B., Bourgeau-Chavez, L., McCarty, J., French, N., and Woodward, R. 2015. "Evaluating wetland mapping techniques for New Brunswick using Landsat TM, ALOS-PALSAR and RADARSAT-2 dual-polarized images." *Canadian Journal of Remote Sensing* (submitted).

Li, J., and Chen, W. 2005. "A rule-based method for mapping Canada's wetlands using optical, radar and DEM data." *International Journal of Remote Sensing*, Vol. 26, No. 22, pp. 5051-5069.

Lillesand, T.M. and Kiefer, R.W. 1994. *Remote Sensing and Image Interpretation*. New York, NY, USA: John Wiley and Sons Inc.

Lynch-Stewart, P., Neice, P., Rubec, C. and Kessel-Taylor, I. 1996. "The Federal Policy on Wetland Conservation – Implementation Guide for Federal Land Managers." Ottawa, Environment Canada. pp. 1-20. Retrieved from http://nawcc.wetlandnetwork.ca/Fed%20Policy%20Wetland%20Conserv_Implement%20Guide%20for%20Fed%20Land%20Mgrs.pdf

Meingast, K. M., Falkowski, M. J., Kane, E. S, Potvin, L. R., Benscoter, B. W., Smith, A. M. S., Bourgeau-Chavez, L. L., and Miller, M. E. 2014. "Spectral detection of near-surface moisture content and water-table position in northern peatland ecosystems." *Remote Sensing of Environment*, Vol. 152, pp. 536-546.

Millard, K. and Richardson, M. 2013 "Wetland mapping with LiDAR derivatives, SAR polarimetric decompositions, and LiDAR–SAR fusion using a random forest classifier." *Canadian Journal of Remote Sensing*, Vol. 39, No. 4, pp. 290-307.

Mitsch, W. J., and Gosselink, J. G. 2007. *Wetlands*. Hoboken, New Jersey, USA: John Wiley & Sons, Inc.

Neily, P., Quigley, E., and Stewart, B. 2008. "Mapping Nova Scotia's Natural Disturbance." Nova Scotia Department of Natural Resources. Retrieved from http://novascotia.ca/natr/library/forestry/reports/NDRreport3.pdf

Nova Scotia Department of Natural Resources. 2011. "Ecosystems and Habitats Program Overview." Retrieved from http://novascotia.ca/natr/wildlife/habitats/wetlands.asp

Ozesmi, S. L., and Bauer, M. E. 2002. "Satellite remote sensing of wetlands." *Wetland Ecology and Management*, Vol. 10, pp. 381-402.

Pennock, D., Zebarth, B., and DeJong, E. 1987. "Landform classification and soil distribution in hummocky terrain, Saskatchewan, Canada." *Geoderma*, Vol. 40, No. 3-4, pp. 297-315.

Pietroniro, A., and Leconte, R. 2005. "A review of Canadian remote sensing and hydrology, 1999-2003." *Hydrological Processes*, Vol. 19, No. 1, pp. 285-301.

Pope, K.O., Rejmankova E., Paris J.F., and Woodruff, R. 1997. "Detecting Seasonal Flooding Cycles in Marshes of the Yucatan Peninsula with SIR-C Polarimetric Radar Imagery." *Remote Sensing of Environment*, Vol. 59, No. 2, pp. 157-166.

Prince Edward Island Environment, Energy and Forestry. nd. "A Guide to Watershed Planning on Prince Edward Island." Retrieved from http://www.gov.pe.ca/photos/original/eef_waterguide.pdf

Rao, B., Dwivedi, R., Kushwaha, S., Bhattacharya, S., Anand, J., and Dasgupta, S. (1999). Monitoring the spatial extent of coastal wetlands using ERS-1 SAR data. *International Journal of Remote Sensing*, Vol. 20, No. 13, pp. 2509-2517.

Touzi, R., Deschamps, A., and Rother, G. 2009. "Phase of Target Scattering for Wetland Characterization Using Polarimetric C-Band SAR." *IEEE Transactions on Geoscience and Remote Sensing*, Vol. 47, No. 9, pp. 3241-3261.

Touzi, R., Deschamps, A., and Rother, G. 2007. "Wetland Characterization using Polarimetric RADARSAT-2 Capability." *Canadian Journal of Remote Sensing*, Vol. 33, Supp. 1, pp. 56-67.

United States Natural Resources Conservation Service. (2012). *Hydric Soils Technical Note 8.* Retrieved from http://www.nrcs.usda.gov/wps/portal/nrcs/detail/soils/use/hydric/?cid=nrcs142p2_053983

van Beijma, S., Comber, A., and Lamb, A. 2014. "Random Forest classification of salt marsh vegetation habitats using quad-polarimetric airborne SAR, elevation and optical RS data." *Remote Sensing of Environment*, Vol. 149, pp. 118-129.

Vitt, D.H. 1994. "An Overview of Factors that Influence the Development of Canadian Peatlands." *Memoirs of the Entomological Society of Canada*. Vol. 126, No. 169, pp. 7-20.

Wang, J., Shang J., Brisco, B., and Brown, R. 1998. "Evaluation of multi-date ERS-1 and multispectral Landsat imagery for wetland detection in Southern Ontario." *Canadian Journal of Remote Sensing*, Vol. 31, pp. 214-224.

Warner, B.G. and Rubec, C.D.A. (Eds.). 1997. "The Canadian Wetland Classification System. (2nd edition)." National Wetlands Working Group. Wetlands Research Centre. University of Waterloo. Ontario, pp. 1-68.

Wilson, J., and Gallant, J. C. 2000. *Terrain analysis: Principles and applications*. New York: Wiley.

Woodhouse, I. 2006. "*Introduction to microwave remote sensing*." Boca Raton, FL, USA: Taylor & Francis.

Chapter 3.   Materials and Methods

3.1   Study Area

The study area is located southwest of Halifax, Nova Scotia, and covers much of Long Lake Provincial Park and the Herring Cove Backlands (Figure 3.1). This area is experiencing increased pressure from urban development though presently much of the landscape is still considered natural. Most of the natural landscape is characterized by forests, lakes, wetlands and a moderately hilly terrain. As measured from the digital elevation model (DEM) (Figure 3.1), the elevation in the study area ranges from 0 m above mean sea level (AMSL) along the coast of Halifax Harbour to 150 m AMSL on Geizer Hill at the northwest edge of the study area. The drainage network is dominated by the McIntosh Run which is approximately 13.5 km long and drains an area of 33.6 km^2. As elsewhere in Nova Scotia, the study area experiences a modified continental climate, but its proximity to the Atlantic Ocean leads to more-frequent rain and fog occurrences (Nova Scotia Museum of Natural History 1989). The physiography and hydrogeography that describe surface and sub-surface water (Schoewe 1951) are likely to be similar across a regional scale (Poff 1996). Conceptually, then, a methodology developed for this study area can be applied to the rest of Nova Scotia. However, physiographic variation does change outside of the study region, according to Ecological Land Classification information for Nova Scotia (Neily et al. 2003). Therefore it is possible that inferences made for my study area on the application of remote sensing, may have to be adapted.
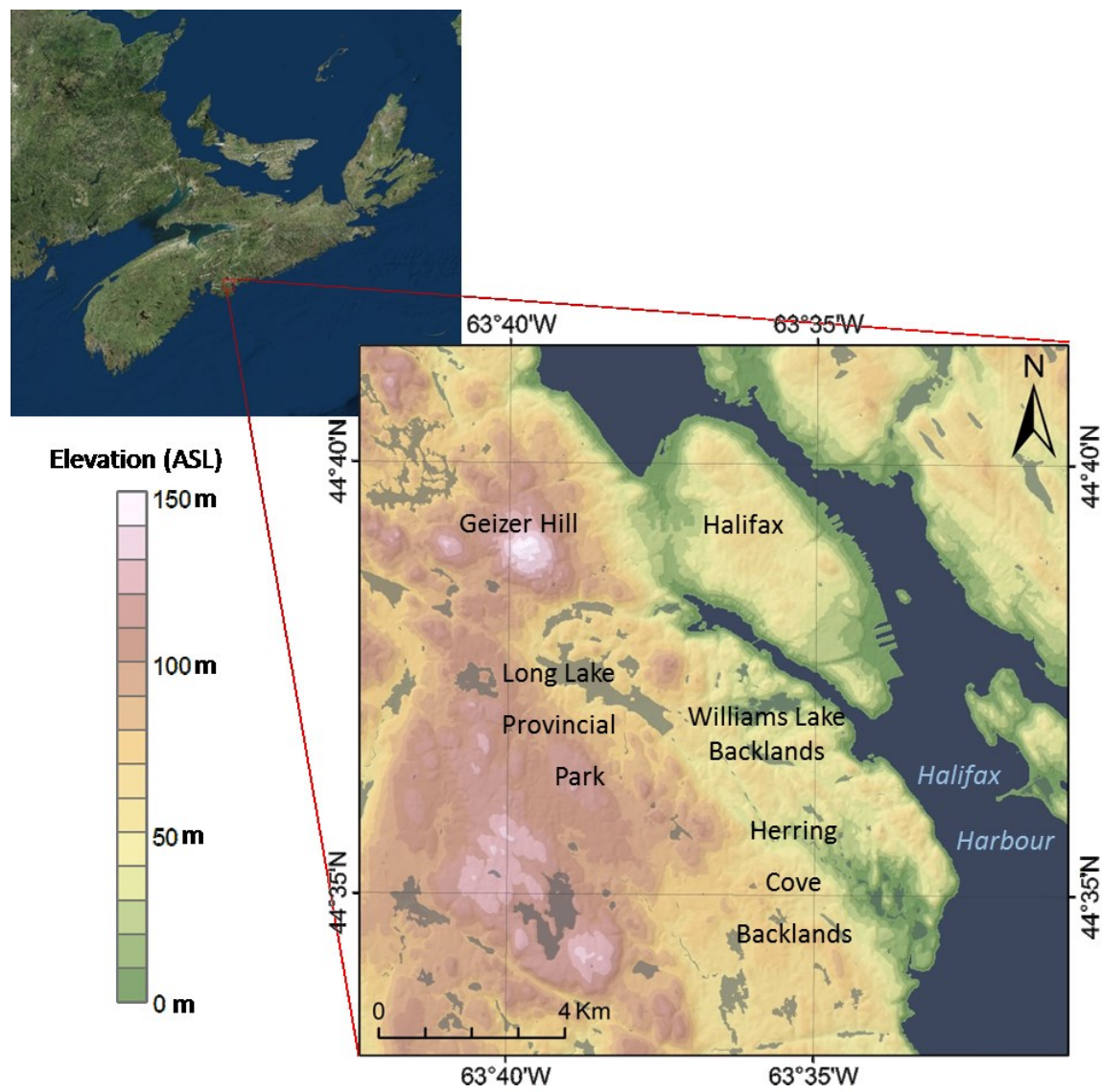
Figure 3.1: Location and digital elevation model of the study area.

Wetland development is related to climate and physiography (Newmaster 1997) so it is important to identify these associations in the study area. The Canadian Wetland Classification System (which Nova Scotia is utilizing) uses both abiotic and biotic parameters that are linked to climate and physiography (Warner and Rubec 1997). Glaciation played a considerable role in wetland formation in Nova Scotia with dramatic effects on the shape of the landscape which influenced hydrology. The last glaciation (i.e. the Wisconsin glaciation) reached the extent shown in Figure 3.2, and retreated about 10,000 years ago (Pielou 1991). As the ice melted, bare ground was exposed, allowing plants and animals to occupy the land and water (Pielou

1991). It resulted in a deranged drainage pattern affecting wetland distribution and is also the reason for basins in Nova Scotia tending to be typically small and disconnected (Pielou 1991).

Figure 3.2: Extent of Wisconsin glaciation in eastern North America (Ehlers and Gibbard 2004).

In Nova Scotia, soils are characterized by podzols which are acidic and generally coarse-textured, and leaching of soil nutrients is common (Canada Committee on Ecological [Biophysical] Land Classification 1988). Cementation of leached organic carbon, iron, and aluminum leads to the creation of hardpan, a condition that can subsequently cause poor drainage with wetland development (Canada Committee on Ecological [Biophysical] Land Classification 1988). Accordingly, wetlands are relatively common in this region.

Nova Scotia's ELC, a tool used in managing forests, describes the landscape using a common set of descriptions or categories. The ELC contains a soil drainage class which describes the removal of excess soil water (Figure 3.3), and shows that the area is a mixture of well drained soils and imperfectly drained soils (Neily et al. 2003). Like the poorly drained class, imperfectly drained soils are also expected to provide suitable conditions for wetland development.
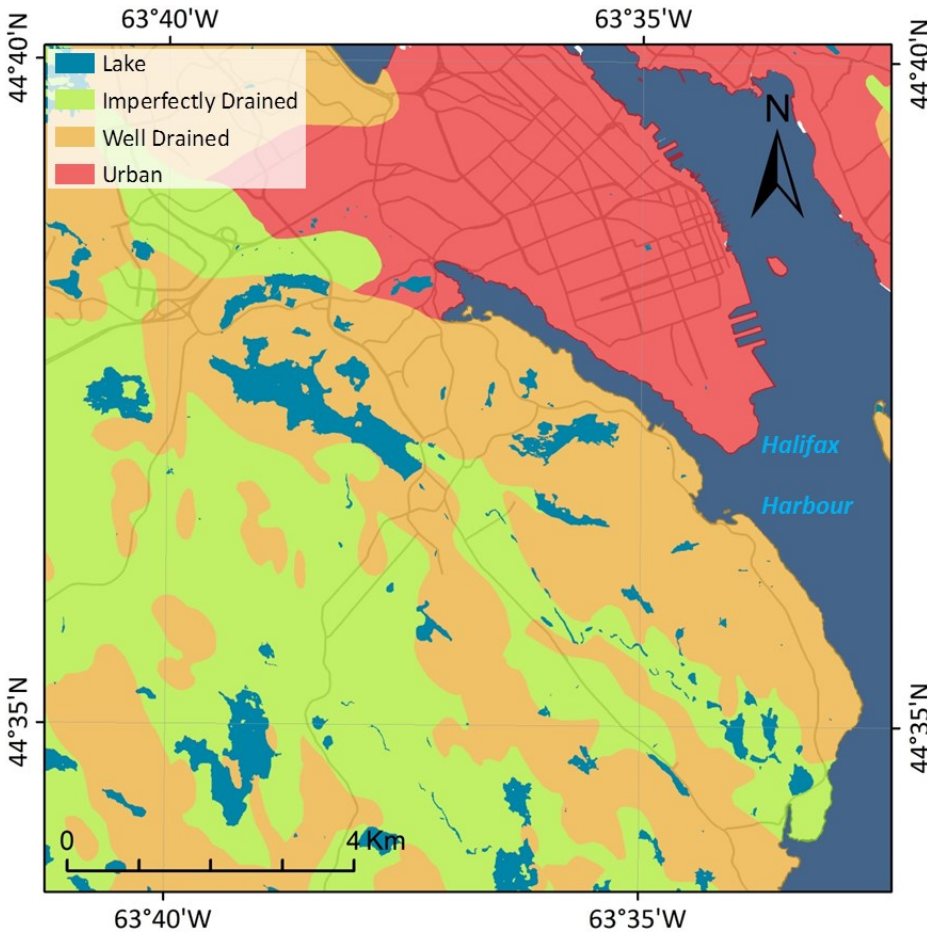
Figure 3.3: Ecological Land Classification drainage shows well drained (light orange) and imperfectly drained (green) soils.

The study area contains most of the relevant wetland classes of interest that can be found in the province of Nova Scotia, such as peatland (includes ombrotrophic peatland like bogs, and minerotrophic peatland such as fens), and swamps. However, because the area is mainly forested, large marshes are absent, so this class was merged with the open-water class to form what is called an open-water/marsh complex. Also, fens and swamps are more common than ombrotrophic bogs in the eastern part of the study area around the Williams Lake Backlands, because it has a barrens landscape that is "flow-through", meaning that definite in- and out-flows are typical (Hill and Patriquin 2014).

3.2 Data Assembly and Data Preparation

3.2.1 Overview

For the first study, two types of satellite imagery were used in the classifications: (1) QuickBird imagery acquired from October 30, 2005 (pixel size = 2.4 m, swath = 16.8 km); and (2) RADARSAT-2 SLC fine quad-pol (FQ) C-band (5.54 cm wavelength) PolSAR imagery from summer 2010 and spring 2013 (pixel spacing of 8 m, nominal resolution of 12 m, and swath of 25 km) (Table 3.3). The QuickBird imagery was available from the Halifax Regional Municipality. It is 11-bit imagery with four multispectral bands (blue 450-520 nm, green 520-600 nm, red 630-690 nm, and near-infrared 760-900 nm). The image was previously georeferenced and has the following projection and datum: UTM zone 20, row T, NAD83.

For the second study, QuickBird imagery was substituted with Landsat 8 imagery from October 6, 2013, available from the United States Geological Survey (pixel size = 30 m, swath = 185 km). It is 12-bit imagery with eight multispectral bands (coastal aerosol 430 – 450 nm, blue 450 – 510 nm, green 530 – 590 nm, red 640 – 670 nm, near infrared 850 – 880 nm, short-wave infrared 1 1570 – 1650 nm, short-wave infrared 2 2110 – 2290 nm, cirrus 1360 – 1380 nm). The image was previously georeferenced and has the same projection and datum as the QuickBird image. The RADARSAT-2 imagery was resampled to 30 m to match the Landsat 8 spatial resolution.

Laser scanning (lidar) data were collected for Halifax Regional Municipality in the spring of 2007 (leaf off). It provides an accurate and dense series of points that was processed to classify points as first return (tree-branch level) and a ground return (ground level). The ground return data were interpolated by the Applied Geomatics Research Group in Middleton, Nova Scotia, to create a 2-m resolution digital elevation model (DEM). The first return data were converted directly to raster (with null values assigned values based on the surrounding neighbourhood) to create the digital surface model (DSM). A canopy height model (CHM) was created as the difference between DSM and DEM.

The Nova Scotia provincial elevation dataset is a series of mass points (general points denoting elevation), plus breaklines and spot heights showing important changes in

topographical shape (Nova Scotia Geomatics Centre 2015). It is derived from aerial photogrammetry procedures (using principles of perspective and projective geometry) and has complete coverage for the province. These data were used in the process to create contour elevation lines from which I created the digital elevation model using the "Topo to Raster" tool in ArcGIS® (ESRI 2015).

Decisions related to the preprocessing of each data input (outlined in the following sections) were based on previously published literature and empirical evidence discovered when experimenting with different parameters while preparing terrain variables from lidar. The extent of lidar, QuickBird, and RADARSAT-2 is shown in Figure 3.4, and the study area is the juncture of these three boundaries. Both Landsat 8 and the NS DEM have complete coverage for the area. Details on these various inputs are described in the following sections, starting with terrain, and then optical imagery and PolSAR.
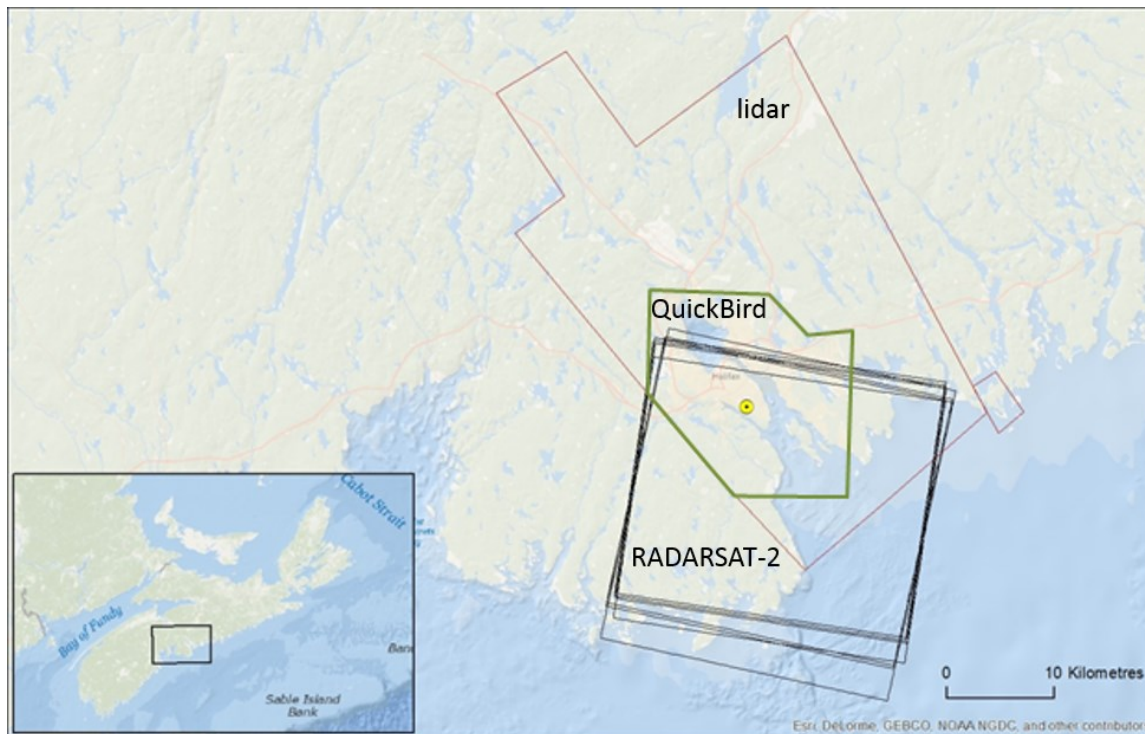
Figure 3.4: Extent of lidar, QuickBird, and RADARSAT-2.

3.2.2 Terrain Processing in Preparation for Classification

Digital terrain analysis was considered a vital element to be included in the data inputs for classification of landcover (Wilson and Gallant 2000). However, Wilson and Gallant (2000) expressed the need to take into account how grid cell size of a DEM will affect its ability to model hydrological processes (Wilson and Gallant 2000). Two elevation models were used, representing a highly accurate and precise DEM interpolated from lidar with a 2 m grid cell size, and a relatively coarse province-wide DEM with a 20 m grid cell size. The lidar DEM has been compared to highly accurate (sub-centimetre) surveyed points but the accuracy of the NS DEM compared to the survey points was unknown. It was necessary to determine the NS DEM accuracy so that any differences in classification results could be attributed to either cell size and/or accuracy.

Laser scanning data, also known as lidar, was collected over a section of Halifax Regional Municipality in 2007. They provide an accurate and dense series of points that was processed to classify points as first return and a ground return (e.g. tree branch level and ground level). The ground return data was interpolated by the Applied Geomatics Research Group using inverse distance weighting (IDW) to create a two-metre resolution digital elevation model (DEM) using Surfer by Golden Software (Monette and Hopkinson 2010). IDW was chosen as the interpolator because the points are dense and location is only precise to the lidar footprint area (Hopkinson, personal communication June 30, 2009). The result was output to an ESRI Grid format and subsequent processing was done using ESRI ArcMap software. The Nova Scotia Topographic Database contours and spot heights were used to interpolate a DEM using the Topo to Raster tool in ArcMap. A second version of the DEM was created with the addition of provincial basemapping water flow data to create a hydrologically correct DEM (i.e. one for which algorithms can direct all modeled flow to pour points in the ocean).

The following DEM derivative variables were calculated: (1) the Slope (SLP) that shows where the surface water runoff is slower (or faster); (2) the Compound Topographic Index (CTI) that shows wetter areas using slope combined with where flow is predicted to accumulate; (3) the Curvature (CRV) that shows deceleration (or acceleration) of water runoff; (4) the Topographic Position Index (TPI) that gives the relative position in the landscape (hilltop to

34

valley bottom); and (5) the Canopy Height Model (CHM) that is a generalized characterization of local tree height estimated by taking the difference between the DEM (as created by AGRG) and the First Return DSM and filtered with a majority filter. The Canopy Height Model could not be calculated with the provincial information.

For illustrative purposes, the values of lidar DEM derivatives were compared using a profile crossing two drumlins (Figure 3.5). The area between and on either side appear to be areas where a wetland could be expected to exist.

- TPI = relative position in the landscape (hilltop to valley bottom)
- SLP = where surface water runoff is slower (or faster)
- CTI = wetter areas using slope + water accumulation
- CRV = deceleration (or acceleration) of water runoff
- CHM = local tree height category (1-5)
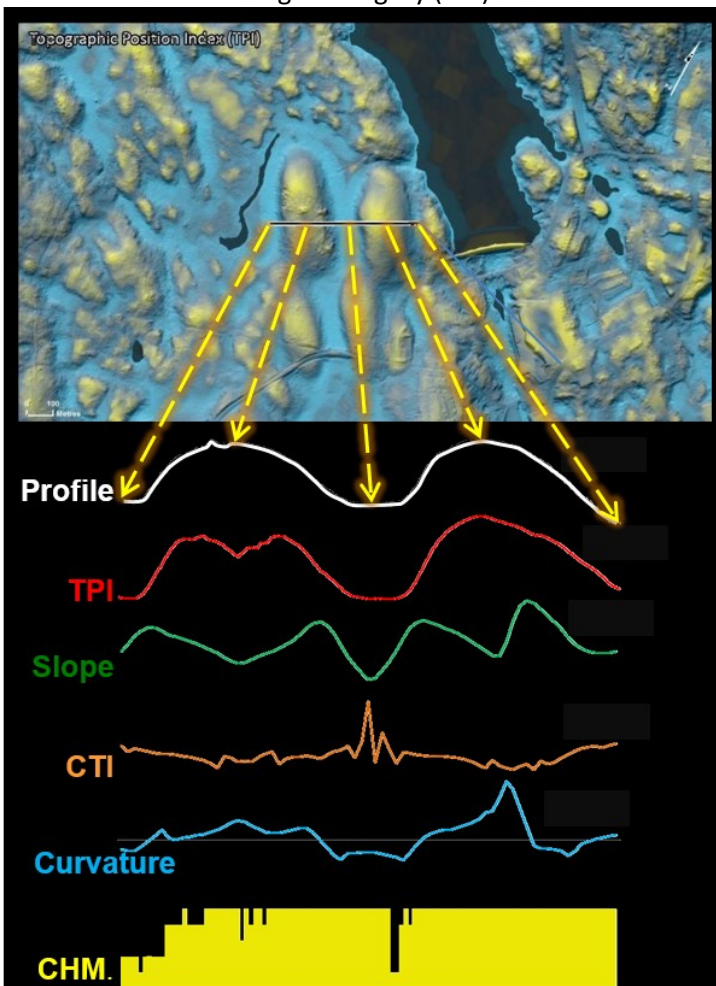
Figure 3.5: Profiles of various elevation derivatives.

The TPI gives the relative position in the landscape (hilltop to valley bottom) for each cell. It is computed in ArcGIS using a modified Jenness method (Jenness 2002) that was designed by S. Cooley (2014), but with parameters adjusted to my study area. My process determines the height of a central cell, as well as the minimum elevation in a 1 ha neighbourhood, and the difference is calculated. The height difference from the neighbourhood minimum is divided by the neighbourhood range (i.e. maximum - minimum), and that value (TPI) is stored in a new raster. The values for this index run between zero and one, and indicate whether the position is near the bottom (valley), near the top (peak), or somewhere in between (slope).

$$\frac{E - nE_{min}}{nE_{max} - nE_{min}}$$

(1)

where

- E = elevation
- nE_{min} = minimum elevation in a neighbourhood
- nE_{max} = maximum elevation in a neighbourhood

Slope is also important but because wetlands are less likely to form on top of hills (like the drumlins in Figure 3.5), it may confuse the model prediction such as the case found on the tops of confined uplands. Here the TPI and slope work together with the TPI providing an extra measure of fine tuning: the flat area on top of the drumlin is reflected in the higher TPI value so that will reduce the influence of the low slope. Figure 3.6 shows an elevation and TPI profile across two drumlins. The left hand drumlin had an excavation at the peak and the right did not, which is more obvious in the TPI profile. TPI is high on the right, very low in the valley and medium in the excavation. Slope is low in all three cases so the TPI will help direct the classification model to show wetland or not. In other words it is unlikely the model would identify a wetland on the right drumlin, more likely on the left drumlin, and very likely in the middle.

Figure 3.6: Profile of the topographic position index crossing two drumlins.

Slope was derived in ArcGIS® using the maximum rate of change from one cell to its eight neighbours to show the steepest downhill descent. Slope, as an input to the classification, is intended to show where surface water runoff is slower (or faster). Preliminary analysis showed that 90% of the area inside Nova Scotia Wetland Inventory polygons was less than or equal to two degrees of slope using the lidar DEM (Figure 3.7). For this proof of concept, a GIS layer was created from the two-degree threshold and matched well with existing wetlands in the field. However, in the case of this research, a binary layer was not used to mask out upland/wetland cases based on any particular threshold. Rather, the information found inside the training areas directed the classification.
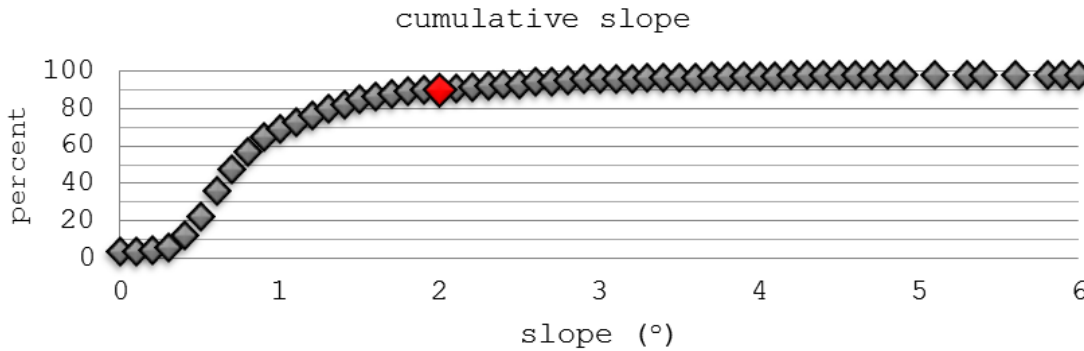
Figure 3.7: Cumulative slope inside Nova Scotia government inventory wetlands. The red diamond indicates 2° slope which 90% of the area of Nova Scotia Wetland Inventory polygons is equal to or under.

Errors in DEMs have been shown to be clearly correlated with terrain slope with the most significant occurring in the steepest part of the study area (Castrignano, Buttafuoco, Comolli and Ballabio 2006). A counterpart problem also exists in flatter regions because although the accuracy is better, there is a limit to calculating a reliable minimum slope value. Work was done in Ontario where it was determined that slope could be considered accurate above 0.12 degrees (Ontario Ministry of Natural Resources 2007). The value of two degrees used in the preliminary testing is easily above the flat accuracy limit.

The CTI shows wetter areas using slope combined with where water is predicted to accumulate (Wilson and Gallant 2000). CTI was calculated as the natural log of the upland contributing area (a) divided by the tan of the slope (beta).

CTI = ln(a / (tan (beta)))   (2)

where:

- a = [(flow accumulation + 1) * (cell size)]
- beta = slope in radians

As an input to CTI, flow accumulation was derived using the D8 single flow method because it is better at delineating channels (Wilson and Gallant 2000). Wilson and Gallant stated that though multiple flow methods show a more realistic flow over slopes, the dispersion this algorithm causes in valleys (where wetlands often are) may not be suitable. It was assumed

that variants in the flow calculation would not be important enough to test, but it may be worthwhile to address in future wetland mapping studies.

CRV is a second derivative of the DEM and was used with the intention of showing deceleration (or acceleration) of water runoff. It has also been used to show convergence or divergence of flow (Moore, Grayson and Ladson 1991). This tool was implemented in ArcGIS® software.

The CHM was constructed to show a generalized characterization of local tree height (Figure 3.8). Vegetation height could then be used to categorize areas based on canopy height (e.g. grass, shrub, trees). Canopy characteristics can provide further interpretation information helpful in wetland identification. To create the CHM, original lidar data in ASCII files (ground and first return) were converted to the binary, public file format *LAS* in ArcGIS® and then converted to ESRI Grid format for analysis. In this case, IDW was not used because IDW interpolation resulted in small artifacts in the CHM that resulted from the unequal distribution of ground points and first points (e.g. when fewer ground points are obtained in dense vegetation compared to first return points). Instead, the LAS point files were converted directly to a grid using *LAS point-to-grid*. A binning option, which selected the maximum elevation value of points within the grid cell resolution and did not fill voids, was used to define the cell value. Finally, the difference between ground and first return was calculated to produce the CHM output grid. The CHM was classified using the numerical categories indicated in Table 3.1 based on a definition found in the Ontario Wetland Evaluation System (OWES) Southern Manual (Ontario Ministry of Natural Resources 2014). Height class was calculated based on using a majority filter using a five-cell kernel as a way to characterize the general canopy type in a 100 m^2 area. Gaps were filled using the expand tool in ArcGIS®.

Table 3.1: Classification of vegetation height (OWES).

Class	Height (m)	Description
1	0.00 – 0.30	low or absent vegetation
2	0.31 – 1.00	low shrub or taller grass/sedge/etc.
3	1.01 – 2.00	medium shrub or taller grass/sedge/etc.
4	2.01 – 6.00	tall shrub
5	> 6.01	tree
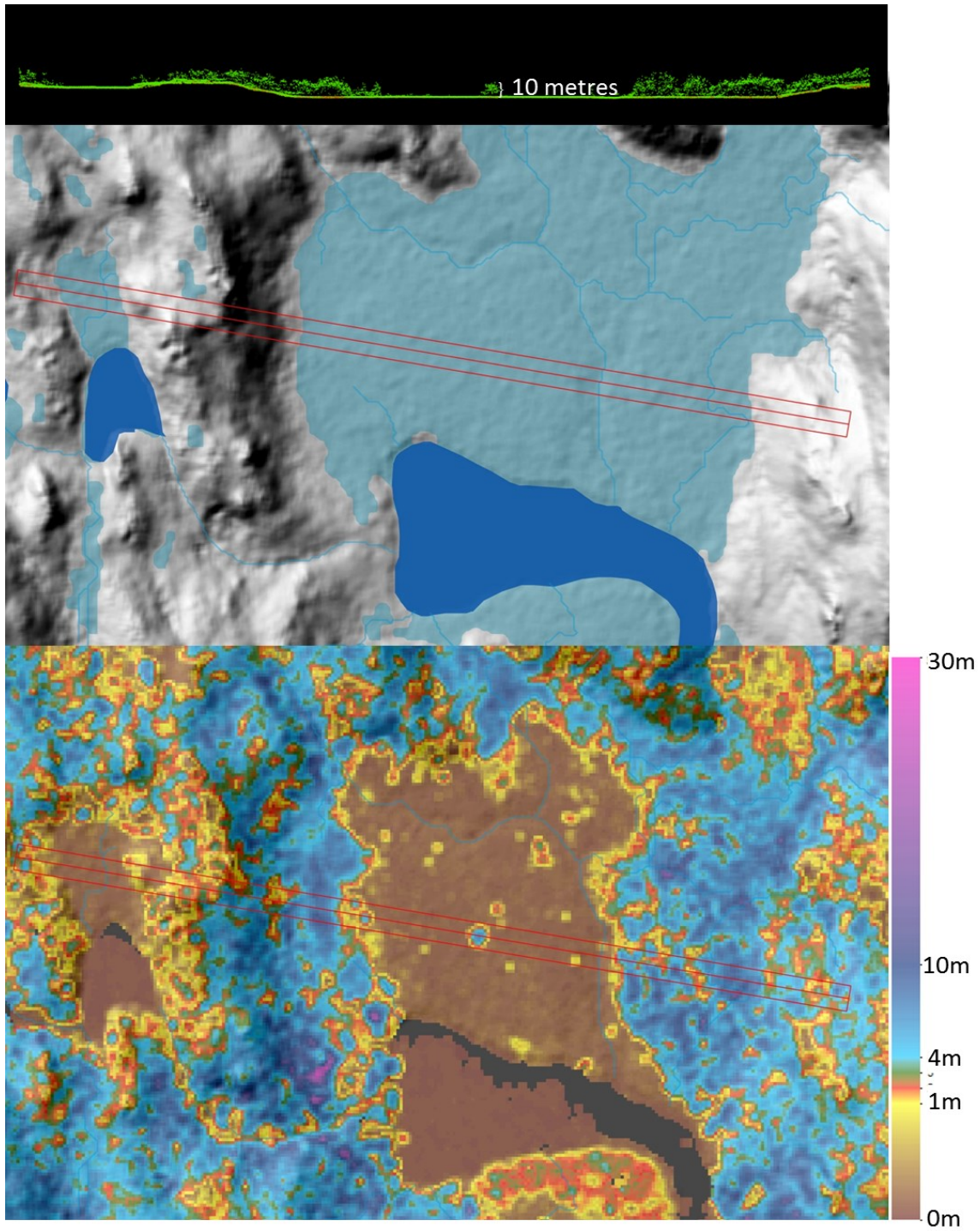
Figure 3.8: Canopy height overlayed on shaded relief.

3.2.3 Optical Imagery Processing in Preparation for Classification

QuickBird imagery was acquired by Halifax Regional Municipality already orthorectified but otherwise in raw format (2.4 m resolution, 11 bit multispectral data stored in 16 bit channels). It was corrected for certain atmospheric conditions in PCI Geomatica (2015) by calculating the top of atmosphere (TOA) reflectance (Krause 2003; GRASS-Wiki 2015) using calibration parameters and metadata. Parameters specifying sensor and bands, sun position, acquisition date, and calibration coefficients were all that was necessary to initiate the workflow, unlike correcting for the apparent surface reflectance which will account for atmospheric conditions during image acquisition. The output in PIX format was used as a direct input to the Random Forests (RF) Classification. Landsat 8 imagery was acquired from October 6, 2013 using the United States Geological Survey (USGS) EarthExplorer web application for the medium resolution phase of the thesis. This date was chosen to be consistent with the QuickBird acquisition season. The 30 metre resolution multi-spectral (8 bit) data were also corrected for top-of-atmosphere reflectance in PCI Geomatica, in preparation for input to the RF Classification.

Most of the image processing was performed in PCI Geomatica 2014®. The QuickBird imagery digital numbers were converted to reflectance values using the top of atmosphere (TOA) reflectances procedure (Krause 2003; GRASS-Wiki 2015). First the top of atmosphere spectral radiance is calculated by:

$$L_{\lambda pixel,band} = \frac{\kappa_{band} * q_{pixel,band}}{\Delta \lambda_{band}} \tag{3}$$

where:

- $L_{\lambda pixel,band}$ = top of atmosphere spectral radiance image pixels [W/(m^2*sr*μm)]
- κ_{band} = absolute radiometric calibration factor [W/(m^2*sr*count)] for a given band
- $q_{pixel,band}$ = radiometrically corrected image pixel
- $\Delta \lambda_{band}$ = effective bandwidth for a given band [μm]

Then the top of atmosphere spectral radiance is used for computing the top of atmosphere reflectance by:

$$\rho = \frac{\pi * L_\lambda * d^2}{E_{sun}\lambda * \cos(\Theta_s)} \qquad (4)$$

- ρ = unitless reflectance

- π = 3.14159265358

- L_λ = spectral radiance at the sensor's aperture [W/(m²*sr*µm)]

- d = Earth/Sun distance in astronomical units (AU), interpolated

- E_{sun} = mean solar exoatmospheric irradiance (W/m²/µm)

- $\cos(\theta_s)$ = cosine of the solar zenith angle from the image's metadata (θ_s 52.26285°)

The values used for κ_{band}, E_{sun} and $\Delta\lambda_{band}$ are given in Table 3.2.

Table 3.2: Values of the three parameters used in the Top of Atmosphere reflectance calculation procedure.

Band	E_{sun} [W/m²/µm]	κ_{band} [W/(m²*sr*count)]	$\Delta\lambda_{band}$ [µm]
Blue	1924.59	0.01604120	0.068
Green	1843.08	0.01438470	0.099
Red	1574.77	0.01267350	0.071
NIR	1113.71	0.01542420	0.114

The Landsat 8 imagery digital numbers were converted to reflectance values using the following top of atmosphere (TOA) reflectances procedure (USGS 2015).

$$\rho\lambda' = M_p Q_{cal} + A_p \qquad (5)$$

where:

- $\rho\lambda'$ = TOA planetary reflectance, without correction for solar angle.
- M_ρ = Band-specific multiplicative rescaling factor from the metadata.
- A_ρ = Band-specific additive rescaling factor from the metadata.
- Q_{cal} = Quantized and calibrated standard product pixel values (DN)

TOA reflectance with a correction for the sun angle is then:

$$\rho\lambda \ = \frac{\rho\lambda'}{\sin(\theta_{SE})} \tag{6}$$

where:

- $\rho\lambda$ = TOA planetary reflectance
- θ_{SE} = Local sun elevation angle provided in the metadata (degrees).
- θ_{SZ} = Local solar zenith angle; $\theta_{SZ} = 90° - \theta_{SE}$ (degrees)

In the case of my Landsat 8 image the following parameters were true for each input band:

- $M_\rho = 0.00002$
- $A_\rho = -0.1$
- $\sin(\theta_{SE}) = 0.62086717793576761544947288739661$

3.2.4 PolSAR

The RADARSAT-2 PolSAR images were provided through the Science and Operational Applications Research Education (SOAR-E) program of the Canadian Space Agency. They were acquired using two fine quad-pol beam modes (FQ6 and FQ30), and a descending (D) orbit. The FQ6 beam mode corresponds to incident angles ranging from 24.6° to 26.4°. The FQ30 beam mode corresponds to incident angles ranging from 47.5° to 48.7°. The images were acquired during the descending orbit, so they were west-looking and acquired early morning. Both beam mode SAR images were acquired in April, when the water level was high in the wetlands and in August-September, when the water level was low (Table 3.3). In addition, the low-water-level images were acquired under dry conditions, while the high-water-level images were acquired under wet conditions.

Table 3.3: Characteristics of the RADARSAT-2 PolSAR images used.

Date	Beam Mode	Water Level	Precipitation (mm) (*)
August 19, 2010	FQ30	low	0
September 1, 2010	FQ6	low	0.6
April 5, 2013	FQ30	high	17.4
April 18, 2013	FQ6	high	16.1

* *Millimetres of rain equivalent recorded at the Shearwater RCS weather station during the six days prior to image acquisition.* (Government of Canada 2015)

The RADARSAT-2 Acquisition Planning Tool (APT) was used to make an independent selection and that choice was submitted to the Canadian Space Agency which managed the data request and subsequently made them available for retrieval. When there was a conflict with another party, a request was made for priority if the other was not urgent. However, in the end, nine fine quad polarized scenes were acquired over the period from August 2010 to April 2013 during spring, summer and fall.

Of the nine original images acquired, seven were collected in descending mode (morning time frame) and two in ascending mode (afternoon). A morning time frame was considered the better choice before solar insolation affected the soil moisture condition. The ascending mode images were initially intended to be used for further comparison but were set aside for a later study. Five had a steep incidence angle and four had a shallow angle; the different angles were chosen to see if this factor would have an effect on classification.

There is no stream gauge on any of the streams in the study area from which to measure water level or degree of flooding, but precipitation information from a nearby weather station (Shearwater RCS) preceding the capture date was used as a proxy to establish water level (Figure 3.9). Final selections of four PolSAR images were chosen based on the precipitation information (in addition to incidence angle). Both a steep angle and shallow incidence angle pair were acquired as close to the same date as possible for summer which was dry and a pair for spring which was wet.
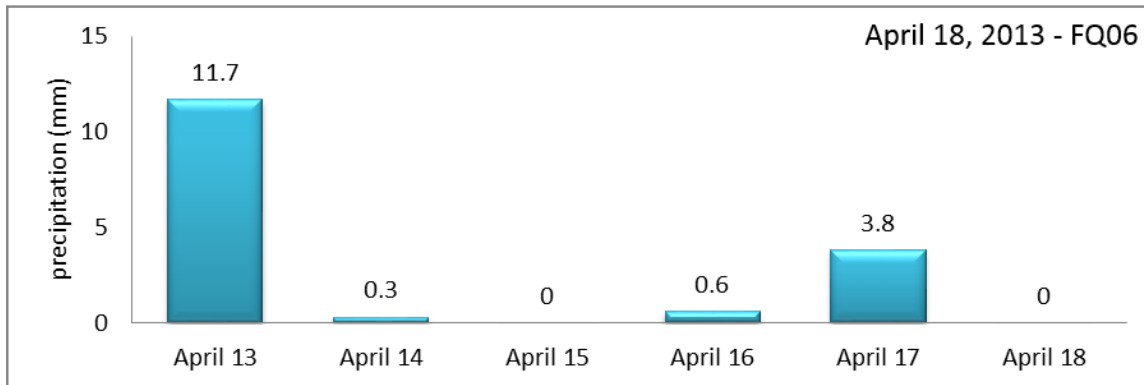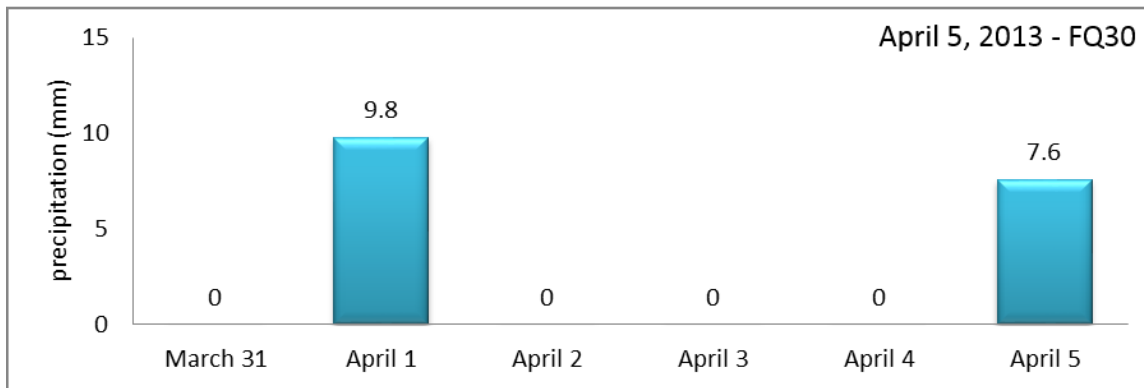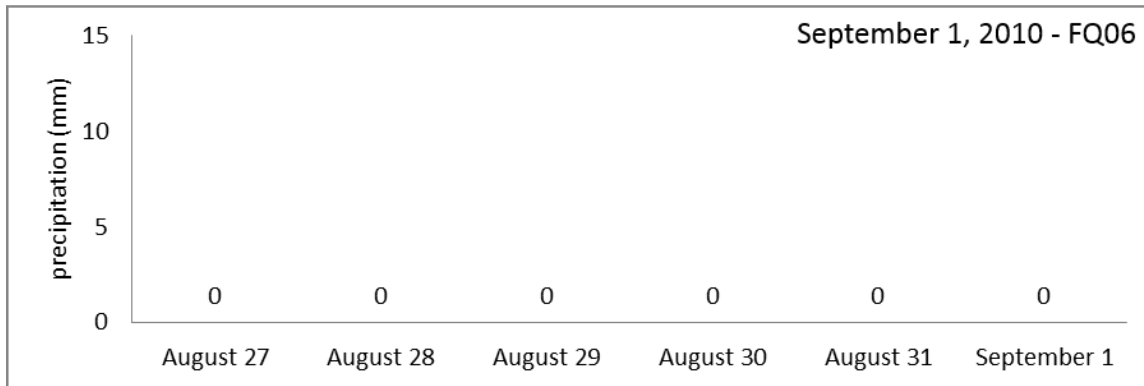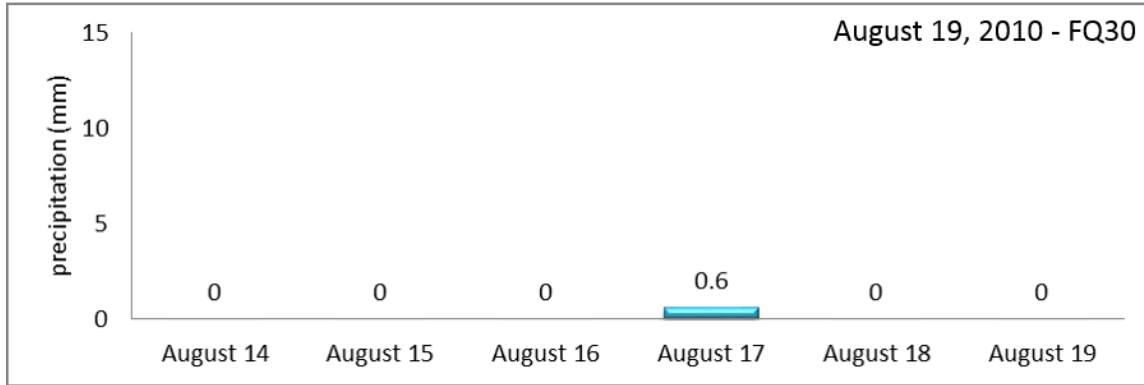
Figure 3.9: Precipitation at Shearwater RCS station (Government of Canada 2015).

All RADARSAT-2 images were received at the single-look complex processing level, meaning that the data are stored in slant range and corrected for satellite reception errors. The RADARSAT-2 PolSAR images were filtered to remove speckle, as speckle can be considered noise and its intensity must be attenuated in order to resolve fine details on SAR images (Goodman 1976). First, the HH, HV, VV, and VH intensity images were filtered using a 7x7 Lee Adaptive filter with the FLE program of PCI Geomatica 2014® (PCI Geomatica 2014). The full polarimetric SAR images were filtered by applying a 5x5 polarimetric Lee speckle filter (Lee et al. 1999) with the PSPOLFIL program of PCI Geomatica 2014®. This filter preserves polarimetric properties by filtering each element of the covariance matrix independently, while maintaining spatial information. Data for PolSAR were run through a number of algorithms designed to extract more information than what the raw channels can offer, including polarimetric variables that are listed in Table 3.4. These algorithms take advantage of the polarimetric and phase information that can be defined between bands.

Specifically, Table 3.4 shows polarimetric parameters (used to differentiate scatterers of different types on the ground), and polarimetric discriminators based on polarimetric synthesis (used for feature characterization because they can identify different types of scattering mechanisms for fully polarized SAR data) (Touzi et al. 1992). Finally, polarimetric variables from three decomposition methods are listed. The Touzi Decomposition was applied using the PSTOUZIDEC algorithm in PCI Geomatica. Work on the analysis of polarized radar data has led to some techniques that can be applied to wetland discrimination. Touzi et al. (2007) had examined existing techniques and, based on their work and a review of the literature, saw a need for an improved method that utilized parameters derived from the scattering matrix. As they have expressed, the goal of incoherent decomposition is to break down the average scattering mechanisms to associate a physical mechanism to each component (Touzi et al. 2007). In this decomposition, the phase of the symmetric scattering type is used to discriminate between wetland vegetation and forest species. So, the dominant scattering type phase with the dominant scattering eigenvalue will enhance the separation of classes, leading to a better wetland classification. The Freeman-Durden Decomposition was applied using the PSFREDUR algorithm. It divides the scene into three scattering mechanisms: rough, double bounce, and

volume. The input is a fully polarimetric dataset in an s4c matrix, but has limitations in that it is not roll-invariant. It also has difficulty in separating rough from volume scatterers (Lee et al. 2004). The Cloude-Pottier decomposition was applied using the PSEABA algorithm. Two parameters are computed: entropy, anistropy, and two angle values are computed: alpha and beta. Entropy shows the importance of one scattering mechanism compared to the other two, as well as the mixing among the three. Anistropy shows the mixing between the second and third scattering mechanism. Alpha angle shows a specific scattering mechanism for an eigen vector. Beta angle is related to the orientation angle of the scatterer and is related to terrain slope.

Table 3.4: List of polarimetric parameters used in the study.

Variable	Definition	Authors
Pedht	Pedestal height = minimum of Pr (copolarized signature)	van Zyl et al. 1987
Totpow	Total power = $|S_{hh}|^2 + 2|S_{hv}|^2 + |S_{vv}|^2$	Lopez-Martinez et al. 2005
γ	correlation coefficient $\gamma = S_{hh}S_{vv}/(|S_{hh}|^2 |S_{vv}|^2)^{1/2}$	Rodriguez and Martin 1992
δ_{HH-VV}	Phase difference	Lopez-Martinez et al. 2005
Pr_{max}	Maximum of the received power	Touzi et al. 1992
Pr_{min}	Minimum of the received power	Touzi et al. 1992
FP	Fractional polarisation = $Pr_{max} - Pr_{min} / Pr_{max} + Pr_{min}$	Zebker et al. 1987
CV	Coefficient of Variation = Pr_{min} / Pr_{max}	van Zyl et al. 1987
S_{max}	Maximum of the scattered intensity	Evans et al. 1988
S_{min}	Minimum of the scattered intensity	Evans et al. 1988
ND	Normalized Difference $ND_s = S_{max} - S_{min} / S_{max} + S_{min}$	Evans et al. 1988
d_{max}	Maximum of the degree of polarization	Touzi et al. 1992
d_{min}	Minimum of the degree of polarization	Touzi et al. 1992
Δd	$d_{max} - d_{min}$	Touzi et al. 1992
α_s	Magnitude of the symmetric scattering	Touzi 2007
$\Phi_{\alpha s}$	Phase of the symmetric scattering	Touzi 2007
ψ	Maximum polarization parameter for orientation	Touzi 2007
τ_m	Maximum polarization parameter for helicity	Touzi 2007
m	Maximum polarization parameter for return	Touzi 2007
FD dbl	Power related to double-bounce scattering	Freeman and Durden 1998
FD surf	Power related to surface scattering	Freeman and Durden 1998
FD vol	Power related to volume scattering	Freeman and Durden 1998
CP H	Entropy $(H) = \sum_{i=3}^{3} -p_i \, log_3(p_i)$	Cloude and Pottier 1997
CP A	Anistropy $(A) = \frac{\lambda_2 - \lambda_3}{\lambda_2 + \lambda_3}$	Cloude and Pottier 1997
CP α	Alpha angle $(\overline{\alpha}) = \sum_{i=3}^{3} \rho_i \, \alpha_i$	Cloude and Pottier 1997
CP β	Beta angle $(\beta) = 2 *$ orientation angle (ψ)	Cloude and Pottier 1997

Both the intensity and polarimetric products, with orbital information (i.e.

georeferencing) transferred from the original file, were orthorectified with PCI Geomatica

Orthoengine using the Radar Satellite Math Modelling method, with the Rational Function

extracted from the image. A resampled lidar DEM was used as input to correct for terrain

variation. Ground control points (GCPs) can be used for the purpose of geocorrection but the Rational Function available in the Radar Satellite Math Modelling method (which extracts information from the image) produced far better results in my study area. According to Woodhouse (2006), GCPs are not necessarily appropriate to use because of the localized effect of topography. To confirm the accuracy of the orthorectification, a visual comparison was made with basemap vector data (i.e. lake and ocean coastline), and a large corner reflector placed at the edge of a wetland before a final image was collected (Figure 3.10). The corner reflector's position was recorded by averaging a GPS signal from a handheld Garmin GPS receiver. In addition, check points were used to test the orthorectification of an image and resulted in a root mean square value to quantify the error.

Figure 3.10: A radar reflector was set up at an open wetland transitioning into treed to assess positional accuracy.

3.3 Experimental Design

3.3.1 Choice of Landcover Classes

Twelve classes (Table 3.5) were chosen to represent the land cover namely: barren, grass, industrial, lake, open-water/marsh complex, open bog, open fen, shrub/treed fen/bog, swamp, upland sparse vegetation, upland forest, and urban. The wetland classes were based on the Canadian Wetland Classification System (Warner and Rubec 1997). The upland classes were chosen mainly to provide differentiation from the wetlands.

Table 3.5: Mapping legend showing classes used for the classification process along with the description from Canadian Wetland Classification System that was used to help identify landcover classes in the field.

Class colour	Class ID and name	Description
	1 - barren	area with more than 50% exposed rock outcrop and less than 25% vegetation.
	2 - grass	area of manicured grass such as recreation fields and golf courses.
	3 - industrial	built-up areas consisting of large, low-rise industrial buildings and parking lots.
	4 - lake	deeper water with no apparent vegetation.
	5 – open-water/ marsh complex	combination of open-water wetland and shallow marsh. Marshes have shallow water levels that can fluctuate daily and expose the soil. Shallow or open-water wetlands have water depths up to 2 m that are typically stable, but soil may occasionally become exposed.
	6 - open bog	ombrotrophic peatland area with primarily ericaceous plants and sphagnum, and less than 25% tree coverage. They have a raised or level surface and are not affected by runoff or ground water.
	7 - open fen	minerotrophic peatland with ericaceous plants, sedges and brown mosses and less than 25% tree coverage. The ground and surface water movement is more stable, and exposed water in channels can form characteristic patterns.
	8 – shrub/treed fen/bog	peatland with more than 25% tree coverage. Treed fens and bogs are not easily differentiated and so are combined for this research.
	9 - swamp	wetlands dominated by trees (typically > 30% cover) that are influenced by minerotrophic groundwater. They can be found on either mineral or peat soils and are typically considered the driest wetland type.
	10 - upland sparse vegetation	area with less than 50% exposed rock outcrop. vegetation primarily low and ericaceous.
	11 - upland forest	forested stand containing trees at least 3m in height.
	12 - urban	built-up areas consisting of high-rise urban core buildings, streets and sidewalks.

The selection of the twelve classes was made to accommodate each wetland class

described by the Canadian Wetland Classification System (Warner and Rubec 1997), with the

exception of the open-water/marsh complex described above. This differs from some other studies which use more generic terms or specific types of vegetation (Brisco et al. 2011, Corcoran et al. 2011, Corcoran et al. 2013). It was not initially known if the input data and the classification process could support the distinction between wetland classes; however, the method allows for comparison of misclassified results to see if the next important class is in fact close. Following McCoy (2005), spectral clusters may be combined afterwards (e.g. industrial + urban = anthropogenic) to create a more generic class. Alternatively, there may be a desire to have two information categories (e.g. open-water and shallow marsh) even if they are not spectrally discernable. While training sites may initially be kept separate, the resulting information classes are combined into one "complex".

3.3.2 Field Data

A stratified purposive sampling approach was used to select training areas and validation sites. A stratified approach is important because of the differing total areas of classes. Though purposive sampling is prone to bias, this method was much more practical in terms of access for site visits (McCoy 2005). A random method without regard to the thematic classes is not appropriate, as some classes are more abundant than others. This could lead to an over-representation of the abundant classes, as well as ignoring rare events (Congalton and Green 1999).

During low water levels in the wetlands mostly in the period from August to September 2012, 1159 points were observed and recorded from sites visited. Site visits were planned to cover as much of the study area as possible (Figure 3.11), especially ensuring that the different types of soil drainage mapped by the Ecological Land Classification (ELC) were covered. Field work was carried out during times when vegetation had not yet senesced so that vegetation could assist in identifying wetlands and non-wetland areas. Among all the visited sites, of which 1159 were recorded, 240 points (137 wetland) were the validation sites that were used to assess the mapping accuracy for each classified image (Table 3.6). The remaining observations were available to delineate training areas for the image classification. Of these, 318 points (170 wetland) were used to create 237 polygons that were used to train the classification process

(Table 3.6). All the sites were selected according to the following criteria: (1) accessibility by road or path; (2) relatively large extent of the related land cover.
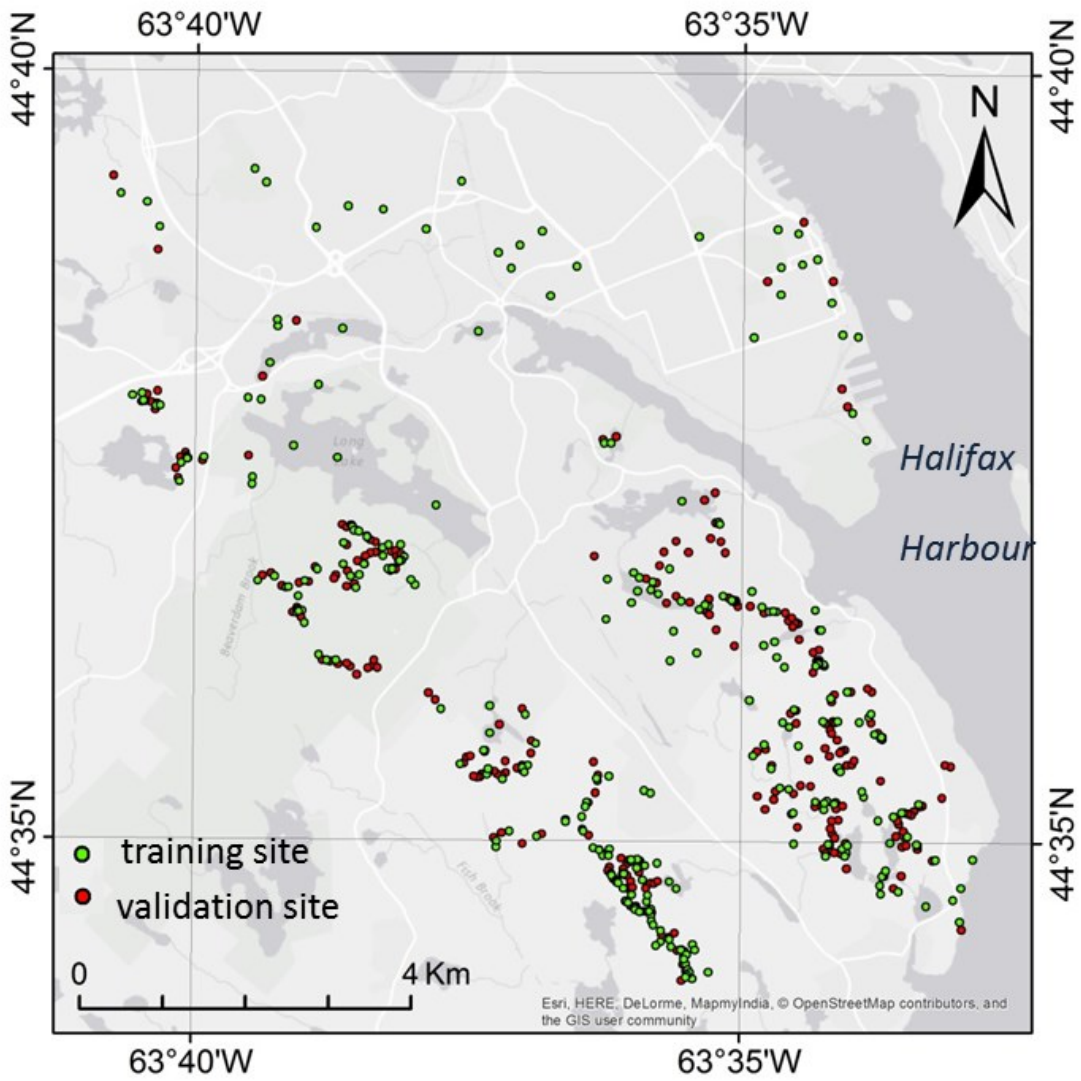
Figure 3.11: Training sites and validation sites of the twelve classes used.

Table 3.6: Number of training sites and validation sites for each class.

Landcover Class	Training Sites (318 points)	GPS Sites (240 points)
barren	19	12
grass	16	3
industrial	10	4
lake	14	6
open-water/marsh complex	12	6
open bog	22	19
open fen	32	30
shrub/treed fen/bog	52	24
swamp	38	52
upland - sparse vegetation	63	34
upland forest	33	47
urban	7	3

Among all the visited sites, 287 sites (170 training sites and 137 validation sites) were considered as being wetland (Table 3.4). Sites were identified as a wetland, such as in Tiner (1999), when the water table is close to (less than 10 cm) or at the surface, or when I found indicator plants, soil hydromorphy, or other evidence of an area that is often saturated with water. Several of the wetland sites were initially found by interpretation of aerial photographs and the slope model, or because they had been previously mapped as wetland on the DNR map currently in use by the Government of Nova Scotia (Figure 3.12).
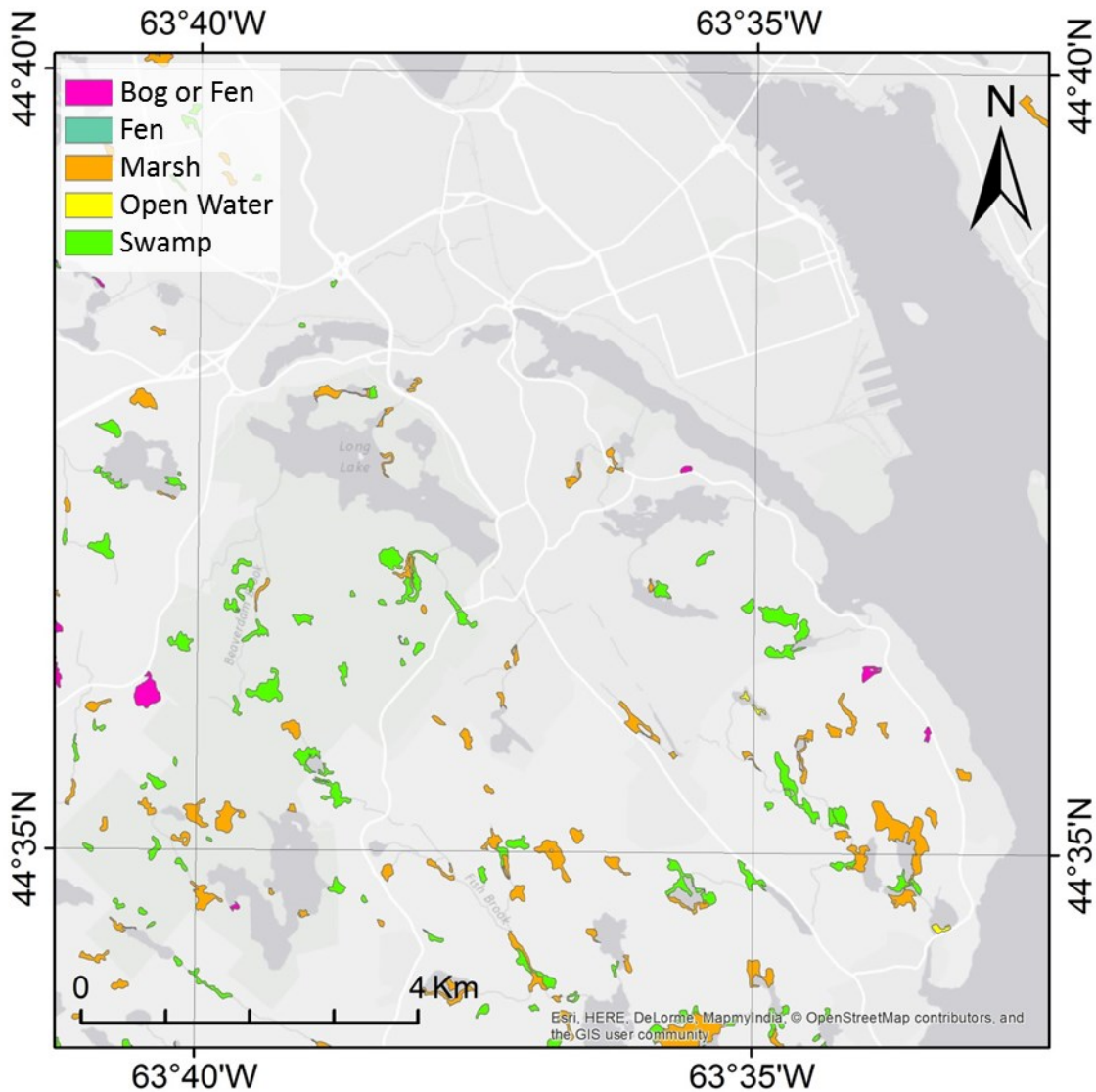
Figure 3.12: Nova Scotia DNR map of the study area.

Planned wetland transects and routes between destinations were not always followed because of the rough terrain or dense vegetation. Custom maps showing trails and a low-slope mask (less than 2°) created from the lidar DEM were made in Mapwel software and uploaded to a Garmin 60cx GPS receiver. On arrival in the field, a GPS fix was acquired and the time on the camera was synchronized with the GPS clock so that the photographs could be geocoded in the lab using GeoSetter software. A compass was used to identify bearing on photos if important and a 1:50,000 topographic paper map (NTS 011D12) was used to aid navigation. In the field, a special effort was made to visit the following sites: sites that represent the transition

between upland and wetland, sites that did not match the low-slope mask, and sites along the route which confirmed the low-slope mask. On each site, the following measurements were made: GPS location, elevation, class identification based on the descriptions in Table 3.5, and ground photographs taken such as those of Figure 3.13.

Figure 3.13: Photographs of typical wetland classes found in the study area.

3.3.3   Input Data Combinations

A prerequisite to the multi-criteria classification stage was to choose which RADARSAT-2 images to use. Of the nine scenes acquired, only four were selected to represent low-water (summer) and high-water (spring) conditions. This initial step required that a classification be run on each image alone using dual polarimetric bands and repeated for various combinations of date and incidence angle. The overall accuracy of each result was compared and the best combination was chosen: in this way it was determined that the best way to proceed with remaining classification was using all four images together.

Two main studies were conducted based on input image resolution with the four RADARSAT-2 image set used in both. The addition of fine resolution optical imagery (QuickBird)

and elevation (lidar DEM) was the basis for the first study, and the addition of medium resolution optical (Landsat 8) and elevation (NS DEM) for the second. The various groupings were necessary to determine the influence of each input on the final accuracy. Altogether, ten combinations were run as listed in Table 3.7.

Table 3.7: List of combinations used for each of the ten classification results.

	resolution (metres)	RADARSAT-2 dual-polarized	RADARSAT-2 Polarimetric Variables plus Intensity	Optical Imagery	Terrain Derivatives
1	8			✓	✓
2	8	✓			
3	8	✓			✓
4	8	✓		✓	✓
5	8		✓		
6	8		✓		✓
7	8		✓	✓	✓
8	30			✓	✓
9	30	✓		✓	✓
10	30		✓	✓	✓

3.4   Data Analysis and Reporting

The primary objective of this thesis was to map wetlands using various combinations of data. Differences are expected and explained by a number of reasons based on input characteristics such as resolution (spatial, spectral, radiometric, and temporal). Before these factors can be compared it was necessary to assess the reliability of the data. The optical and SAR inputs have been extensively tested and calibrated, however no information was found to indicate accuracy of the NS DEM. Tests of DEM accuracy were fairly simple but were a necessary first step to start explaining the differences in results.

3.4.1   Wetland Mapping

A nonparametric classification approach was chosen because of the differing nature of the input data to model. A technique that did not rely on data following any particular distribution was needed. The Random Forests classifier was selected because it is able to accommodate many layers of input bands including those from different types of data. So it is acceptable that multi-temporal SAR imagery is used (Waske, Heinzel, Braun, and Menz 2007),

along with optical imagery and with elevation derivatives (Van Beijma, Comber and Lamb 2014). For instance, Van Beijma, Comber, and Lamb (2014) found that Random Forests models were highly effective in classifying salt-marsh vegetation habitats and I anticipated that it would also work well for wetland differentiation in Nova Scotia.

The RF algorithm, built by Leo Breiman and Adele Cutler, takes advantage of tree learning and promising error rates with good noise handling (Breiman 2001). RF creates multiple trees and settles on the best class from each iteration (Figure 3.14) through a voting process. Used as a classifier, it is run in the R Statistical Programming interface where variable importance is output along with a classification.
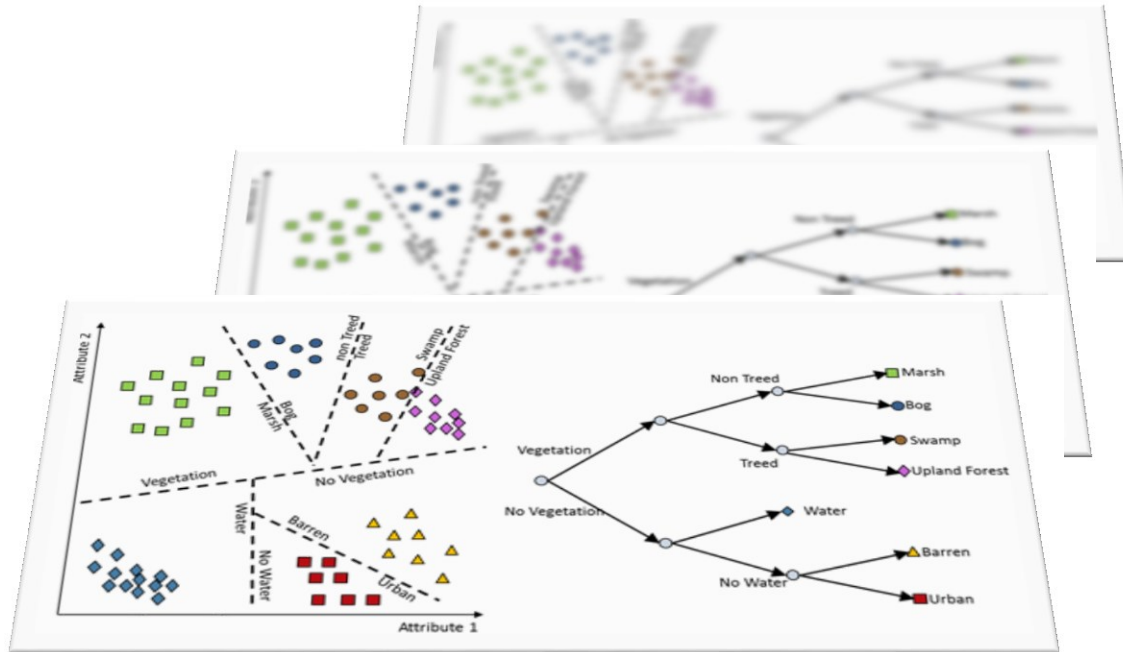
Figure 3.14: Conceptual schematic of Random Forests Classifier (adapted from SAR-EDU remote sensing education initiative).

RF follows an ensemble classification practice, which is a method of combining multiple classifiers into one, and results in a generally more accurate outcome (Maclin and Opitz 2011). It works by using many decision trees to create a predictive model based on observation of the

input data; and each tree contributes a vote that can be tallied into a particular classification (Breiman and Cutler nd).

Classification accuracy was measured first using a confusion matrix (or error matrix), where training areas are compared to the equivalent land cover in the classified map. Each cell in the matrix shows the number of pixels classified compared to a particular class as defined by the training areas (Congalton 1991). The matrix computes individual class User's and Producer's accuracies and their related error of omission and commission as described in Congalton (1991). The User's accuracy identifies the probability that a pixel from the classification map is in the right class, plus the associated number of pixels misclassified to the wrong class (error of omission). The Producer's accuracy corresponds to the probability that a reference pixel is well classified, and the associated number of misclassified pixels that actually belong to another class (error of commission).

The best combination of input images was selected based on the highest overall accuracy that visually represents a suitable map. However, this method only gives an assessment of the classified image accuracy, which is different from the true mapping accuracy. An independent accuracy assessment is more robust and compares the resulting classified map with an independent set of field observation data acquired over the validation sites which are points recorded with GPS coordinates. Each validation site was compared to the classified map, and the map is considered to be correct. These comparisons were tabulated to produce the percentage of correct identifications computed as a function of the total number of wetland validation sites. A confusion matrix was not calculated because only wetland classes were used and some misidentification is due to confusion with non-wetland classes.

Finally, a visual assessment is qualitatively undertaken based on visual interpretation, context, and expert knowledge. Though this method is subjective, it is valuable to assess the overall look of the resulting map and to pick out examples of successful or unsuccessful results which will give insight into the process.

3.4.2 Analysis for comparing the NS DEM and the Lidar DEM

Aside from wetland classification, further analysis was needed to compare the elevation datasets. Based on anecdotal evidence, the NS DEM is not an accurate model of the terrain.

Even at its intended scale of 1:20,000 it has visual discrepancies compared to other data. However, because the purpose of the DEM in this thesis is to model the shape of the terrain and not the elevation value, the NS DEM may still be able to function to show where water will flow and accumulate. The assessment of how well it can model water flow is based on relative accuracy. This was measured by comparing elevation values, as well as one derivative (namely slope) of the NS DEM and the lidar DEM (which is assumed to be the benchmark at this stage).

Firstly, part of the Nova Scotia Coordinate Referencing System (NSCRS) infrastructure maintains survey markers recorded with a very accurate position and elevation value. These points were compared in a GIS to the lidar DEM and the NS DEM. Though some survey markers are unreliable according to staff at Service Nova Scotia and Municipal Relations (personal communication 2015), there are enough to conduct a reliable root-mean-squared error (RMSE). The RMSE will give an indication of the error of the predicted elevation data (the DEMs) by aggregating the magnitude of error made up of the difference in elevation at each survey marker. This error, referred to in this thesis as *absolute error*, is compared to a precise vertical datum used for the survey markers (i.e. orthometric height).

Secondly, two other tests were conducted to determine relative accuracy of the NS DEM compared to the lidar DEM. These comparisons were done mainly to help provide an explanation to differences anticipated in the wetland mapping classification accuracy assessments, and to see if the NS DEM could be used if lidar is not available.

For the first test of relative accuracy, lidar DEM values were extracted for each NSTDB elevation point (from which the NS DEM was interpolated) and the differences in elevation were displayed on a map in order to visually determine if there were systematic errors. Systematic errors can result from miscalibrated equipment or other operator error. If there is an error, the assumption that relative accuracy (i.e. elevation accuracy of a point compared to surrounding points in close proximity) is good will be adopted for the analysis in Chapter 4 if the errors are broad and generally clustered together. This would mean that the local terrain morphology is accurate enough so that the coarser NS DEM can still help predict wetland location. For the second test of relative accuracy, additional information to quantify the difference was done by comparing the slope value of the NS DEM against the slope value of the

lidar DEM using a cross tabulation analysis in SPSS Statistics software (IBM 2015). Slope was chosen since it is a straightforward calculation involving a small neighbourhood of pixels.

3.5   References

Breiman, L. 2001. "Random Forest". *Machine Learning*, Vol. 45, No. 1, pp. 5-32.

Breiman, L., and Cutler, A. nd. Random Forests*.* Retrieved from https://www.stat.berkeley.edu/~breiman/RandomForests/cc_home.htm

Brisco, B., Kapfer, M., Hirose T., Tedford, B., and Liu, J. 2011. "Evaluation of C-band polarization diversity and polarimetry for wetland mapping." *Canadian Journal of Remote Sensing*, Vol. 37, pp. 82-92.

Canada Committee on Ecological (Biophysical) Land Classification. 1988. "Wetlands of Canada." Ottawa: Sustainable Development Branch, Canadian Wildlife Service, Conservation and Protection, Environment Canada. pp. 1-61.

Castrignano, A., Buttafuoco, G., Comolli, R., and Ballabio, C. 2006. "Accuracy assessment of digital elevation model using stochastic simulation." *Proceedings of the 7th International Symposium on Spatial Accuracy Assessment in Natural Resources and Environmental Sciences.* pp. 490–498.

Cloude, S., and Pottier, E. 1997. "An entropy based classification scheme for land applications of polarimetric SAR." *IEEE Transactions on Geoscience and Remote Sensing*, Vol. 35, No. 1, pp. 68-78.

Congalton, R. 1991. "A review of assessing the accuracy of classifications of remotely sensed data." *Remote Sensing of Environment*, Vol. 37, pp. 35–46.

Congalton, R.G., and Green, K. 1999. "Sample Design. In Assessing the accuracy of remotely sensed data: principles and practices." New York, NY, USA: CRC Press Inc. pp. 17-25.

Cooley, S. 2015. "Terrain Roughness." Retrieved July 5, 2014 from http://gis4geomorphology.com/roughness-topographic-position/

Corcoran, J. M., Knight, J. F., Brisco, B., Kaya, S., Cull, A., and Murnagahn, K. 2011. "The integration of optical, topographic, and radar data for wetland mapping in Northern Minnesota." *Canadian Journal of Remote Sensing*, Vol. 37, No. 5, pp. 564-582.

Corcoran, J. M., Knight, J. F., and Gallant, A. L. 2013. "Influence of multi-source and multi-temporal remotely sensed and ancillary data on the accuracy of Random Forest classification of wetlands in Northern Minnesota." *Remote Sensing*, Vol. 5, No. 7, pp. 3212-3238.

Ehlers, J., and Gibbard, P. L. 2004. "*Quaternary glaciations: Extent and chronology*." Amsterdam, Netherlands: Elsevier. GIS data retrieved from http://booksite.elsevier.com/9780444534477/digital_maps.php

ESRI [Computer software]. 2015. Retrieved from http://www.esri.com

Evans, D.L., Farr, T.G., van Zyl, J.J., and Zebker, H.A. 1988. "Radar polarimetry: Analysis tools and applications." *IEEE Transactions on Geoscience and Remote Sensing*, Vol. 26, No. 6, pp. 774-789.

Freeman, A., and Durden, S. 1998. "A three-component scattering model for polarimetric SAR data." *IEEE Transactions on Geoscience and Remote Sensing*, Vol. 36, No. 3, pp. 963-973.

Goodman, J. W. 1976. "Some fundamental properties of speckles." Journal of the Optical Society of America, Vol. 66, No. 11, pp. 1145-1150.

Government of Canada. 2015. "Climate Data. Shearwater RCS, Environment Canada." Retrieved from http://climate.weather.gc.ca/index_e.html

GRASS-Wiki. 2015. "QuickBird." Retrieved from https://grasswiki.osgeo.org/wiki/QuickBird

Hill, N, and Patriquin, D. 2014. "Ecological Assessment of the Plant Communities of the Williams Lake Backlands." Retrieved from Williams Lake Conservation Company: http://www.williamslakecc.org/documents/WLBFinalRep12Feb2014.pdf pp. 1-83.

IBM SPSS Statistics [Computer software]. 2015. Retrieved from http://www-01.ibm.com/software/analytics/spss/

Jennes, J. 2002. "Topographic Position Index." Retrieved May 1, 2014 from http://www.jennessent.com/downloads/tpi_documentation_online.pdf/

Krause, K. 2003. "Radiance Conversion of QuickBird Data – Technical Note." Retrieved from: https://apollomapping.com/wp-content/user_uploads/2011/09/Radiance_Conversion_of_QuickBird_Data.pdf

Lee, J.S., Grunes, M.R., Ainsworth, TL., Du, LJ., and Schuler, DL. 1999. "Unsupervised classification using polarimetric decomposition and the complex Wishart classifier." *IEEE Transactions on Geoscience and Remote Sensing*, Vol. 37, No. 5, pp. 2249-2258.

Lee, J.S., Pottier, G., and Ferro-Famil, L. 2004. "Unsupervised terrain classification preserving polarimetric scattering characteristics." *IEEE Transactions on Geoscience and Remote Sensing*, Vol. 42, No. 4, pp. 722-731.

Lopez-Martinez, C., Pottier, E., and Cloude, S.R. 2005. "Statistical assessment of eigenvector-based target decomposition theorems in radar polarimetry." *IEEE Transactions on Geoscience and Remote Sensing*, Vol. 43, No. 9, pp. 2058-2074.

Maclin, R., and Opitz, D. 2011. "Popular Ensemble Methods: An Empirical Study." *Journal Of Artificial Intelligence Research*, Vol. 11, pp. 169-198.

McCoy, R. 2005. *Field methods in remote sensing*. New York, NY, USA: Guilford Press.

Monette, S. and Hopkinson, C. 2010. "Development of an Urban Forest Canopy Model for input into a Lidar-based Storm Water Runoff Model for Halifax Harbour Watersheds." Retrieved from http://atlanticadaptation.ca/sites/discoveryspace.upei.ca.acasa/files/HRM%20Forest%20Canopy%20Final%20Report_0.pdf

Moore, Grayson, and Ladson. 1991. "Digital terrain modelling: A review of hydrological, geomorphological, and biological applications." *Hydrological processes*, Vol. 5, No. 1, pp. 3-30.

Neily, P. D., Quiget, E., Benjamin, L., Stewart, B., and Duke, T. 2003. "Ecological land classification for Nova Scotia: Volume I, mapping Nova Scotia's terrestrial ecosystems." Halifax, N.S.: Nova Scotia Department of Natural Resources, Renewable Resources Branch. pp. 1-77.

Newmaster, S.G., Harris, A.G. and Kershaw, L.J. 1997. *Wetland Plants of Ontario.* Edmonton, AB, Canada: Lone Pine Publishing.

Nova Scotia Geomatics Centre. 2015. "Digital Elevation Model Specifications." Retrieved from http://www.nsgc.gov.ns.ca/mappingspecs/Specifications/Compilation/Resource_NSTDB/default.htm

Nova Scotia Museum of Natural History. 1989. "Natural History of Nova Scotia, The Dynamics of Nova Scotia's Climate." pp. 94-103. Retrieved from https://ojs.library.dal.ca/NSM/article/download/3752/3438

Ontario Ministry of Natural Resources. 2007. "Evaluation of Lidar Elevation Derivatives." Unpublished Internal Document.

Ontario Ministry of Natural Resources. 2014. "Ontario Wetland Evaluation System Southern Manual 3rd edition, version 3.3." pp. 1-284. Queen's Printer for Ontario. Retrieved from http://files.ontario.ca/environment-and-energy/parks-and-protected-areas/ontario-wetland-evaluation-system-southen-manual-2014.pdf

PCI Geomatica [Computer software]. 2014. Retrieved from http://www.pcigeomatics.com

Pielou, E. 1991. "After the Ice Age the return of life to glaciated North America." Chicago, IL, USA: University of Chicago Press.

Poff, N.L. 1996. "A hydrogeography of unregulated streams in the United States and an examination of scale-dependence in some hydrological descriptors." *Freshwater Biology.* Vol. 36, pp. 71-91.

Rodriguez, E. and Martin, J.M. 1992. "Theory and design of interferometric synthetic aperture radars." *IEE Proceedings F Radar and Signal Processing*, Vol. 139, No. 2, pp. 147-159.

Schoewe, W.H. 1951. "The Geography of Kansas: PART III. *Hydrogeography." Transactions of the Kansas Academy of Science.* Vol. 54, No. 3 , pp. 263-329.

Tiner, R.W. 1999. *Wetlands indicators: a guide to wetland identification, delineation, classification, and mapping*. Lewis Publishers, Boca Raton (Florida, USA).

Touzi, R. 2007. "Target Scattering Decomposition in Terms of Roll-Invariant Target Parameters." *IEEE Transactions on Geoscience and Remote Sensing*, Vol. 45, No. 1, pp. 73-84.

Touzi, R., Deschamps, A., and Rother, G. 2007. "Wetland Characterization using Polarimetric RADARSAT-2 Capability." *Canadian Journal of Remote Sensing*, Vol. 33, Supp. 1, pp. 56-67.

Touzi, R., Goze, S., Le Toan, T., Lopes, A., and Mougin, E. 1992. "Polarimetric discriminators for SAR images." *IEEE Transactions on Geoscience and Remote Sensing*, Vol. 30, No. 5, pp. 973-980.

van Beijma, S., Comber, A., and Lamb, A. 2014. "Random Forest classification of salt marsh vegetation habitats using quad-polarimetric airborne SAR, elevation and optical RS data." *Remote Sensing of Environment*, Vol. 149, pp. 118-129.

van Zyl, J.J., Zebker, H.A., and Elachi, C. 1987. "Imaging radar polarization signatures: Theory and observation." *Radio science*, Vol. 22, No. 4, pp. 529-543.

Warner, B.G. and Rubec, C.D.A. (Eds.). 1997. "The Canadian Wetland Classification System. (2nd edition)." National Wetlands Working Group. Wetlands Research Centre. University of Waterloo. Ontario, pp. 1-68.

Waske, B., Heinzel, V., Braun, M., and Menz, G. 2007. "Random Forests for classifying multi-temporal SAR data." *In Proceedings Envisat Symposium*, Montreux, Switzerland. April 23-27, 2007.

Wilson, J., and Gallant, J. C. 2000. *Terrain analysis: Principles and applications*. New York: Wiley.

Woodhouse, I. 2006. "*Introduction to microwave remote sensing*." Boca Raton, FL, USA: Taylor & Francis.

Zebker, H.A., van Zyl, J.J., and Held, D.N. 1987. "Imaging radar polarimetry from wave synthesis." *Journal of Geophysical Research*, Vol. 92, No. B1, pp. 683-701.

Chapter 4.   Mapping wetlands in Nova Scotia with multi-beam RADARSAT-2 Polarimetric SAR, QuickBird and Lidar data

Abstract

Wetlands were mapped in an area southwest of Halifax, Nova Scotia by classifying a combination of multi-date and multi-beam RADARSAT-2 C-band polarimetric SAR (polSAR) images with spring lidar, and fall QuickBird data using the Random Forests (RF) classifier. The resulting maps were evaluated in comparison to GPS field data collected in 2012 as well as to wetland maps currently in use by the Province of Nova Scotia, namely the Department of Natural Resources (DNR) wetland inventory map and the swamp wetland classes of the DNR forest map. The comparison with the 137 wetland validation sites I collected in situ shows that only 66.4% of the wetland sites are correctly identified using the QuickBird classified image. With the addition of variables derived from lidar, the number of correctly identified wetlands increases to 86.1%. The accuracy remained the same with the addition of RADARSAT-2 (86.1%). However, when I tested the accuracy of specific wetland classes (instead of wetland versus upland), the accuracy improved from 59.9% with only QuickBird and lidar, to 63.5% with QuickBird, lidar, and RADARSAT-2. These percentages of correctly identified wetland sites are well above the accuracy of the DNR wetland and forest maps (46.7%) using my field validation sites. For the SAR-based classifications combined with lidar and QuickBird, the majority of the misidentifications are due to wetlands not being classified in the right wetland class and much fewer being classified as a non-wetland class. For the DNR maps, about half (53.3%) of the misclassifications are field validated wetlands that are not mapped as a wetland, and the remaining half are wetland sites mapped in the wrong wetland class (37.2%).

Keywords: wetland mapping, wetlands, RADARSAT-2, lidar, QuickBird, Landsat 8, polarimetric SAR

4.1 Introduction

Wetlands are complex ecological systems and only form when processes of hydrology, geomorphology and biology work collectively to create the necessary conditions (Lynch-Stewart et al. 1996). Accurate mapping of wetlands is important to many applications (including long-term monitoring and natural resource management) so there is a need to explore methods which can help improve wetland mapping. In 2011, Nova Scotia released a wetland conservation policy implemented in part to ensure no net loss of wetlands (i.e. equal offsetting of loss using reclamation or restoration). It is a critical policy that aims to protect an essential feature of the landscape. The application of such policy requires an accurate and up-to-date mapping of the wetlands.

The current wetland map of Nova Scotia was produced by the Nova Scotia Department of Natural Resources (NSDNR) in 2004. The map provides the most recent estimates for the number, location and class of wetlands in the province. It was produced by photo-interpretation of digitized aerial photographs that were acquired in the 1980s and 1990s (Nova Scotia Environment 2009). The wetland inventory was subsequently integrated with the forest resource inventory, a geospatial dataset primarily designed to guide timber harvesting and land management activities within the province. However, a number of authors have suggested that photo-interpretation of digitized aerial photography is unreliable for the identification, delineation, and classification of wetlands (Jacobson et al. 1987; Sader et al. 1995; Hogg and Todd 2007). This is particularly true in forested regions because of errors due to dense tree cover (Hogg and Todd 2007). Such limitations also exist for satellite optical imagery that are acquired with short wavelength radiation, but not for synthetic aperture radar (SAR) imagery that is acquired with longer wavelengths that have a deeper penetration. In addition, by contrast to optical imagery, SAR images can be acquired whatever the sky conditions because the sensor transmits its own energy and is not subject to sunlight.

Single polarized SAR has been tested in Canada for mapping wetlands as part of the Canadian Wetland Inventory (Li and Chen 2005; Grenier et al. 2007; Fournier et al. 2007). Wetland classification can be improved through the use of multiple polarizations as opposed to single polarized imagery (Ozesmi and Bauer 2002; Wang et al. 1998). Indeed, multiple

polarizations can provide more information than single polarizations. The launch of fully polarimetric SAR X, C and L-band sensors (TerraSAR-X and RADARSAT-2 in 2007, and PALSAR in 2006) provides data that allow a complete description of the scattering properties because it provides the full scattering matrix. Such an advantage offers an additional opportunity to develop improved tools for mapping wetlands. These tools include polarization synthesis, polarimetric variables and polarimetric decomposition parameters. Polarimetric data have already been shown to be highly effective for wetland mapping (Touzi et al. 2007).

My study presents a method to map wetlands by applying the non-parametric classifier Random Forests (RF), to a combination of RADARSAT-2 C-band polarimetric SAR images, QuickBird images, and lidar data in an area close to Halifax, Nova Scotia; an area comprised of forests, barrens and a chaotic topography (Neily et al. 2005). While most of the previous wetland mapping studies have used optical satellite images (see the review of Ozesmi and Bauer 2002), some have also used radar images, mainly single-polarized images (Ozesmi and Bauer 2002) or dual-polarized images (LaRocque et al. 2015). More recently, radar polarimetric SAR (polSAR) images have been tested, but in a landscape that is less complex than ours and is mainly located over flat areas (Brisco et al. 2011; Millard and Richardson 2013; Corcoran et al. 2011; Corcoran et al. 2013; van Biejma et al. 2014). Also, these polSAR studies only assess the accuracy of the resulting maps against training areas in the classified images (Brisco et al. 2011; Millard and Richardson 2013; Corcoran et al. 2011; Corcoran et al. 2013; van Biejma et al. 2014), or against maps derived from aerial photography (Millard and Richardson 2013); while in my case, I compare the classified image with GPS field data. In my study, I also assess the sources of confusion errors with the upland classes and amongst the wetland classes for each wetland class.

4.2   Materials and Methods

4.2.1   Study Area
The study area is located just south of Halifax, Nova Scotia between 44° 30' N and 44° 40' N, and 63° 32' W and 63° 41' W (Figure 4.1), on the National Topographic System Map sheet 011D12. Much is accessible through public land in Long Lake Provincial Park and the Herring

Cove Backlands. Although there are significant zones that are experiencing increased pressure from urban development, most of the study area still has natural forested landscapes.
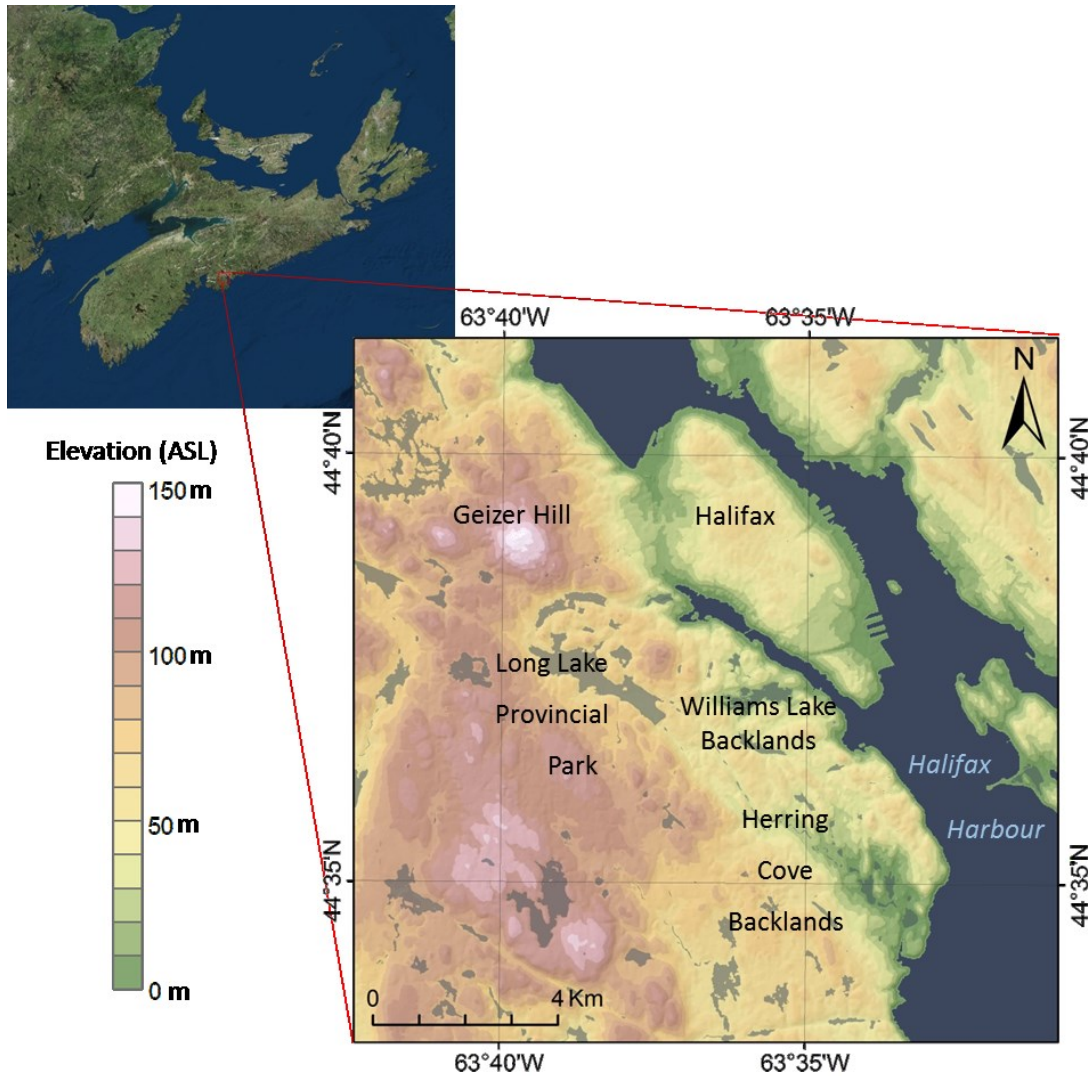
Figure 4.1: Location and digital elevation model of the study area.

As measured from the digital elevation model (DEM) (Figure 4.1), the elevation in the study area ranges from 0 m above mean sea level (AMSL) along the coast of Halifax Harbour to 150 m AMSL on Geizer Hill at the northwest edge of the study area. The drainage network is dominated by the McIntosh Run which is approximately 13.5 km long and drains an area of 33.6 km^2. As elsewhere in Nova Scotia, the study area experiences a modified continental climate, but its proximity to the Atlantic Ocean leads to more frequent rain and fog occurrences (Nova Scotia Museum of Natural History 1989).

According to the Nova Scotia's Ecological Land Classification (ELC) soil drainage classes, the area is a mixture of well drained soils and imperfectly drained soils (Figure 4.2) (Neily et al. 2003). Like poorly drained soils, imperfectly drained soils are also expected to provide suitable conditions to promote wetland development. In addition, most of the forested soils are acidic and generally coarse textured podzols where leaching of soil nutrients is common (Canada Committee on Ecological Biophysical Land Classification 1988). Cementation of leached organic carbon, iron, and aluminum leads to the creation of hardpan, which can subsequently cause poor drainage and wetland development (Canada Committee on Ecological Biophysical Land Classification 1988).
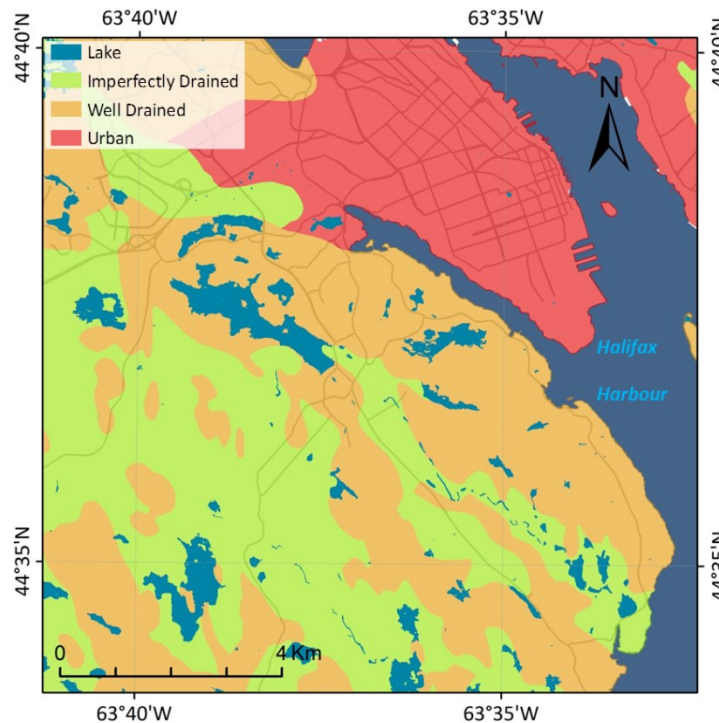
Figure 4.2: ELC soil drainage classes for the study area.

The study area contains most of the relevant wetland classes of interest that can be found in the province of Nova Scotia, such as peatland (which includes ombrotrophic peatlands or bogs, and minerotrophic peatlands or fens), and swamps. However, because the area is mainly forested, large marshes are absent in the area, so this class was merged with the open-water class to form a so-called open-water/marsh complex. Also, fens and swamps are more common than ombrotrophic bogs in eastern part of the study area around the Williams Lake

Backlands, because it has a barrens landscape that is "flow-through", meaning that definite in- and out-flows are typical (Hill and Patriquin 2014).

Twelve classes (Table 4.1) were chosen to represent the land cover of the study area, namely: barren, grass, industrial, lake, open-water/marsh complex, open bog, open fen, shrub/treed fen/bog, swamp, upland sparse vegetation, upland forest, and urban. The wetland classes were based on the Canadian Wetland Classification System (Warner and Rubec 1997).

Table 4.1: Mapping legend showing classes used for the classification process along with the description from Canadian Wetland Classification System that was used to help identify landcover classes in the field.

Class colour	Class ID and name	Description
	1 - barren	Area with more than 50% exposed rock outcrop and less than 25% vegetation.
	2 - grass	Area of manicured grass such as recreation fields and golf courses.
	3 - industrial	Built-up areas consisting of large, low-rise industrial buildings and parking lots.
	4 - lake	Deeper water with no apparent vegetation.
	5 – open-water/marsh complex	Combination of open-water wetland and shallow marsh. Marshes have shallow water levels that can fluctuate daily and expose the soil. Shallow or open-water wetlands have water depths up to 2m that are typically stable, but soil may occasionally become exposed.
	6 - open bog	Ombrotrophic peatland area with primarily ericaceous plants and sphagnum, and less than 25% tree coverage. They have a raised or level surface and are not affected by runoff or ground water.
	7 - open fen	Minerotrophic peatland with ericaceous plants, sedges and brown mosses and less than 25% tree coverage. The ground and surface water movement is more stable, and exposed water in channels can form characteristic patterns.
	8 – shrub/treed fen/bog	Peatland with more than 25% tree coverage. Treed fens and bogs are not easily differentiated and so are combined for this research.
	9 - swamp	Wetlands dominated by trees (typically > 30% cover) that are influenced by minerotrophic groundwater. They can be found on either mineral or peat soils and are typically considered the driest wetland type.
	10 - upland sparse vegetation	Area with less than 50% exposed rock outcrop. Vegetation primarily low and ericaceous.
	11 - upland forest	Forested stand containing trees at least 3m in height.
	12 - urban	Built-up areas consisting of high-rise urban core buildings, streets and sidewalks.

4.2.2 Imagery

Two types of satellite imagery were used in the classifications: (1) Multispectral QuickBird imagery acquired on October 30, 2005 (pixel size = 2.4 m, swath = 16.8 km); and (2) RADARSAT-2 SLC fine quad-pol (FQ) C-band (5.54 cm wavelength) polarimetric SAR imagery (pixel spacing of 8 m, nominal resolution of 12 m, and swath of 25 km). The QuickBird imagery was available from the Halifax Regional Municipality. It is 11-bit imagery with four multispectral bands (blue 450-520 nm; green 520-600 nm; red 630-690 nm; and near-infrared 760-900 nm). The image was previously georeferenced with the following projection and datum: UTM zone 20, row T, NAD83.

The RADARSAT-2 polarimetric SAR images were provided through the Science and Operational Applications Research Education (SOAR-E) program of the Canadian Space Agency. They were acquired using two fine quad-pol beam modes (FQ6 and FQ30) and a descending (D) orbit. The FQ6 beam mode corresponds to incident angles ranging from 24.6° to 26.4°. The FQ30 beam mode corresponds to incident angles ranging from 47.5° to 48.7°. The images were acquired during the descending orbit, so they were west-looking and acquired early morning. Both beam mode SAR imagery were acquired in April, when the water level is high in the wetlands and in August-September, when the water level is low (Table 4.2). In addition, the low water level images were acquired under dry conditions in late summer, while the high water level images were acquired under wet conditions, in early spring under no frost or snow condition but from a different year.

Table 4.2: Characteristics of the RADARSAT-2 polarimetric SAR images used.

Date	Beam mode	Water level	Precipitation (mm) (*)
August 19, 2010	FQ30	low	0
September 1, 2010	FQ6	low	0.6
April 5, 2013	FQ30	high	17.4
April 18, 2013	FQ6	high	16.1

Millimeters of rain equivalent recorded at the Shearwater RCS weather station during the six days prior to image acquisition. (Government of Canada 2015)

4.2.3 Other data

Laser scanning (lidar) data was collected for Halifax Regional Municipality in spring 2007 using the ALTM2050 lidar system that was flown at 1200m above ground at 70m/s on average. The system has a laser repetition rate of 50 kHz, a scan angle of $\pm 20^{\circ}$, a beam divergence (dual) of 0.2 mrad, and provides a series of points with a vertical and horizontal accuracy of 15 cm or better.

Finally the wetland map extracted from the classified image was compared to GPS field data (see details in the next section) and to a wetland map that is currently in use by the government of Nova Scotia (Figure 4.3) and that can be requested from the Nova Scotia Department of Natural Resources (DNR). It will be called hereafter *"DNR map"*.
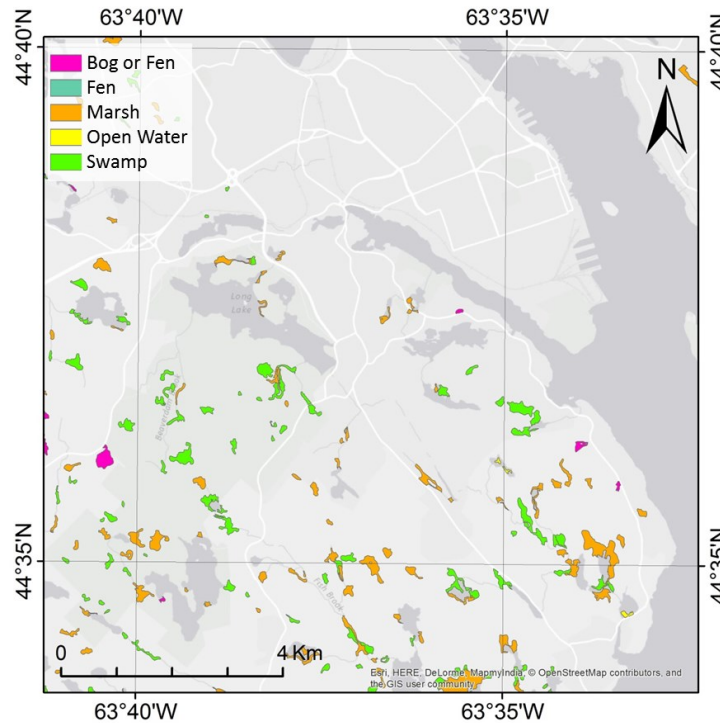
Figure 4.3: Nova Scotia DNR map of the study area.

4.2.4 Field data collection

During low water levels in the wetlands mostly in the period from August to September 2012, field observations were made at 558 GPS sites. Site visits were planned to cover as much of the study area as possible (Figure 4.4), especially ensuring that the different soil drainage classes mapped by the Ecological Land Classification (ELC) were considered. All the sites were

selected according to the following criteria: (1) accessibility by road or path; (2) relatively large extent of the related land cover.

Field work was carried out during times when vegetation had not yet senesced so that vegetation could assist in identifying wetlands and non-wetland areas. Among all the 558 visited sites, 318 sites were used to delineate training areas for the image classification and 240 points being used to assess the mapping accuracy for the map produced from the image classification (Table 4.3).
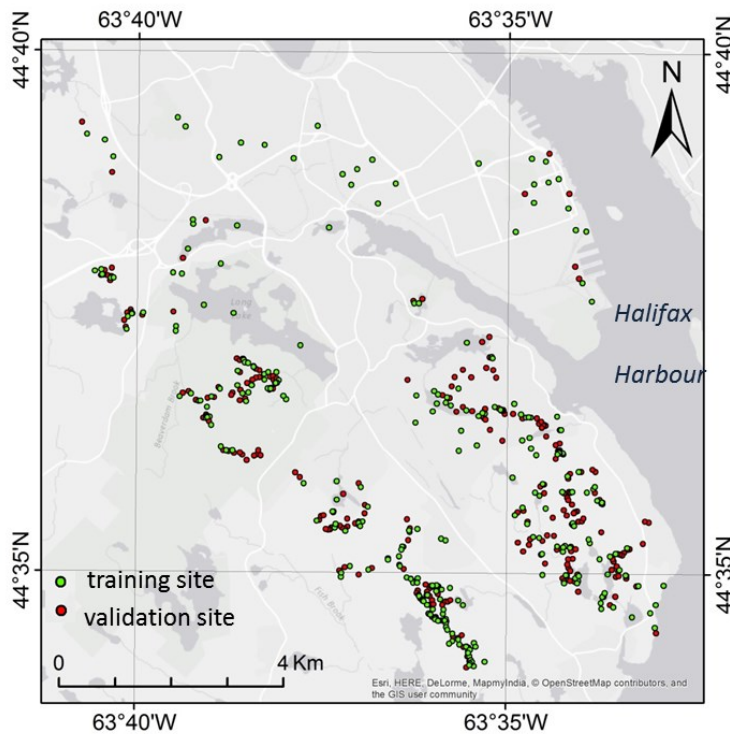
Figure 4.4: Training and validation sites of for the twelve classes used.

Table 4.3: Number of training and validation sites for each class.

Class name	Training Sites	Validation Sites
Barren	19	12
Grass	16	3
Industrial	10	4
Lake	14	6
Open-water/marsh complex	12	6
Open bog	22	19
Open fen	32	30
Shrub/treed fen/bog	52	24
Swamp	38	52
Upland - sparse vegetation	63	34
Upland forest	33	47
Urban	7	3
Total	318	240

Among all the visited sites, 287 sites (170 training sites and 137 validation sites) were considered as being wetland (Table 4.3). Sites were defined as a wetland, such as in Tiner (1999), when the water table is close to (less than 10 cm) or at the surface, or when I found indicator plants, soil hydromorphy, or other evidence of an area that is often saturated with water. Several of the wetland sites were initially found by interpretation of aerial photographs and the slope model, or because they had been previously mapped as wetland on the DNR (Figure 4.3).

Planned wetland transects and routes between destinations were not always followed because of the rough terrain or dense vegetation. Custom maps showing trails and a low-slope mask (less than 2°) created from the lidar DEM were made in Mapwel software and uploaded to a Garmin 60cx GPS receiver. On arrival in the field a GPS fix was acquired and the time on the camera was synchronized with the GPS clock so that the photographs could be geocoded in the lab using GeoSetter software. A compass was used to identify bearing on photos if important and a 1:50,000 topographic paper map (NTS 011D12) was used to aid navigation. In the field, a special effort was made to visit the following sites: sites that represent the transition between upland and wetland, sites that did not match the low-slope mask, and sites along the route which confirmed the low-slope mask. On each site, the following measurements were made:

GPS location, elevation, class identification based on the descriptions in Table 4.1, and ground photographs taken such as those of Figure 4.5.

lake   open water/marsh complex   open bog

open fen   treed fen or bog   swamp

Figure 4.5: Field photographs of typical wetland classes found in the study area.

4.2.5 Lidar data processing

Raw lidar points were classified as first return (tree branch level) and ground return (ground level) using TerraScan software. The ground return data was interpolated with an Inverse Distance Weighting (IDW) algorithm to create a 2 m resolution digital elevation model (DEM) using Surfer (Golden Software). IDW was chosen as the interpolator because the points are dense and location is only precise to the lidar footprint area (Hopkinson, personal communication June 30, 2009). This DEM was used for computing the following four derivative variables: (1) the slope (SLP); (2) the Compound Topographic Index (CTI); (3) the Curvature (CRV) and (4) the Topographic Position Index (TPI).

The Slope (SLP) shows where the surface water runoff is slower (or faster). It was derived in ArcGIS using the maximum rate of change from one cell to its eight neighbours to show the steepest downhill descent. In my study area, 90% of the area inside Nova Scotia Wetland Inventory polygons was less than or equal to two degrees of slope. The Compound

Topographic Index (CTI) shows wetter areas using slope combined with where flow is predicted to accumulate (Wilson and Gallant 2000). CTI was calculated as the natural log of the upland contributing area (a) divided by the tangent of the slope (β).

$$CTI = \ln(a/\tan\beta) \qquad\qquad (1)$$

where

- a = [(flow accumulation + 1) * (cell size)]
- β = slope in radians

The flow accumulation of Equation 1 was derived using the D8 single flow direction method that calculates accumulated flow for a cell from flow accumulation values of the eight surrounding cells (Wilson and Gallant 2000). This method was used because it is better at delineating channels (Wilson and Gallant 2000). Indeed, a multiple flow method shows a more realistic flow over slopes, but it also produces high dispersion in valleys (where wetlands often are) that may not be suitable (Wilson and Gallant 2000).

The Curvature (CRV) shows deceleration (or acceleration) of water runoff. It can also be used to show flow convergence or divergence (Moore, Grayson, and Ladson 1991). It is computed in ArcGIS as the second derivative of the DEM. The Topographic Position Index (TPI) gives the relative position in the landscape (hilltop to valley bottom) for each cell. It is computed in ArcGIS using a modified Jenness method (Jenness 2002) that was designed by S. Cooley (2014), but with parameters adjusted to my study area (equation 2). My process determines the height of a central cell, as well as the minimum elevation in a 1 ha neighbourhood, and the difference is calculated. The height difference from the neighbourhood minimum is divided by the neighbourhood range (i.e. maximum - minimum), and that value (TPI) is stored in a new raster. The values for this index run between zero and one, and indicate whether the position is near the bottom (valley), near the top (peak), or somewhere in between (slope).

$$\frac{E - nE_{min}}{nE_{max} - nE_{min}} \qquad\qquad (2)$$

where

- E = elevation
- nE_{min} = minimum elevation in a neighbourhood
- nE_{max} = maximum elevation in a neighbourhood

A fifth lidar variable was derived based on the DEM and the DSM. It is the Canopy Height Model (CHM) that is the difference between the DEM and the DSM and further categorized into five height classes. To create the CHM, original lidar data in ASCII files (ground and first return) was converted to LAS format in ArcGIS and then converted to ESRI Grid format for analysis. In this case, IDW was not used because this interpolation resulted in small artifacts in the CHM due to unequal distribution of ground points and first points (fewer ground points are obtained in dense vegetation). Instead, the LAS point files were interpolated using the *LAS dataset to raster* conversion tool of ArcGIS. A binning option was used to define the cell value. It selected the maximum elevation value of points within the grid cell resolution, but did not fill voids. Finally, the difference between ground and first return was calculated to produce the CHM output grid. Height class was calculated using a majority filter with a five by five cell kernel as a way to characterize the general canopy type in a 100 m^2 area. Gaps were filled with values from adjacent cells using the *Expand* tool of ArcGIS. The resulting height data was classified using the categories of Table 4.4 that are based on a definition adapted from the Ontario Wetland Evaluation System (OWES) Southern Manual (2014).

Table 4.4: Vegetation height class definition (adapted from the Ontario Wetland Evaluation System (OWES) Southern Manual (2014)).

Class	Height (m)	Description
1	0.00 – 0.30	low vegetation
2	0.31 – 1.00	low shrub or taller grass/sedge/etc.
3	1.01 – 2.00	medium shrub or taller grass/sedge/etc.
4	2.01 – 6.00	tall shrub
5	> 6.01	tree

All the lidar-derived products were then resampled to 8 m to match the RADARSAT-2 images prior to classification.

4.2.6   Satellite Image processing

Most of the image processing was performed in PCI Geomatica 2014®. The QuickBird imagery digital numbers were converted to reflectance values using the top of atmosphere (TOA) reflectance procedure (Krause 2003; GRASS-Wiki 2015). First the top of atmosphere spectral radiance is calculated by:

$$L_{\lambda pixel,band} = \frac{\kappa_{band} * q_{pixel,band}}{\Delta\lambda_{band}} \tag{3}$$

with

- $L_{\lambda pixel,band}$ = top of atmosphere spectral radiance image pixels [W/(m²*sr*μm)]
- κ_{band} = absolute radiometric calibration factor [W/(m²*sr*count)] for a given band
- $q_{pixel,band}$ = radiometrically corrected image pixel
- $\Delta\lambda_{band}$= effective bandwidth for a given band [μm]

Then the top of atmosphere spectral radiance is used for computing the top of atmosphere reflectance by:

$$\rho = \frac{\pi * L_\lambda * d^2}{E_{sun}\lambda * \cos(\Theta_s)} \tag{4}$$

- ρ = unitless reflectance
- π = 3.14159265358
- L_λ = spectral radiance at the sensor's aperture [W/(m²*sr*μm)]
- d = Earth/Sun distance in astronomical units (AU), interpolated
- E_{sun} = mean solar exoatmospheric irradiance (W/m²/μm)
- $\cos(\theta_s)$ = cosine of the solar zenith angle from the image's metadata (θ_s 52.26285°)

The values used for κ_{band}, E_{sun}, and $\Delta\lambda_{band}$ are given in Table 4.5.

Table 4.5: Values of the three parameters used in the Top of Atmosphere reflectance calculation procedure.

Band	E_{sun} [W.m^{-2}.μm^{-1}]	κ_{band} [W. m^{-2}. sr^{-1}. count^{-1}]	$\Delta\lambda_{band}$ [μm]
Blue	1924.59	0.01604120	0.068
Green	1843.08	0.01438470	0.099
Red	1574.77	0.01267350	0.071
NIR	1113.71	0.01542420	0.114

The RADARSAT-2 polarimetric SAR images were filtered for removing speckle, as speckle can be considered noise and its intensity must be attenuated in order to resolve fine details on SAR images (Goodman 1976). First, the HH, HV, VV, and VH intensity images were filtered using a 7x7 Lee Adaptive filter with the FLE program of PCI Geomatica 2014® (PCI Geomatica 2014). The full polarimetric SAR images were filtered by applying a 5x5 polarimetric Lee speckle filter (Lee et al. 1999) with the PSPOLFIL program of PCI Geomatica 2014®. This filter preserves polarimetric properties by filtering each element of the covariance matrix independently, while maintaining spatial information. These filtered images were then used to compute the polarimetric variables that are listed in Table 4.6.

Table 4.6: List of polarimetric parameters used in the study.

Variable	Definition	Authors
Pedht	Pedestal height = minimum of Pr (copolarized signature)	van Zyl et al. (1987)
Totpow	Total power = $|S_{hh}|^2 + 2\,|S_{hv}|^2 + |S_{vv}|^2$	Lopez-Martinez et al. (2005)
γ	correlation coefficient $\gamma = S_{hh}S_{vv} / (|S_{hh}|^2\,|S_{vv}|^2)^{1/2}$	Rodriguez and Martin (1992)
$\delta_{HH\text{-}VV}$	Phase difference	Lopez-Martinez et al. (2005)
Pr$_{max}$	Maximum of the received power	Touzi et al. (1992)
Pr$_{min}$	Minimum of the received power	Touzi et al. (1992)
FP	Fractional polarisation = Pr$_{max}$- Pr$_{min}$ / Pr$_{max}$+Pr$_{min}$	Zebker et al. (1987)
CV	Coefficient of Variation = Pr$_{min}$ / Pr$_{max}$	van Zyl et al. (1987)
S$_{max}$	Maximum of the scattered intensity	Evans et al. (1988)
S$_{min}$	Minimum of the scattered intensity	Evans et al. (1988)
ND	Normalized Difference ND$_s$ = S$_{max}$ - S$_{min}$ / S$_{max}$ + S$_{min}$	Evans et al. (1988)
d$_{max}$	Maximum of the degree of polarization	Touzi et al. (1992)
d$_{min}$	Minimum of the degree of polarization	Touzi et al. (1992)
Δd	d$_{max}$ − d$_{min}$	Touzi et al. (1992)
α_s	Magnitude of the symmetric scattering	Touzi (2007)
$\Phi_{\alpha s}$	Phase of the symmetric scattering	Touzi (2007)
ψ	Maximum polarization parameter for orientation	Touzi (2007)
τ_m	Maximum polarization parameter for helicity	Touzi (2007)
λ	Touzi dominant eigenvalue	Touzi (2007)
FD dbl	Power related to double-bounce scattering	Freeman and Durden (1998)
FD surf	Power related to surface scattering	Freeman and Durden (1998)
FD vol	Power related to volume scattering	Freeman and Durden (1998)
CP H	Entropy $(H) = \sum_{i=3}^{3} -p_i\, log_3(p_i)$	Cloude and Pottier (1997)
CP A	Anistropy $(A) = \frac{\lambda_2 - \lambda_3}{\lambda_2 + \lambda_3}$	Cloude and Pottier (1997)
CP α	Alpha angle $(\alpha) = \sum_{i=3}^{3} \rho_i\, \alpha_i$	Cloude and Pottier (1997)
CP β	Beta angle (β) = 2 * orientation angle (ψ)	Cloude and Pottier (1997)

Both the intensity and polarimetric products were orthorectified with PCI Geomatica 2014® Orthoengine using the *Radar Satellite Math Modelling* method, with the Rational Function extracted from the image and a DEM. Fourteen check points were used to test the orthorectification of an image and resulted in a root mean square of 0.24 pixels in the x and 0.76 in the y (see appendix C). This resulted in an output which corresponded very well with a corner reflector placed in the field and other features such as roads and coastlines in the QuickBird image. All the georeferenced images were clipped to the area of interest polygon and the background was assigned a grey level value matching the null value in my classifier.

4.2.7   Image classification

Representative training areas of each of the twelve land cover classes of Table 4.1 were delineated in ArcGIS as polygon shapefiles, by using information collected in the field (from 318 GPS training sites), high resolution aerial photography and profiles of raw first and ground lidar points. Training areas have at least 500 pixels per class for adequate class representation in the classification and were delineated away from transition edges. The training areas were randomly located throughout the study area, but the number of training areas by class reflected the relative frequency of the different land covers inside the study area, as shown in Figure 4.6.
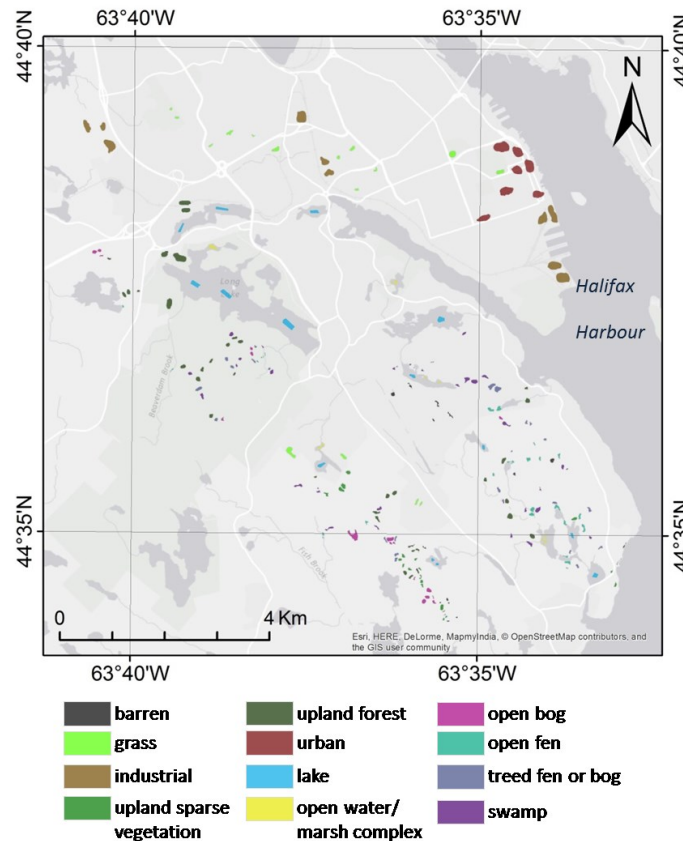
Figure 4.6: Location of the training areas for each class delineated using GPS points, aerial photography, and the raw lidar point cloud.

In this study, a non-parametric decision tree type classifier, Random Forests (RF) was used. The RF algorithm was originally developed by Leo Breiman and Adele Cutler at the University of California, Berkeley (http://www.stat.berkeley.edu/~breiman/ RandomForests/) (Breiman 2001, 2003). The algorithm used for this study was developed in the R programming language (R Development Core Team 2012) and has been used successfully in recent studies on wetland mapping with RADARSAT-2 images in New Brunswick (LaRocque et al. 2015) and in the Hudson Bay Lowlands in Ontario (Ou et al. 2014). RF can be run with "sub-polygon" and "all-polygon" (http://www.amnh.org/our-research/center-for-biodiversity-conservation/biodiversity-informatics/open-source-software-and-scripts). The *sub-polygon* version randomly selects a user-determined number of training area pixels from each class. The *all-polygon* version, which I applied, uses all of the pixels in all of the training area polygons to define class training areas and has the advantage of using the actual class size. The RF classifier

was set to a forest of 500 independent decision trees with the default number of variables randomly sampled as candidates at the split of every node (i.e. *mtry*). The default values for *mtry* for a classification are calculated as the square root of *p*, where *p* is the number of variables in x, i.e., the matrix of predictors for the classification (https://cran.r-project.org/web/packages/randomForest/randomForest.pdf). Using the default value gives a setting which includes all of the input features, or in other words, all pixels will be randomly sampled as candidates at each split of every node.

The RF classifier is calibrated using two thirds of the training area data and is called "*In Bag*" data. "*Out of Bag*" data is the remaining third which is used to test the forest to validate the resulting classification. The 500 individual decision trees are created using "*In Bag*" data, and are applied to produce independent classifications which are subsequently combined into the final classification map (Waske and Braun 2009). RF will allow for bootstrap aggregating of "*In Bag*" data when there is relatively limited training data for some classes in order to increase the number of training pixels. However bootstrapping was not required in my study area as I had enough training sites.

RF was chosen because of its multiple advantages. It does not assume normal distribution of the input data. It can therefore accommodate the data distribution differences between polarimetric SAR (Wishart) (Lee et al. 1994) and optical (Gaussian) data. Also, several other studies found that RF improves the classification over the maximum likelihood classifier (MLC) (e.g. Waske and Braun 2009; Ozdarici-Ok et al. 2014; LaRocque et al. 2014; Millard and Richardson 2015). RF is also able to accommodate many layers of input bands including those from different types of data. So it is an ideal classifier for a classification where multi-temporal SAR imagery is used with optical imagery (Waske et al. 2007) or with elevation derivatives (Van Beijma et al. 2014). RF is also not sensitive to noise or over classifying. Finally, RF is able to rank the importance of each variable to the classification in order that the most influential variables in the classification can be identified (Gislason et al. 2006; Waske and Braun 2009). This ranking is presented in the "Mean Decrease Accuracy" plot. The higher the image is on the "Mean Decrease Accuracy" plot Y axis, the more useful the image was in performing the classification (Strobl *et al.* 2008; Louppe *et al.* 2013).

RF was used to classify the following combinations of lidar, QuickBird and RADARSAT-2 polarimetric SAR images:

1. Five lidar elevation derivative variables
2. QuickBird blue, green, red and NIR images
3. RADARSAT-2 dual-polarized (HH and HV) intensity images
4. Lidar derivatives and four QuickBird images
5. Lidar derivatives and RADARSAT-2 dual-polarized
6. Lidar derivatives and RADARSAT-2 dual-polarized and QuickBird images
7. RADARSAT-2 HH, HV, VH, VV intensity and polarimetric variable images
8. Lidar derivatives and RADARSAT-2 HH, HV, VH, VV intensity and polarimetric variable images
9. Lidar derivatives and RADARSAT-2 HH, HV, VH, VV intensity and polarimetric variable images and four QuickBird images

Classification accuracy was measured first using a confusion matrix (or error matrix), where training areas are compared to the equivalent land cover in the classified map. Each cell in the matrix shows the number of pixels classified compared to a particular class as defined by the training areas (Congalton 1991). The matrix computes individual class User's and Producer's accuracies and their related error of omission and commission as described in Congalton (1991). The User's accuracy identifies the probability that a pixel from the classification map is in the right class, plus the associated number of pixels misclassified to the wrong class (error of omission). The Producer's accuracy corresponds to the probability that a reference pixel is well classified, and the associated number of misclassified pixels that actually belong to another class (error of commission).

The best combination of input images was selected based on the highest overall accuracy that visually represents a suitable map. However, this method only gives an assessment of the classified image accuracy, which is different from the true mapping accuracy. An independent accuracy assessment is more robust and compares the resulting classified map with an independent set of field observation data acquired over the validation sites which are points recorded with GPS coordinates. Each validation site was compared to the classified map,

and the map is considered to be correct. These comparisons were tabulated to produce the percentage of correct identifications computed as a function of the total number of wetland validation sites. A confusion matrix was not calculated because only wetland classes were used and some misidentification is due to confusion with non-wetland classes.

4.3   Results

4.3.1   Effect of wetland water level on the radar images

RADARSAT-2 imagery acquisition was tasked for late summer and early spring to get images with low and high water levels in the wetlands. The effect of different water levels is visible on the false colour composites of the RADARSAT-2 images (Figure 4.7). For the shallow incidence angle (FQ30), open wetlands look darker and forested wetlands are greener in appearance, as the interaction between water and trees produces a double-bounce scattering resulting in a brighter return. The similar is true for the steep incidence angle (FQ6); however some of the open wetlands appear brighter than with the shallow incidence angle (FQ30). This is, in part, due to the fact that the FQ30 signal cannot penetrate the forested canopy cover as easily as FQ6.
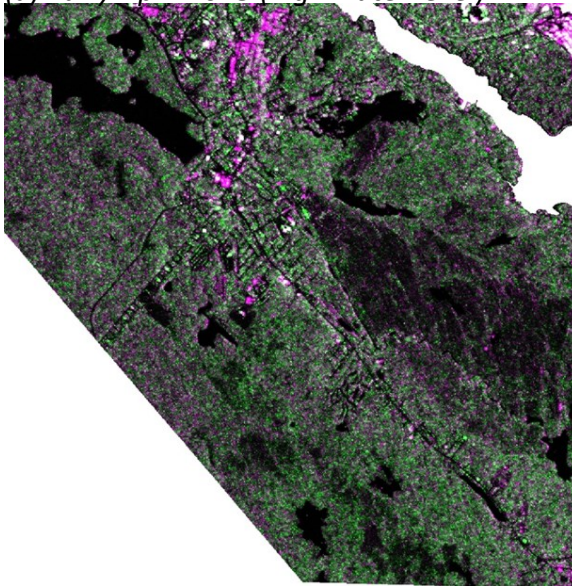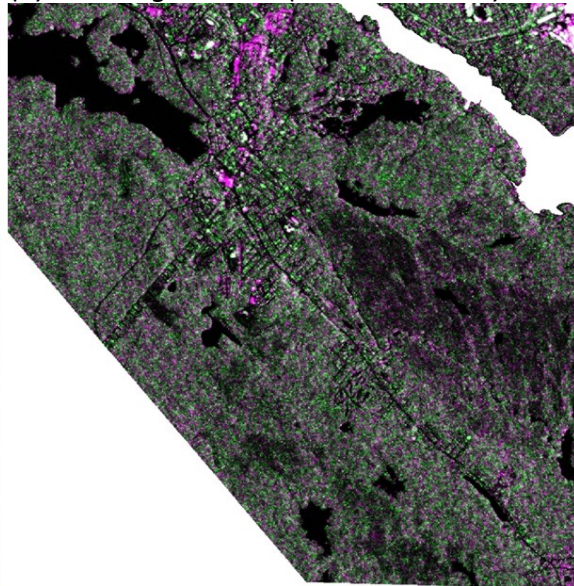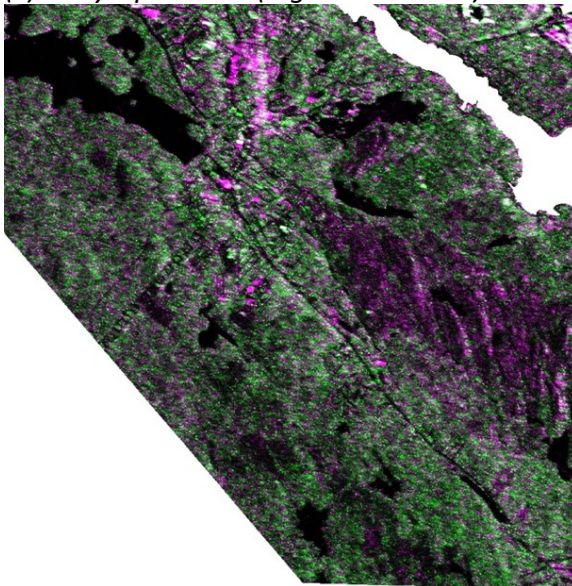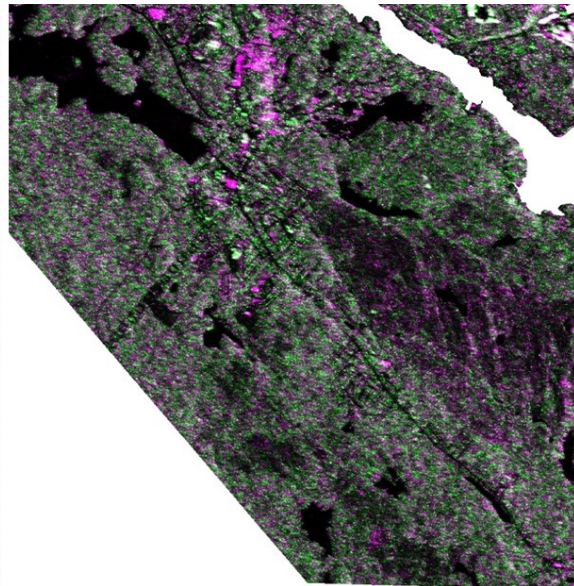
Figure 4.7: False colour composite of RADARSAT-2 FQ30 dual-polarized HH and HV images acquired (a) during high water level, and (b) during low water level, and false colour composite of RADARSAT-2 FQ6 dual-polarized HH and HV images acquired (c) during high water level, and (d) during low water level. The composite is HH in red, HV in green and HH in blue.

4.3.2 Classified images

Table 4.7 shows the overall classification accuracy when the classifier was applied to various combinations of input data. The lowest overall accuracy occurs when only one type of data is used, i.e., the lidar variables (63.3%), the RADARSAT-2 dual-pol HH and HV images (60.8%) or the QuickBird images (62.1%). There is a notable increase in accuracy, from 60.8% to 76.1%, when RADARSAT-2 HH, HV, VH, VV intensity and polarimetric variables are used instead of the RADARSAT-2 dual-pol images, A strong accuracy improvement occurs when lidar variables are combined with either the QuickBird or the RADARSAT-2 images, the highest classification accuracy occurring with the RADARSAT-2 HH, HV, VH, VV intensity and polarimetric variables (87.6%). The overall highest accuracy is obtained with the combination of all three types of data, with the accuracy reaching 88.8% with the RADARSAT-2 HH and HV images and 90.2% with the RADARSAT-2 HH, HV, VH, VV intensity and polarimetric variables.

Table 4.7: Overall classification accuracy (%) for the various data set combinations.

Data Combination	Overall accuracy (%)
QuickBird	62.1
Lidar	63.3
RADARSAT-2 HH/HV	60.8
RADARSAT-2 HH, HV, VH, VV intensity and polarimetric	76.1
Lidar & QuickBird	84.6
Lidar & RADARSAT-2 HH/HV	84.0
Lidar & RADARSAT-2 HH, HV, VH, VV intensity and polarimetric	87.6
Lidar & RADARSAT-2 HH/HV & QuickBird	88.8
Lidar & RADARSAT-2 HH, HV, VH, VV intensity and polarimetric & QuickBird	90.2

Table 4.8 compares the User's accuracies of each individual class and their related average accuracies, when the classifier was applied to the following data combinations: 1) QuickBird alone; 2) lidar & QuickBird; 3) lidar & QuickBird & RADARSAT-2 HH and HV; and 4) lidar & QuickBird & RADARSAT-2 intensity (HH, HV, VH, VV) and polarimetric variable images. The addition of RADARSAT-2 data has the strongest effect on the class accuracies for the treed wetland classes, such as "*Shrub/Treed fen/bog*" and "*Swamp*", as well as for the "*Barren*", "*Upland Sparse Vegetation*", "*Industrial*" and "*Urban area*" classes.

Table 4.8: User's class accuracies using the RF classifier applied to various data combinations

Class	QuickBird	Lidar + QuickBird	Lidar + QuickBird + RADARSAT-2 HH & HV	Lidar + QuickBird + RADARSAT-2 intensity & polarimetric variables
Barren	40.2	62.6	76.0	75.0
Grass	95.7	97.8	98.1	97.1
Industrial	75.7	88.0	93.4	95.1
Lake	99.2	99.6	99.8	99.8
Open-water/marsh complex	83.5	92.5	95.7	95.4
Open bog	51.2	79.1	81.0	81.5
Open fen	42.4	84.5	85.6	85.9
Shrub/treed fen/bog	27.7	52.6	54.8	59.3
Swamp	24.6	82.0	84.7	87.6
Upland sparse vegetation	29.3	73.0	77.2	80.2
Upland forest	69.8	94.9	95.4	96.9
Urban	54.4	77.1	89.7	91.6
Average User's accuracy	57.8	82.0	86.0	87.1
Overall accuracy	62.1	84.6	88.8	90.2

Figure 4.8 and Figure 4.9 show the resulting classified maps. Like Table 4.7, it shows the benefit of using additional datasets. There is a notable improvement with the addition of lidar to QuickBird, over QuickBird by itself. Also, the addition of RADARSAT-2 images result in a better mapping of the barren class.

a) QuickBird

barren
grass
industrial
lake
open water/marsh complex
open bog
open fen
shrub/treed fen/bog
swamp
upland sparse vegetation
upland forest
urban
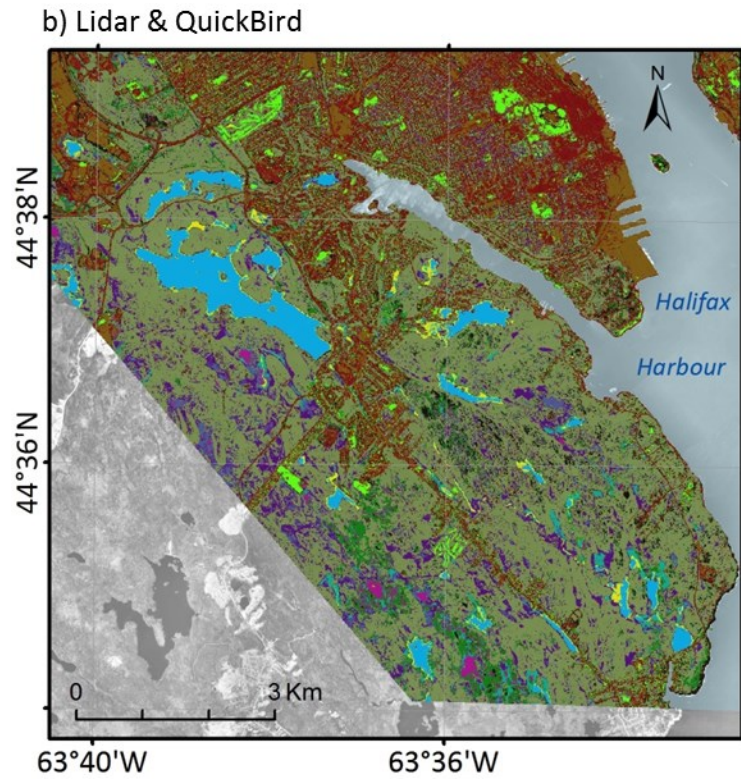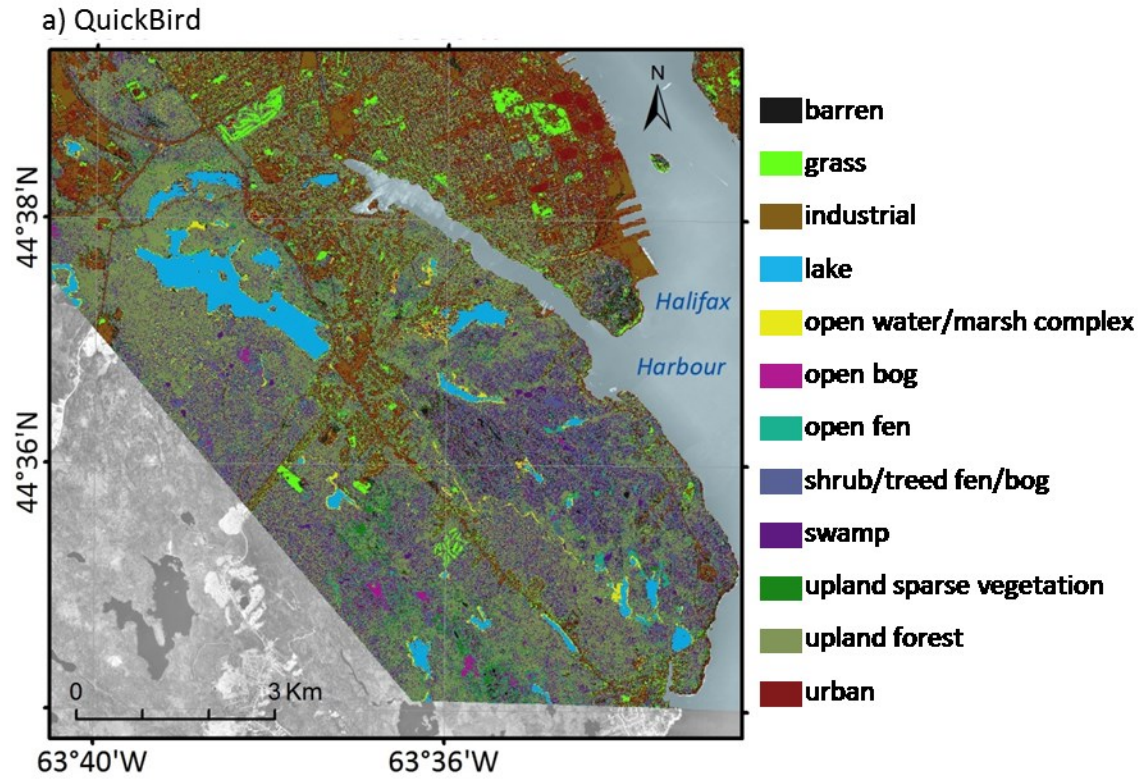
b) Lidar & QuickBird

Figure 4.8: Classified images using the RF classifier applied to: a) QuickBird; b) lidar & QuickBird images.
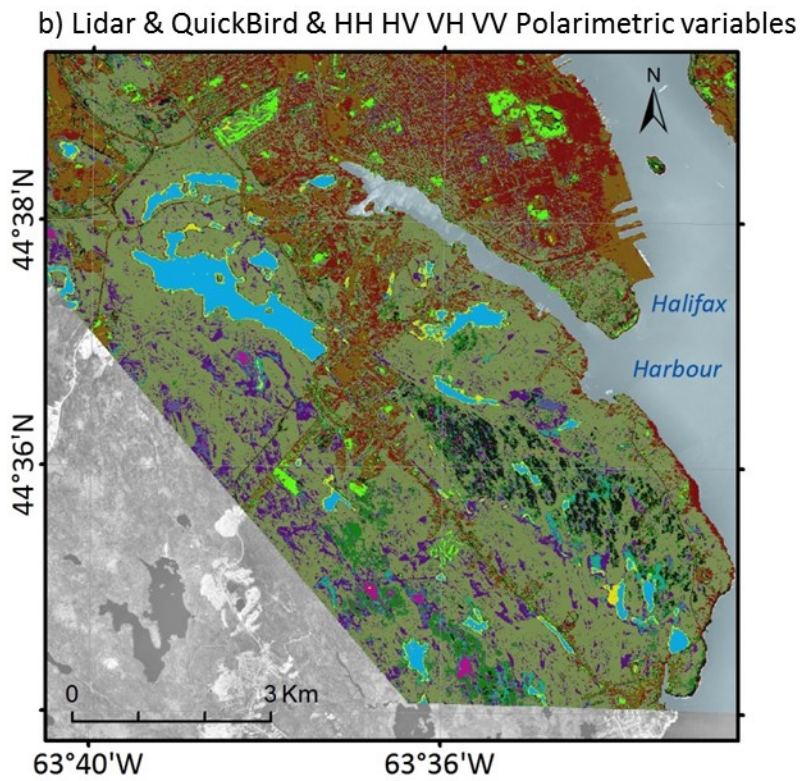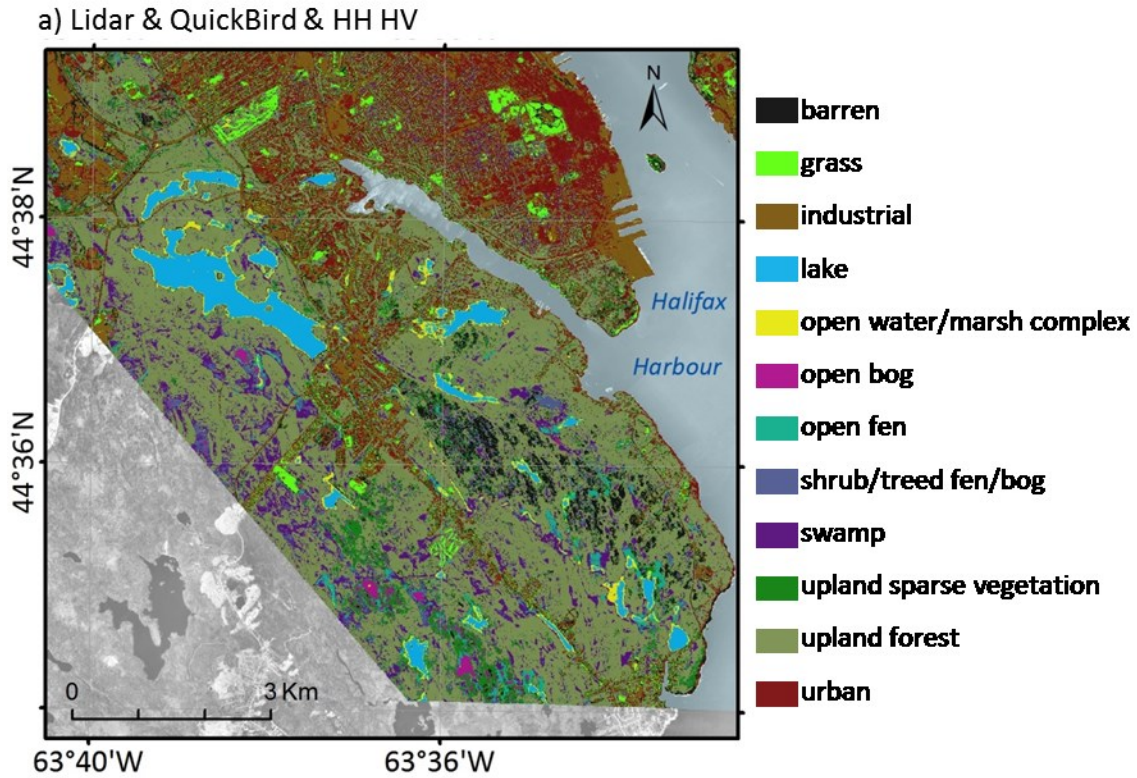
Figure 4.9: Classified images using the RF classifier applied to: a) lidar & QuickBird & RADARSAT-2 Dual Pol; and b) lidar & QuickBird & RADARSAT-2 intensity and polarimetric variable images.

90

The overall classification accuracy (Table 4.7), and the corresponding classified images (Figure 4.8 and Figure 4.9) only give a general idea about the classification accuracy so it is necessary to identify where confusion between classes occurs. This is shown in the confusion matrix of Table 4.9, which also gives the User's and Producer's accuracies and the related omission and commission errors. Table 4.8 corresponds to the classification of the combination of lidar, QuickBird and RADARSAT-2 intensity and polarimetric variable data, which had the highest overall classification accuracy (90.2%).

Most of the off-diagonal cells have a low value, indicating that most of the pixels are reasonably well classified. All the non-wetland classes have a Producer's or User's accuracy higher than 85%, except for the *barren* which has a low User's accuracy of 72.7% and the *upland sparse vegetation* classes which has a low Producer's accuracy of 78.9% and a low User's accuracy of 80.4%. With a higher Producer's accuracy (87.1%), *barren* field training areas were well chosen, but due to the similarity with *upland sparse vegetation* (which also exhibits some bare ground), there is a too high commission error (27.3%). *Upland sparse vegetation* had an omission error of 21.1%, and commission error of 19.6%, with confusion occurring with barren and upland forest.

Half the wetland classes have a Producer's accuracy higher than 85%, and lower than 85% for *open fen*, *shrub/treed fen/bog*, and *swamp*. Accordingly, *open fen* has errors of omission (18%) due to confusion with mostly *shrub/treed fen/bog* and some *open bog*. *Shrub/treed fen/*bog has errors of omission (30.2%) due to confusion with *open bog*, *open fen*, and *swamp. Swamp* has an error of omission (24.0%) mostly due to confusion with *shrub/treed fen/bog*.

Four out of six wetland classes have a User's accuracy higher than 85% but *open bog,* and *shrub/treed fen/bog* are lower. So, *open bog* has an error of commission of 20.3% mostly due to confusion with *shrub/treed fen/bog*, and some from *open fen* and *upland sparse vegetation*. The *shrub/treed fen/bog* class has a large error of commission of 40.5% mostly due to confusion with *swamp*, with some due to *open fen*.

From these results it is possible to see that the higher errors are mostly between the two wetland classes with tree or shrub canopy, and between the open fen or bog classes and the shrub/treed fen/bog class. Furthermore, there is a better distinction between *swamp* and any of the *open* wetland classes, compared to *shrub/treed fen/bog* with the open wetland classes. This is because of the variability in canopy ranging from shrub height to tree height. The biggest discrepancy between general wetland and non-wetland classes is seen in the confusion between *open bog* and *upland sparse vegetation*; however both classes support ericaceous vegetation so this may be the reason.

Table 4.9: Confusion matrix (in pixels) from the RF Classifier for the best case scenario (RADARSAT-2 polarimetric intensity and variables, with QuickBird, and lidar DEM derivatives).

Classified Data	Reference Data												row total	User's accuracy (%)	Error of commission (%)
	1 - barren	2 - grass	3 - industrial	4 - lake	5 – open-water / marsh complex	6 - open bog	7 - open fen	8 - shrub/treed fen/bog	9 - swamp	10 - upland sparse vegetation	11 - upland forest	12 - urban			
1 - barren	**521**	3	27	0	0	12	4	5	0	124	14	7	717	72.7	27.3
2 - grass	2	**1577**	14	0	0	0	3	0	1	3	2	13	1615	97.6	2.4
3 - industrial	7	0	**4496**	0	1	0	2	2	0	1	1	219	4729	95.1	4.9
4 - lake	0	0	0	**2416**	4	0	0	0	0	0	0	0	2420	99.8	0.2
5 – open-water/marsh complex	0	0	2	17	**558**	0	10	0	1	0	0	0	588	94.9	5.1
6 - open bog	0	1	0	0	2	**1067**	62	102	35	60	9	0	1338	**79.7**	20.3
7 - open fen	0	1	0	0	1	32	**1219**	102	60	5	1	0	1421	85.8	14.2
8 – shrub/treed fen/bog	0	1	0	0	0	67	146	**921**	385	11	17	0	1548	**59.5**	40.5
9 - swamp	0	1	0	0	0	0	29	123	**1763**	2	88	0	2006	87.9	12.1
10 - upland sparse vegetation	53	2	5	0	0	36	11	43	1	**880**	59	4	1094	80.4	19.6
11 - upland forest	3	0	0	0	0	0	0	18	72	27	**3877**	2	3999	96.9	3.1
12 - urban	12	7	256	0	0	0	1	3	3	3	21	**3392**	3698	91.7	8.3
Column total	598	1593	4800	2433	566	1214	1487	1319	2321	1116	4089	3637	Overall accuracy = 90.1% Kappa coefficient = 88.8%		
Producer's accuracy (%)	87.1	99.0	93.7	99.3	98.6	87.9	**82.0**	**69.8**	**76.0**	78.9	94.8	93.3			
Error of omission (%)	12.9	1.0	6.3	0.7	1.4	12.1	18.0	30.2	24.0	21.1	5.2	6.7			

The RF classifier outputs a list which ranks the importance of each input variable (see Mean Decrease Accuracy plot in Appendix D). In my best case scenario (using the combination of lidar variables with RADARSAT-2 HH, HV, VH, and VV intensity and polarimetric and QuickBird images), the five lidar variables are found in the top six most important variables in the classification with the following order: TPI, SLP, CHM, CTI and CRV. This shows the importance of the terrain features and the vegetation height in the classification. Near-infrared wavelengths are very sensitive to the vegetation of each class and vegetation seems thereby to be a determinant for classifying various land covers. Amongst all the RADARSAT-2 products, the HV and VH intensity images as well as the real component of the correlation coefficient of the spring FQ6 RADARSAT-2 image are the most important variables. HV and VH images are sensitive to volume scattering that again depends mainly on the vegetative component of each class.

4.3.3 Validation with the independent in-situ field sites

Analyzing the performance of the image combination based solely on classification accuracies is not enough and it is necessary to compare the classified images with independent validation data sets in order to assess how accurate the map produced from each classification is. The classified maps were compared against the 137 wetland validation sites. Out of these 137 sites, 66.4% and 68.6% were correctly identified when only QuickBird or lidar were used individually (Table 4.10). The accuracy increased to 86.1% when QuickBird or RADARSAT-2 dual-pol HH and HV images were added in the classification, but when RADARSAT-2 HH, HV, VH, VV and polarimetric variables are used the accuracy dropped to 82.5%. The accuracy increased again when all three types of images were used but the percentage for the combination with the RADARSAT-2 HH, HV, VH, VV and polarimetric variable images (86.1%) is lower than for the combination with the RADARSAT-2 dual-pol HH and HV images (86.9%). In all cases, the percentage of sites that are correctly identified as wetland are well above the one obtained with the DNR map that is currently used for wetland mapping by the government of Nova Scotia (46.7%). This map was produced mainly by photo-interpretation and field survey.

Table 4.10: Overall statistics of the identification of the 137 wetland in situ sites on the classified images or the DNR maps.

Source of data	Correctly identified as wetland		Correctly identified wetland class	
	N	%	N	%
NS DNR map	64	46.7	13	9.5
QuickBird	91	66.4	44	32.1
Lidar	94	68.6	57	41.6
Lidar & QuickBird	118	86.1	82	59.9
Lidar & RADARSAT-2 dual pol (HH/HV)	118	86.1	81	59.1
Lidar & RADARSAT-2 dual pol (HH/HV) & QuickBird	119	86.9	87	63.5
Lidar & RADARSAT-2 intensity & polarimetric images	113	82.5	78	56.9
Lidar& RADARSAT-2 intensity & polarimetric & QuickBird	118	86.1	88	64.2

Identifying the GPS wetland sites in their proper wetland class is a more challenging task, and the related percentages are well below the correct identifications of the wetland/non-wetland classes. Again, the lowest accuracy is with the DNR map, on which only 9.5% of the GPS wetland validation sites are mapped in the right wetland class (Table 4.10). The highest rate in identifying the proper wetland class was achieved when the triple combinations were used; i.e. 63.5% with the RADARSAT-2 dual-pol HH and HV, and 64.2% with the RADARSAT-2 HH, HV, VH, VV and polarimetric variables. It seems that both from the classification accuracy point of view (Table 4.7) and from the mapping accuracy point of view (Table 4.10) that the combination of lidar, QuickBird and the RADARSAT-2 HH, HV, VH, VV and polarimetric variable images gave the best accuracies. It is why that only this case will be considered further. In each of the following analyses, it will be compared to accuracy obtained with the DNR map.

With the classified image, 21.9% of the misidentifications are due to wetland sites not being classified in the correct wetland class, but only 13.9% are wetland sites being classified into a non-wetland class (Table 4.11). With the DNR map, 37.2% of the misidentifications are due to confusion among wetland classes and 53.3% is due to confusion with a non-wetland class (Table 4.11).

Table 4.11: Distribution of the incorrectly identified wetland GPS observations as a function of the identification error source for the classified map and the DNR map.

Source of errors	Lidar & QuickBird & RADARSAT-2 intensity & polarimetric variables		DNR map	
	N	%	N	%
Non-wetland class	19	13.9	73	53.3
Not the right wetland class	30	21.9	51	37.2
Total	49	35.8	124	90.5

In order to determine which wetland class the classified map or the DNR map gives the poorest identification results (by comparison with the GPS wetland validation sites), I have calculated the number and the percentage of correctly identified wetland validation sites for each wetland class (Table 4.12). All the classes are better identified on the classified image than on the DNR map. In both cases, the lakes and the open-water/marsh complex gave the highest mapping accuracy. The lowest accuracy (42.1%) is for the "open bog" class on the classified map, and for the "open fen" and "shrub/treed fen/bog" classes (0%) on the DNR map.

Table 4.12: Number and percentage of the correctly identified wetland GPS observations as a function of the wetland class.

Wetland class	Total count	Lidar & QuickBird & RADARSAT-2 intensity & polarimetric variables		DNR map	
		N (correct class)	%	N (correct class)	%
Lake	6	6	100	6	100
Open-water/marsh complex	6	5	83.3	3	50
Open bog	19	8	42.1	1	5.3
Open fen	30	22	73.3	0	0
Shrub/treed fen/bog	24	11	45.8	0	0
Swamp	52	36	69.2	3	5.8

On the classified map, except for the swamp, misidentifications are mainly due to wetlands being identified in the wrong wetland class (Table 4.13), instead of having wetlands being identified as a non-wetland (Table 4.14). On the DNR map, the confusion mainly occurred

with other wetland classes for the non-treed wetlands (Table 4.13) but with the non-wetland classes for the treed wetlands ("swamp" or "shrub/treed fen/bog") because of confusion with the upland forests (Table 4.14).

Table 4.13: Number and percentage of the wetland GPS observations that were not identified in the right wetland class on the classified map and the DNR map.

Wetland class	Total count	Lidar & QuickBird & RADARSAT-2 intensity & polarimetric variables		DNR map	
		N	%	N	%
Lake	6	0	0	0	0
Open-water/marsh complex	6	0	0	3	50
Open bog	19	9	47.4	11	57.9
Open fen	30	7	23.3	28	93.3
Shrub/treed fen/bog	24	12	50.0	9	37.5
Swamp	52	2	3.9	0	0
Total	137	30	21.9	51	37.2

Table 4.14: Number and percentage of the wetland GPS observations that were identified as a non-wetland class on the classified map and the DNR map.

Wetland class	Total count	Lidar & QuickBird & RADARSAT-2 intensity & polarimetric variables		DNR map	
		N	%	N	%
Lake	6	0	0	0	0
Open-water/marsh complex	6	1	16.7	0	0
Open bog	19	2	10.5	7	36.8
Open fen	30	1	3.3	2	6.7
Shrub/treed fen/bog	24	1	4.2	15	62.5
Swamp	52	14	26.9	49	94.2
Total	137	19	13.9	73	53.3

4.4   Discussion

The present study tested various combinations of RADARSAT-2 polarimetric SAR, lidar and QuickBird imagery for land cover classifications with the RF classifier. My best overall classification accuracy (90.2%) was obtained by using the combination of RADARSAT-2 HH, HV, VH, VV intensity and polarimetric variables, and lidar. This overall classification accuracy is

higher than those obtained in previous wetland mapping studies that use RADARSAT-2 or airborne CV-580 C-band intensity and/or polarimetric variables (Brisco et al. 2011 (64.65%), Corcoran et al. 2011 (63%), Corcoran et al. 2013 (69%), Millard and Richardson 2013 (88.0%), and van Biejma et al. 2014 (78.2%)) despite the more heterogeneous and rougher area considered in my study. My better results can be explained by several reasons. By comparison to Brisco et al. (2011), I also used lidar data in the classification that provided the largest increase in the overall accuracy. In addition, Brisco et al. (2011) only used Cloude-Pottier decomposition parameters in the classification, while I also used here other polarimetric decomposition variables, such as the Freeman-Durden decomposition variables. By contrast to Brisco et al. (2011) and Millard and Richardson (2013), I also used optical images and LaRocque et al. (2012) already showed that compared to using solely RADARSAT-2 images, a better mapping accuracy is achieved when RADARSAT-2 images are combined with optical images. Indeed, SAR and optical images are highly complementary. SAR has a unique ability to detect surface texture and provides information on scattering mechanisms that are related to surface roughness (and thus to the presence or absence of vegetation as well as to the vegetation type) and moisture content. Optical images, such as QuickBird, allow acquiring information on the reflective properties that are related to the presence or absence of vegetation, vegetation type, and to the surface moisture content if the canopy is sparse enough. The study by van Beijma et al. (2014) used higher resolution imagery than I did and also used polSAR bands not as commonly used (S- and X-Bands). However, van Beijma et al. (2014) were attempting to classify coastal vegetation at the species level which is more difficult than wetland class.

My overall accuracy was higher than those of Corcoran et al. (2011) (63%) and Corcoran et al. (2013) (69%), for which the study area was similar to ours in terms of topography and forest cover in contrast to that of Brisco et al. (2011) which was primarily a gently rolling, agricultural region. My better accuracy can be explained by the fact that I used polSAR images that were acquired in May during high water levels and in late August/early September during low water levels, while Corcoran et al. (2011, 2013) did not account for such a change in water level. In addition, Corcoran et al. (2011, 2013) only used RADARSAT-2 acquired with a steep incidence angle (FQ8 26.9° – 28.7°), whereas I used both steep (FQ6 24.6° – 26.4°) and shallow

(FQ30 47.5° – 48.7°) angle images. By contrast to Corcoran et al. (2011, 2013), I also used several layers derived from a lidar DEM, and a canopy height layer that is impossible to derive from the National Elevation Dataset DEM used by Corcoran et al. (2011, 2013). Also the resolution of my lidar DEM (2 m resampled to 8 m) was also much better than the National Elevation Dataset DEM.

However, my overall classification accuracy (90.2%) is lower than those obtained by LaRocque et al. (2015) (94.3%). By contrast to my study, they used images acquired during flooding conditions as well as ALOS-PALSAR L-band images, both showing an improved accuracy. Because of its longer wavelength, L-band beam is able to penetrate the vegetation canopy better than the C-band that I used and thus L-band images are better to map forested wetlands. Finally, LaRocque et al. (2015) used optical and SAR images that were acquired within a short time frame (three years), while in my case, the data were acquired over eight years. Indeed, lidar data were acquired in May 2007, the QuickBird image was acquired in October, 2005, and the RADARSAT-2 images were acquired during summer 2010 for the dry condition, and during spring 2013 for the wet condition.

In addition to a multi-sensor approach, my study also used a multi-temporal data approach for the RADARSAT-2 acquisition. Combining both approaches was already showed to produce more accurate wetland maps in Africa (Rebelo 2010), USA (Bourgeau-Chavez et al. 2008, 2015a; Corcoran et al. 2011, 2013) and New Brunswick (LaRocque et al. 2015). A multi-temporal approach allows for capturing seasonal differences in the vegetation and water level conditions, which allow for better wetland type discrimination.

The DEM is the most important input data in my classification. A similar result was obtained by Millard and Richardson (2013) who mapped wetlands in Ontario and by LaRocque et al. (2015) who mapped wetlands in New Brunswick. It can be explained by the fact that topography relates to the way water flows across or into a wetland. Wetlands can form in a variety of landscapes, but topography helps direct the distribution of surplus water and consequently the location of wetlands (Canada Committee on Ecological [Biophysical] Land Classification 1988). For example, wetlands are most often found in lowlands. In Corcoran et al. (2011) the DEM was third in importance, but it was not part of the top fifteen variables in

Corcoran et al. (2013). However, Corcoran et al. (2013) still determined that the accuracy is reduced without the DEM. The low importance of DEM variables in Corcoran et al. (2011, 2013) studies can be explained by a low resolution of the DEM used (30 m), which can make a difference in the detection of small or narrow wetlands. van Beijma et al. (2014) found that the lidar DSM was the most important variable possibly due to the fact that the homogenous coastal wetland vegetation often matches a distinct vertical position compared to the water level.

Also in the top ten important variables of my study are QuickBird images (near infrared, red, blue, and green). Such a result is in agreement with LaRocque et al. (2015) who found that the infrared bands of Landsat 5 images acquired under high and low water levels were the most important variable after the DEM and more important than SAR images. Similarly, Corcoran et al. (2011, 2013) found that optical imagery was more important than SAR images when classifying wetlands. In several old studies, optical imagery was already found to be suitable for mapping wetlands, particularly in the case of open wetlands with low vegetation (Pietroniro and Leconte 2005; Harris et al. 2005, 2006; Meingast et al. 2014). van Biejma et al. (2014) found that NDVI derived from optical imagery to be next in importance after the DSM. Furthermore, for the polSAR data, decomposition variables were useful to measure different characteristics particular to each vegetation habitat and increased accuracy significantly (van Beijma et al. 2014). van Beijma et al. (2014) used X-band polSAR, with a relatively short wavelength, to successfully map vegetation extent; however the longer wavelength S-band was more useful for differentiating vegetation habitat. Since they were mapping marsh (i.e. lacking trees) the need for even longer wavelengths (e.g. L-band) was not needed, as was evident from other studies (Corcoran et al. 2011, 2013; LaRocque et al. 2015). The smaller wavelengths may have been better at resolving smaller differences in the structure of the marsh vegetation.

RADARSAT-2 images acquired in the spring during high water have a greater influence on the classification than those acquired during low water levels. This is in agreement with LaRocque et al. (2015)'s study that showed that polSAR acquired during flooding or high water levels was more important. A similar observation was made by Corcoran et al. (2013) with spring Landsat 5 TM images. It means that the presence of water in the wetlands as observed

on the SAR images is critical for mapping wetlands. Brisco et al. (2011), Corcoran et al. (2011), and Millard and Richardson (2013), did not use spring imagery with higher water levels.

FQ6 images are more important than the FQ30 images. The steep incidence angle of RADARSAT-2 FQ6 images seems to be more favorable for wetland mapping than the shallow incidence angle of FQ30 images for my study. This happens during the spring leaf-off season, probably because of a better canopy penetration of the radar beam. For shrub and treed wetlands in Labrador Sokol et al. (2004) found that the ability of C-HH images to separate flooded and non-flooded forested areas increases with steep incidence angles, because of a greater interaction by the radar beam with the forest floor.

Similarly, Kandus et al. (2001) found that a combination of shallow and steep incidence angle is essential for mapping wetlands in treed and open areas because shallow incidence angles are important for delineating open water and steep incidence angles are required for mapping flooding zones in forested areas. Steep incidence angles are also better for mapping wetlands in forested areas during leaf-on season (Corcoran et al. 2011, 2013) for mapping wetlands in treed areas. To map both open wetlands and forested wetlands, LaRocque et al. (2015) were able to use images acquired with shallow incidence angles, but during leaf-off conditions. They identified the need of testing images acquired with steep incidence angles for their study area in New Brunswick.

With respect to the SAR variables, the most important variables are the HV and VH intensity images which are sensitive to volume scattering that depends mainly on the vegetative component of each class. RADARSAT-2 HV intensity images acquired during flooding and high water levels were already shown to be the most important for identifying wetlands in New Brunswick (LaRocque et al. 2015). I found in my study that the spring HV backscatter from the steep incidence angle, followed by the VH backscatter from the same acquisition were the most important polSAR images. Without the high water acquisition, Millard and Richardson (2013) and Corcoran et al. (2013) found that HH intensity images, followed by HV, were most important; and then VH and VV intensity images. With respect to the polarimetric products, I found that the real component of the correlation coefficient and the Cloude-Pottier α and β

angles were the most important, while the Freeman-Durden volume scattering variable was the most important followed by HV for Corcoran et al. (2011). From a temporal perspective my study follows a similar pattern to LaRocque et al. (2015), showing high water levels to be more important but with an important contribution from the contrasting drier period.

As stated, the DNR map provides the most recent estimates for the number, location and class of wetlands in the province that are greater than or equal to ½ hectare (Nova Scotia Environment 2009). My study resulted in a better accuracy in part as a result of this area constraint of the larger minimum mappable unit (mmu) for the DNR map, plus the fact that no forested polygons on site class 3 or higher could be classified as wetland. The discrepancy due to these restrictions was not accounted for, however upon visual inspection there are still substantial areas of non-treed wetlands that have been omitted and areas that were incorrectly classified.

4.5   Conclusions

My study showed that with RADARSAT-2 SAR polarimetric images acquired during high and low water levels, at steep and shallow incidence angles, with QuickBird optical and lidar DEM derivative data, allows an improved mapping of wetland areas in a part of Nova Scotia, over the current DNR map. The majority of misidentification of the GPS wetland validation sites is mainly due to wetlands not being classified in the right wetland class. The DNR map that the government of Nova Scotia is currently using has a lot of misidentification of the GPS validation sites. Most of the error in non-treed wetlands is associated to not being in the right wetland class, and most of the errors in treed wetlands are misclassified as upland.

There are several limitations in this study. I found confusions between the treed wetland and upland forest classes that might be reduced by using L-Band radar which is better able to penetrate the tree canopy (Touzi et al. 2009, LaRocque et al. 2015). My accuracy was lower than the one of LaRocque et al. (2015), who used images acquired in flooding conditions that were shown to strongly improve the classification accuracy. Finally, in this study, I used images and lidar data acquired during different years. Given that parts of my study area experienced

significant changes from fire and development over 2005 – 2013 periods, it would be better to get images acquired during closer years.

4.6   Acknowledgements

4.7   References

Bourgeau-Chavez, L. L., Endres, S., Battaglia, M., Miller, M. E., Banda, E., Laubach, Z., Higman, P., Chaw-Fraser, P., and Marcaccio, J. 2015. "Development of a bi-national Great Lakes coastal wetland and land use map using three-season PALSAR and Landsat imagery." *Remote Sensing*, Vol. 7, No. 7, pp. 8655-8682.

Bourgeau-Chavez, L. L., Riordan, K., Miller, N., Nowels, M., and Powell, R. B. 2008. "Remotely monitoring Great Lakes coastal wetlands with multi-sensor, multi-temporal SAR and multi-spectral data." *Proceedings of the 2008 International Geoscience and Remote Sensing Symposium (IGARSS 2008)*: pp. I-428 - I-429.

Breiman, L. 2001. "Random Forest". *Machine Learning*, Vol. 45, No. 1, pp. 5-32.

Breiman, L. 2003. "Manual of Setting up, Using and Understanding Random Forest", V4.0, University of California Berkeley, Statistics Department, Berkeley.

Brisco, B., Kapfer, M., Hirose T., Tedford, B., and Liu, J. 2011. "Evaluation of C-band polarization diversity and polarimetry for wetland mapping." *Canadian Journal of Remote Sensing*, Vol. 37, pp. 82-92.

Canada Committee on Ecological (Biophysical) Land Classification. 1988. "Wetlands of Canada." Ottawa: Sustainable Development Branch, Canadian Wildlife Service, Conservation and Protection, Environment Canada. pp. 1-61.

Cloude, S., and Pottier, E. 1997. "An entropy based classification scheme for land applications of polarimetric SAR." *IEEE Transactions on Geoscience and Remote Sensing,* Vol. 35, No. 1, pp. 68-78.

Congalton, R. 1991. "A review of assessing the accuracy of classifications of remotely sensed data." *Remote Sensing of Environment*, Vol. 37, pp. 35–46.

Cooley, S. 2015. "Terrain Roughness." Retrieved July 5, 2014 from http://gis4geomorphology.com/roughness-topographic-position/

Corcoran, J. M., Knight, J. F., Brisco, B., Kaya, S., Cull, A., and Murnagahn, K. 2011. "The integration of optical, topographic, and radar data for wetland mapping in Northern Minnesota." *Canadian Journal of Remote Sensing*, Vol. 37, No. 5, pp. 564-582.

Corcoran, J. M., Knight, J. F., and Gallant, A. L. 2013. "Influence of multi-source and multi-temporal remotely sensed and ancillary data on the accuracy of Random Forest classification of wetlands in Northern Minnesota." *Remote Sensing*, Vol. 5, No. 7, pp. 3212-3238.

Evans, D.L., Farr, T.G., van Zyl, J.J., and Zebker, H.A. 1988. "Radar polarimetry: Analysis tools and applications." *IEEE Transactions on Geoscience and Remote Sensing*, Vol. 26, No. 6, pp. 774-789.

Fournier, R., Grenier, A, M., Lavoie, A., and Hélie, R. 2007. "Towards a strategy to implement the Canadian Wetland Inventory using satellite remote sensing." *Canadian Journal of Remote Sensing*, Vol. 33, Supp. 1, pp. S1–S16.

Freeman, A., and Durden, S. 1998. "A three-component scattering model for polarimetric SAR data." *IEEE Transactions on Geoscience and Remote Sensing*, Vol. 36, No. 3, pp. 963-973.

Gislason, P., Benediktsson, J., and Sveinsson, J. 2006. "Random Forest for land cover classification." *Pattern Recognition Letters*, Vol. 27, pp. 294-300.

Goodman, J. W. 1976. "Some fundamental properties of speckles." *Journal of the Optical Society of America*, Vol. 66, No. 11, pp. 1145-1150.

Government of Canada. 2015. "Climate Data. Shearwater RCS, Environment Canada." Retrieved from http://climate.weather.gc.ca/index_e.html

GRASS-Wiki. 2015. "QuickBird." Retrieved from https://grasswiki.osgeo.org/wiki/QuickBird

Grenier, M., Demers, A.-M., Labrecque, S., Benoit, M., Fournier, R. A., and Drolet, B. 2007. "An object-based method to map wetland using RADARSAT-1 and Landsat ETM images: Test case on two sites in Quebec, Canada." *Canadian Journal of Remote Sensing*, Vol. 33, Supp. 1, pp. S2-S45.

Harris, A., Bryant, R. G., and Baird, A. J. 2005. "Detecting water stress in Sphagnum spp." *Remote Sensing of Environment*, Vol. 97, No. 3, pp. 371–381.

Harris, A., Bryant, R. G., and Baird, A. J. 2006. "Mapping the effects of water stress on Sphagnum: Preliminary observations using airborne remote sensing." *Remote Sensing of Environment*, Vol. 100, No. 3, pp. 363-378.

Hill, N, and Patriquin, D. 2014. "Ecological Assessment of the Plant Communities of the Williams Lake Backlands." Retrieved from Williams Lake Conservation Company: http://www.williamslakecc.org/documents/WLBFinalRep12Feb2014.pdf pp. 1-83.

Hogg, A., and Todd, K. 2007. "Automated discrimination of upland and wetland using terrain derivatives." *Canadian Journal of Remote Sensing*, Vol. 33, pp. S68-S83.

Jacobson, J. E., Ritter, R. A. and Koeln, G. T. 1987. "Accuracy of Thematic Mapper derived wetlands as based on National Wetland Inventory data." *American Society Photogrammetry and Remote Sensing Technical Papers*, 1987 ASPRS-ACSM Fall Convention, Reno, NV. pp. 109-118.

Jennes, J. 2002. "Topographic Position Index." Retrieved May 1, 2014 from http://www.jennessent.com/downloads/tpi_documentation_online.pdf/

Kandus, P., Karszenbaum, H., Pultz, T., Parmuchi, G., and Bava, J. 2001. "Influence of flood conditions and vegetation status on the radar backscatter of wetland ecosystems", *Canadian Journal of Remote Sensing*, Vol. 27, No. 6, pp. 651-662.

Krause, K. 2003. "Radiance Conversion of QuickBird Data – Technical Note." Retrieved from: https://apollomapping.com/wp-content/ user_uploads/2011/09/Radiance_Conversion_of_QuickBird_Data.pdf

LaRocque, A., Leblon, B., Bourgeau-Chavez, L., McCarty, J., French, N., and Woodward, R. 2015. "Evaluating wetland mapping techniques for New Brunswick using Landsat TM, ALOS-PALSAR and RADARSAT-2 dual-polarized images." *Canadian Journal of Remote Sensing* (submitted).

Lee, J.S., Grunes, M.R., Ainsworth, TL., Du, LJ., and Schuler, DL. 1999. "Unsupervised classification using polarimetric decomposition and the complex Wishart classifier." *IEEE Transactions on Geoscience and Remote Sensing*, Vol. 37, No. 5, pp. 2249-2258.

Lee J.S., Grunes, M.R., and Kwok R. 1994. "Classification of multi-look polarimetric SAR imagery based on the complex Wishart distribution." *International Journal of Remote Sensing*, Vol. 15, No. 11, pp. 2299-2311.

Li, J., and Chen, W. 2005. "A rule-based method for mapping Canada's wetlands using optical, radar and DEM data." *International Journal of Remote Sensing*, Vol. 26, No. 22, pp. 5051-5069.

Lopez-Martinez, C., Pottier, E., and Cloude, S.R. 2005. "Statistical assessment of eigenvector-based target decomposition theorems in radar polarimetry." *IEEE Transactions on Geoscience and Remote Sensing*, Vol. 43, No. 9, pp. 2058-2074.

Louppe, G., Wehenkel, L., Sutera, A., and Geurts, P. 2013. "Understanding variable importances in forests of randomized trees." *Advances in Neural Information Processing Systems*, Vol. 26, pp. 431-439.

Lynch-Stewart, P., Neice, P., Rubec, C. and Kessel-Taylor, I. 1996. "The Federal Policy on Wetland Conservation – Implementation Guide for Federal Land Managers." Ottawa, Environment Canada. pp. 1-20. Retrieved from http://nawcc.wetlandnetwork.ca/Fed%20Policy%20Wetland%20Conserv_Implement%20Guide%20for%20Fed%20Land%20Mgrs.pdf

Meingast, K. M., Falkowski, M. J., Kane, E. S, Potvin, L. R., Benscoter, B. W., Smith, A. M. S., Bourgeau-Chavez, L. L., and Miller, M. E. 2014. "Spectral detection of near-surface moisture content and water-table position in northern peatland ecosystems." *Remote Sensing of Environment*, Vol. 152, pp. 536-546.

Millard, K. and Richardson, M. 2013 "Wetland mapping with LiDAR derivatives, SAR polarimetric decompositions, and LiDAR–SAR fusion using a random forest classifier." *Canadian Journal of Remote Sensing*, Vol. 39, No. 4, pp. 290-307.

Millard, K., and Richardson, M. 2015. "On the importance of training data sample selection in random forest image classification: A case study in peatland ecosystem mapping." *Remote sensing*, Vol. 7, No. 7, pp. 8489-8515.

Moore, Grayson, and Ladson. 1991. "Digital terrain modelling: A review of hydrological, geomorphological, and biological applications." *Hydrological processes*, Vol. 5, No. 1, pp. 3-30.

Neily, P. D., Quiget, E., Benjamin, L., Stewart, B., and Duke, T. 2003. "Ecological land classification for Nova Scotia: Volume I, mapping Nova Scotia's terrestrial ecosystems." Halifax, N.S.: Nova Scotia Department of Natural Resources, Renewable Resources Branch. pp. 1-77.

Neily, P. D., Quigley, E., Benjamin, L., Stewart, B., and Duke, T. 2005. "Ecological land classification for Nova Scotia." Halifax, N.S.: Nova Scotia Department of Natural Resources, Renewable Resources Branch. pp. 1-70.

Nova Scotia Environment. 2009. "Nova Scotia Wetland Conservation Policy (Draft for Consultation)." pp. 1-24. Retrieved from http://www.gov.ns.ca/nse/wetland/docs/Nova.Scotia.Wetland.Conservation.Policy.pdf

Nova Scotia Museum of Natural History. 1989. "Natural History of Nova Scotia, The Dynamics of Nova Scotia's Climate." pp. 94-103. Retrieved from https://ojs.library.dal.ca/NSM/article/download/3752/3438

Ontario Ministry of Natural Resources. 2014. "Ontario Wetland Evaluation System Southern Manual 3rd edition, version 3.3." pp. 1-284. Queen's Printer for Ontario. Retrieved from http://files.ontario.ca/environment-and-energy/parks-and-protected-areas/ontario-wetland-evaluation-system-southen-manual-2014.pdf

Ou, C., Zhang, Y., LaRocque, A., Leblon, B., Webster, K., McLaughlin, J., and Barnett, P. 2014. "Model calibration for mapping permafrost using Landsat-5 TM and RADARSAT-2 images." *Proceedings of the 2014 IEEE International Geoscience and Remote Sensing Symposium (IGARSS 2014)*: pp. 4883-4886.

Ozdarici-Ok, A., Akar, O., and Gungor, O. 2012. "Evaluation of Random Forest method for agricultural crop classification." *European Journal of Remote Sensing*, Vol. 45, No. 3, pp. 421-432.

Ozesmi, S. L., and Bauer, M. E. 2002. "Satellite remote sensing of wetlands." *Wetland Ecology and Management*, Vol. 10, pp. 381-402.

PCI Geomatica [Computer software]. 2014. Retrieved from http://www.pcigeomatics.com

Pietroniro, A., and Leconte, R. 2005. "A review of Canadian remote sensing and hydrology, 1999-2003." *Hydrological Processes*, Vol. 19, No. 1, pp. 285-301.

R Development Core Team 2012. "R: A language and environment for statistical computing." Vienna, R Foundation for Statistical Computing. Retrieved from https://www.r-project.org/

Rebelo, L. S. 2010. "Eco-hydrological characterization of inland wetlands in Africa using L-Band SAR." *IEEE Journal of Selected Topics in Applied Earth Observations and Remote Sensing*, Vol. 3, No. 4, pp. 554-559.

Rodriguez, E. and Martin, J.M. 1992. "Theory and design of interferometric synthetic aperture radars." *IEE Proceedings F Radar and Signal Processing*, Vol. 139, No. 2, pp. 147-159.

Sader, A., Ahl, D., and Liou, W. 1995. "Accuracy of Landsat-TM and GIS rule-based methods for forest wetland classification in Maine." *Remote Sensing of Environment,* Vol. 53, pp. 133-144.

Sokol, J., McNairn, H., and Pultz, T. 2004. "Case studies demonstrating the hydrological applications of C-band multipolarized and polarimetric SAR." *Canadian Journal of Remote Sensing,* Vol. 30, No. 3, pp. 470-483.

Strobl, C., Boulesteix, A.-L., Kneib, T., Augustin, T., and Zeileis, A. 2008. "Conditional variable importance for Random Forests." *BMC Bioinformatics*, Vol. 9, No. 1, pp. 307.

Tiner, R.W. 1999. *Wetlands indicators: a guide to wetland identification, delineation, classification, and mapping*. Lewis Publishers, Boca Raton (Florida, USA).

Touzi, R. 2007. "Target Scattering Decomposition in Terms of Roll-Invariant Target Parameters." *IEEE Transactions on Geoscience and Remote Sensing*, Vol. 45, No. 1, pp. 73-84.

Touzi, R., Deschamps, A., and Rother, G. 2009. "Phase of Target Scattering for Wetland Characterization Using Polarimetric C-Band SAR." *IEEE Transactions on Geoscience and Remote Sensing*, Vol. 47, No. 9, pp. 3241-3261.

Touzi, R., Deschamps, A., and Rother, G. 2007. "Wetland Characterization using Polarimetric RADARSAT-2 Capability." *Canadian Journal of Remote Sensing*, Vol. 33, Supp. 1, pp. 56-67.

Touzi, R., Goze, S., Le Toan, T., Lopes, A., and Mougin, E. 1992. "Polarimetric discriminators for SAR images." *IEEE Transactions on Geoscience and Remote Sensing*, Vol. 30, No. 5, pp. 973-980.

van Beijma, S., Comber, A., and Lamb, A. 2014. "Random Forest classification of salt marsh vegetation habitats using quad-polarimetric airborne SAR, elevation and optical RS data." *Remote Sensing of Environment*, Vol. 149, pp. 118-129.

van Zyl, J.J., Zebker, H.A., and Elachi, C. 1987. "Imaging radar polarization signatures: Theory and observation." *Radio science*, Vol. 22, No. 4, pp. 529-543.

Wang, J., Shang J., Brisco, B., and Brown, R. 1998. "Evaluation of multi-date ERS-1 and multispectral Landsat imagery for wetland detection in Southern Ontario." *Canadian Journal of Remote Sensing*, Vol. 31, pp. 214-224.

Warner, B.G. and Rubec, C.D.A. (Eds.). 1997. "The Canadian Wetland Classification System. (2nd edition)." National Wetlands Working Group. Wetlands Research Centre. University of Waterloo. Ontario, pp. 1-68.

Waske, B., Heinzel, V., Braun, M., and Menz, G. 2007. "Random Forests for classifying multi-temporal SAR data." *In Proceedings Envisat Symposium*, Montreux, Switzerland. April 23-27, 2007.

Waske, B. and Braun, B. 2009. "Classifier ensembles for land cover mapping using multi-temporal SAR Imagery." *ISPRS Journal of Photogrammetry and Remote Sensing*, Vol. 64, pp. 450-457.

Wilson, J., and Gallant, J. C. 2000. *Terrain analysis: Principles and applications*. New York: Wiley.

Zebker, H.A., van Zyl, J.J., and Held, D.N. 1987. "Imaging radar polarimetry from wave synthesis." *Journal of Geophysical Research*, Vol. 92, No. B1, pp. 683-701.

Chapter 5.   Mapping wetlands in Nova Scotia with multi-beam RADARSAT-2 Polarimetric SAR, Landsat 8 and the Nova Scotia Digital Elevation Model.

Abstract

Wetlands were mapped in an area southwest of Halifax, Nova Scotia using combinations of multi-date RADARSAT-2, provincial Digital Elevation Model and fall Landsat 8 imagery. Twelve classes were established at the outset for this project, of which six were wetland classes. Field data was collected with geographic coordinates recorded using a GPS receiver. Most points were used to help create a series of representative polygon areas used to train the software during the automated computer processing stage. For classification, a technique that did not rely on data following any particular distribution was needed so the Random Forests (RF) Classifier was chosen. The RF Classifier could also accommodate the many layers of input bands including those from different types of data and imagery. 237 GPS points collected in-situ were set aside to assess the accuracy of the resulting classification maps and the Nova Scotia Government wetland inventory maps.

The best accuracy for discrete wetland classes (52.6%) was achieved from the combination of all three sources and the general wetland classification (77.4%) was achieved from the combination of the provincial DEM with Landsat 8. The provincial DEM alone was 22.6% and 56.2% and the Nova Scotia Government wetlands were lowest at 9.5% for wetland class and 46.7% for the nonspecific-class wetlands. Higher resolution inputs, used in a preceding study, still produced a better accuracy for discrete wetland classes (64.2%) and the general wetland classification (86.9%). However, though the provincial DEM is less accurate and the input spatial resolution is coarser, the higher radiometric resolution of Landsat 8 compared to QuickBird may have offset the errors for some classes.

Keywords: wetland mapping, wetlands, RADARSAT-2, lidar, QuickBird, Landsat 8, polarimetric SAR

5.1 Introduction

Nova Scotia's "no net loss" program for wetlands (i.e. equal offsetting of loss using reclamation or restoration) is a critical policy that aims to protect an essential feature of the landscape. However, because some wetlands have not yet been identified, the Nova Scotia Department of Natural Resources (NSDNR) wetland inventory is incomplete. Thus, it is important that methods which can help improve the inventory be explored. An ideal mapping method is able to identify both the type (e.g. marsh, fen, bog, or swamp) and location of wetlands. This study used medium resolution data (30 m) to map wetlands and accuracy was measured against field data. Further comparisons were made at the basin level for the McIntosh Run to evaluate generalized land classification information.

As stated by Schott (2007), remote sensing provides a synoptic viewpoint which, after processing and interpreting the data, leads to a land classification that can be used for long-term monitoring and other natural resource management applications. Furthermore, by looking beyond the visible range of the electromagnetic spectrum (such as aerial photography), much more information can be derived. The perspective afforded by a classified, georeferenced land cover map allows for analysis of patterns and interactions in the surrounding landscape. In addition, care must be taken as well when formulating a policy or mapping program. For instance, the government of New Brunswick enforced wetland designation meant to assess the cost of damage experienced in flood-prone areas of the province. It was meant to protect development from the risks of flooding however because it was a predictive layer it was not always accurate and could potentially delay development needlessly (Telegraph Journal 2011). The answer is to ensure the proper use of the results. In the case of this study, like the situation in New Brunswick, the output is meant as an analytical result to assessing alternative wetland mapping techniques. Planning applications likely require an output with more certainty only available with individual wetland assessments.

It was expected that using medium resolution data would result in a lower accuracy for mapping individual wetlands, because there is a spatial limit to what can be resolved. However, it is important to understand wetlands from a regional perspective such as a secondary basin level because wetlands act as reservoirs, provide fire protection, attenuate flooding and reduce

pollutants and sediment (Brooks et al. 2013). Even when the resolution is lower it provides a source of information that can help identify where development may conflict with features in sensitive areas. Thus, a system is necessary that is standard to the region - in the case of Nova Scotia, lidar is not yet available for the entire province. The cost of acquiring high resolution data may be prohibitive, so in the meantime it is important to initiate a mapping program now as it provides a baseline of information from which to build on. The use of RADARSAT-2 imagery would be practical for a larger wetland mapping project but lack of available high resolution optical imagery and lidar means that alternatives should be considered. For this reason, this paper examined the same principle of mapping wetlands using a radar, terrain and optical imagery combination, but using data that is easier to obtain and process. In this case the provincial elevation model is used and Landsat 8 imagery; both of which are freely available.

In my study, the comparison of limited availability data (high resolution) with data that is easier to obtain at the province level (medium resolution) was shown. Following the combination of data and processing detail established in the previous high resolution study, the medium resolution data was compared against the high resolution accuracy for mapping individual wetlands. When comparing accuracy only the classification from the best case high resolution classification was used. In addition to discrete location, other basin level metrics were quantified and assessed. This method, using medium resolution data, could have an application to map wetland location in the province as well as quantifying a wetland presence generalized at the watershed scale. Further analysis was also done to understand the differences in DEMs aside from their spatial resolution.

5.2   Materials and Methods

5.2.1   Study Area

The study area, situated by the Atlantic Ocean, is located just south of Halifax, Nova Scotia between 44° 30' N and 44° 40' N, and 63° 32' W and 63° 41' W (Figure 5.1). Much of the study area is accessible through public land in Long Lake Provincial Park and the Herring Cove Backlands. Although there are significant zones that are experiencing increased pressure from urban development, most of the study area still has natural forested landscapes.
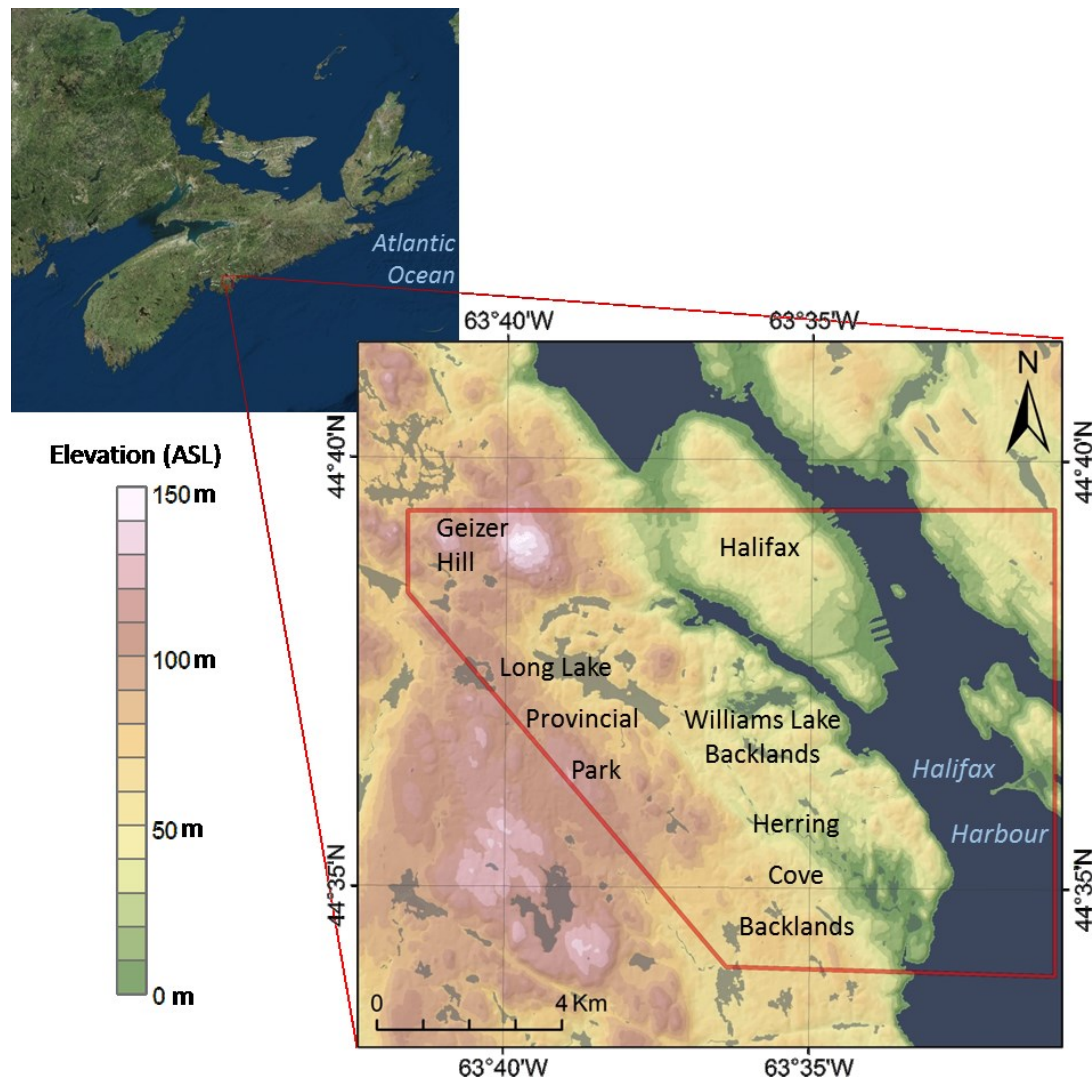
Figure 5.1: Location and digital elevation model of the study area.

As measured from the digital elevation model (DEM) (Figure 5.1), the elevation in the study area ranges from 0 m above mean sea level (AMSL) along the coast of Halifax Harbour to 150 m AMSL on Geizer Hill at the northwest edge of the study area. The drainage network is dominated by the McIntosh Run which is approximately 13.5 km long and drains an area of 33.6 km². As elsewhere in Nova Scotia, the study area experiences a modified continental climate, but its proximity to the Atlantic Ocean leads to more frequent rain and fog occurrences (Nova Scotia Museum of Natural History 1989).

According to the Nova Scotia's Ecological Land Classification (ELC) soil drainage classes show that the area is a mixture of well drained soils and imperfectly drained soils (Neily et al.

2003). Like poorly drained soils, imperfectly drained soils are also expected to provide suitable conditions to promote wetland development. In addition, most of the forested soils are acidic and generally coarse textured podzols where leaching of soil nutrients is common (Canada Committee on Ecological Biophysical Land Classification 1988). Cementation of leached organic carbon, iron, and aluminum leads to the creation of hardpan, which can subsequently cause poor drainage and wetland development (Canada Committee on Ecological Biophysical Land Classification 1988). The study area contains most of the relevant wetland classes of interest that can be found in the province of Nova Scotia, such as peatland (which includes ombrotrophic peatlands or bogs, and minerotrophic peatlands or fens), and swamps. However, because the area is mainly forested, large marshes are absent in the area, so this class was merged with the open-water class to form a so-called open-water/marsh complex. Also, fens and swamps are more common than ombrotrophic bogs in eastern part of the study area around the Williams Lake Backlands, because it has a barrens landscape that is "flow-through", meaning that definite in- and out-flows are typical (Hill and Patriquin 2014).

Twelve classes (Table 5.1) were chosen to represent the land cover of the study area, namely: barren, grass, industrial, lake, open-water/marsh complex, open bog, open fen, shrub/treed fen/bog, swamp, upland sparse vegetation, upland forest, and urban. The wetland classes were based on the Canadian Wetland Classification System (Warner and Rubec 1997).

Table 5.1: Mapping legend showing classes used for the classification process along with the description from Canadian Wetland Classification System that was used to help identify landcover classes in the field.

Class colour	Class ID and name	Description
	1 - barren	area with more than 50% exposed rock outcrop and less than 25% vegetation.
	2 - grass	area of manicured grass such as recreation fields and golf courses.
	3 - industrial	built-up areas consisting of large, low-rise industrial buildings and parking lots.
	4 - lake	deeper water with no apparent vegetation.
	5 – open-water/marsh complex	combination of open-water wetland and shallow marsh. Marshes have shallow water levels that can fluctuate daily and expose the soil. Shallow or open-water wetlands have water depths up to 2m that are typically stable, but soil may occasionally become exposed.
	6 - open bog	ombrotrophic peatland area with primarily ericaceous plants and sphagnum, and less than 25% tree coverage. They have a raised or level surface and are not affected by runoff or ground water.
	7 - open fen	minerotrophic peatland with ericaceous plants, sedges and brown mosses and less than 25% tree coverage. The ground and surface water movement is more stable, and exposed water in channels can form characteristic patterns.
	8 – shrub/treed fen/bog	peatland with more than 25% tree coverage. Treed fens and bogs are not easily differentiated and so are combined for this research.
	9 - swamp	wetlands dominated by trees (typically > 30% cover) that are influenced by minerotrophic groundwater. They can be found on either mineral or peat soils and are typically considered the driest wetland type.
	10 - upland sparse vegetation	area with less than 50% exposed rock outcrop. vegetation primarily low and ericaceous.
	11 - upland forest	forested stand containing trees at least 3m in height.
	12 - urban	built-up areas consisting of high-rise urban core buildings, streets and sidewalks.

5.2.2 Imagery

Two types of satellite imagery were used in the classifications: (1) Multispectral Landsat 8 imagery acquired from October 6, 2013 (pixel size = 30 m, swath = 185 km); and (2) RADARSAT-2 SLC fine quad-pol (FQ) C-band (5.54 cm wavelength) polarimetric SAR imagery (pixel spacing of 8 m, nominal resolution of 12 m, and swath of 25 km) (Table 5.2). The Landsat 8 imagery was available from the United States Geological Survey. It is 12-bit imagery with eight multispectral bands (coastal aerosol 430 – 450 nm, blue 450 – 510 nm, green 530 – 590 nm, red 640 – 670 nm, near infrared 850 – 880 nm, short-wave infrared-1 1570 – 1650 nm, short-wave infrared-2 2110 – 2290 nm, cirrus 1360 – 1380 nm). The image was previously georeferenced, and I reprojected it using the same projection and datum with the following: UTM zone 20, row T, NAD83. The RADARSAT-2 imagery was resampled to 30 m to match the Landsat 8 spatial resolution.

The RADARSAT-2 polarimetric SAR images were provided through the Science and Operational Applications Research Education (SOAR-E) program of the Canadian Space Agency. They were acquired using two fine quad-pol beam modes (FQ6 and FQ30) and a descending (D) orbit. The FQ6 beam mode corresponds to incident angles ranging from 24.6° to 26.4°. The FQ30 beam mode corresponds to incident angles ranging from 47.5° to 48.7°. The images were acquired during the descending orbit, so they were west-looking and acquired early morning. Both beam mode SAR imagery were acquired in April, when the water level is high in the wetlands and in August-September, when the water level is low (Table 5.2). In addition, the low water level images were acquired under dry conditions in late summer, while the high water level images were acquired under wet conditions, from a different year, in early spring (no frost or snow).

Table 5.2: Characteristics of the RADARSAT-2 polarimetric SAR images used.

Date	Beam mode	water level	Precipitation (mm) (*)
August 19, 2010	FQ30	low	0
September 1, 2010	FQ6	low	0.6
April 5, 2013	FQ30	high	17.4
April 18, 2013	FQ6	high	16.1

Millimetres of rain equivalent recorded at the Shearwater RCS weather station during the six days prior to image acquisition.

5.2.3   Other data

The Nova Scotia provincial elevation dataset is a series of mass points (general points denoting elevation), plus breaklines and spot heights showing important changes in topographical shape (Nova Scotia Geomatics Centre 2015). It is derived from aerial photogrammetry procedures (using principles of perspective and projective geometry) and has complete coverage for the province. While the input elevation point data is relatively sparse and accuracy equal to lidar is not practical (especially in treed areas), this dataset is still of value as a start to calculate terrain variables such as low slope needed for isolating potentially wetter areas. These points were used in the process to create contour elevation lines.

The Nova Scotia provincial elevation contour dataset was used to interpolate the DEM for this study. It will be called hereafter *"NS DEM"*. Unlike lidar, the original contours were derived using coarser data and different techniques and there is no canopy height model. The following derivatives were created from the NS DEM:

- Slope (SLP)
- Compound Topographic Index (CTI)
- Curvature (CRV)
- Topographic Position Index (TPI)

Nova Scotia has a thematic layer which models wet areas. This Wet Areas Map layer was created using the Wet Areas Mapping (WAM) process (an algorithm constructed by, and the intellectual property of, the Nexfor/Bowater Forest Watershed Research Centre at the University of New Brunswick) (http://novascotia.ca/natr/forestry/gis/Wam_wtbl_2012.xml). Rather than use this layer, similar outputs using the NS DEM were redone for this study. This provides consistency in this study compared to the high resolution study and gives more transparency to modeling procedure.

Other data needed for the study included in situ observations at a number of points collected with GPS, with information recorded to show wetland type. The wetland map extracted from the classified image was compared to GPS field data (see details in the next section). Finally the wetland map that is currently in use by the government of Nova Scotia (Figure 5.2) and that can be requested from the Nova Scotia Department of Natural Resources

(DNR) was obtained. It was also used as a comparison to the GPS points during the accuracy stage. It will be called hereafter *"DNR map".*
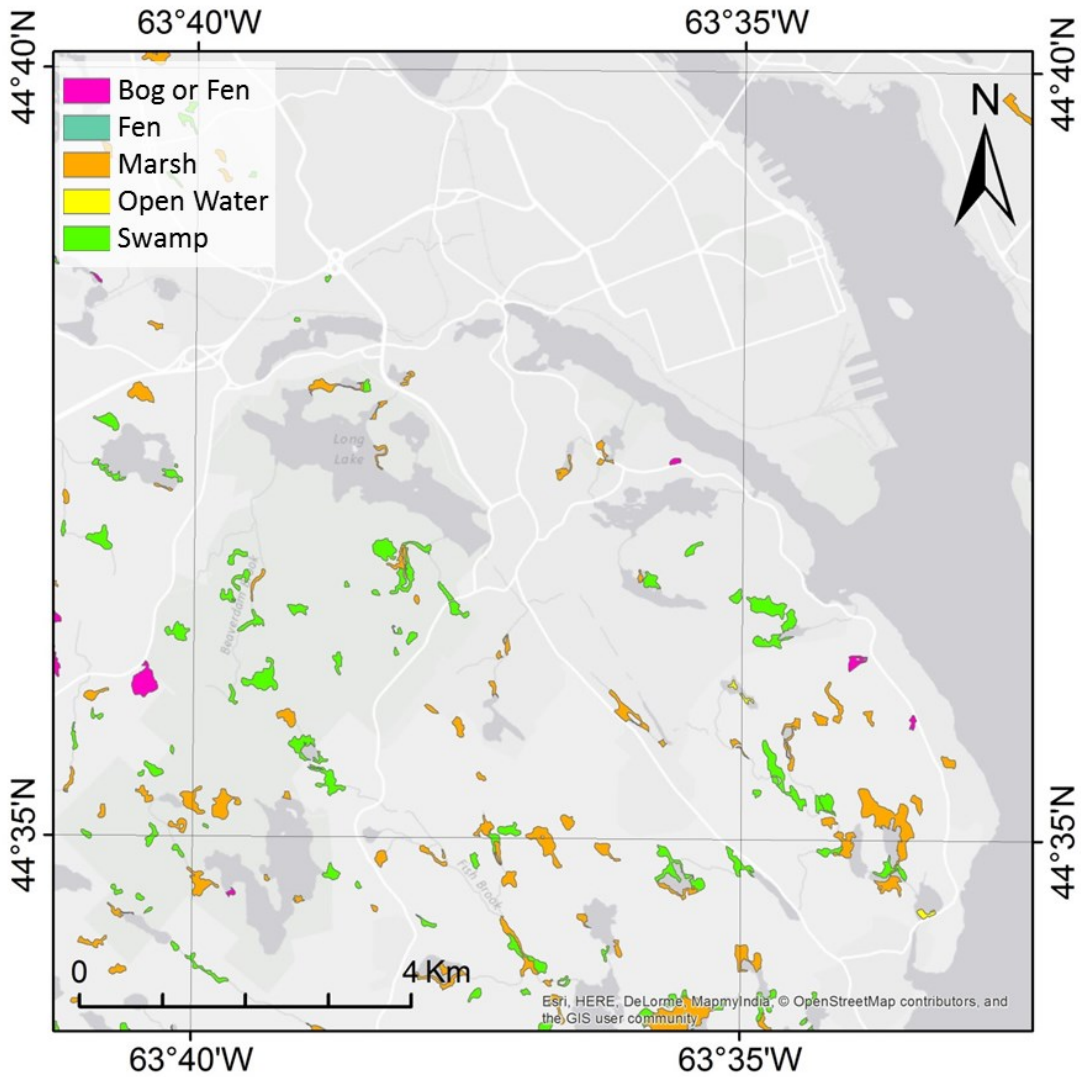
Figure 5.2: Nova Scotia DNR map of the study area.

5.2.4   Field data collection

During low water levels in the wetlands mostly in the period from August to September 2012, field observations were made at 558 GPS sites. Site visits were planned to cover as much of the study area as possible (Figure 5.3), especially ensuring that the different soil drainage classes mapped by the ELC were considered. All the sites were selected with a relatively large extent of the particular land cover. Field work was carried out during times when vegetation had not yet senesced so that vegetation could assist in identifying wetlands and non-wetland

areas. Among all the 558 visited sites, 318 sites were used to delineate training areas for the image classification and 240 points being used to assess the mapping accuracy for the map produced from the image classification (Table 5.3).
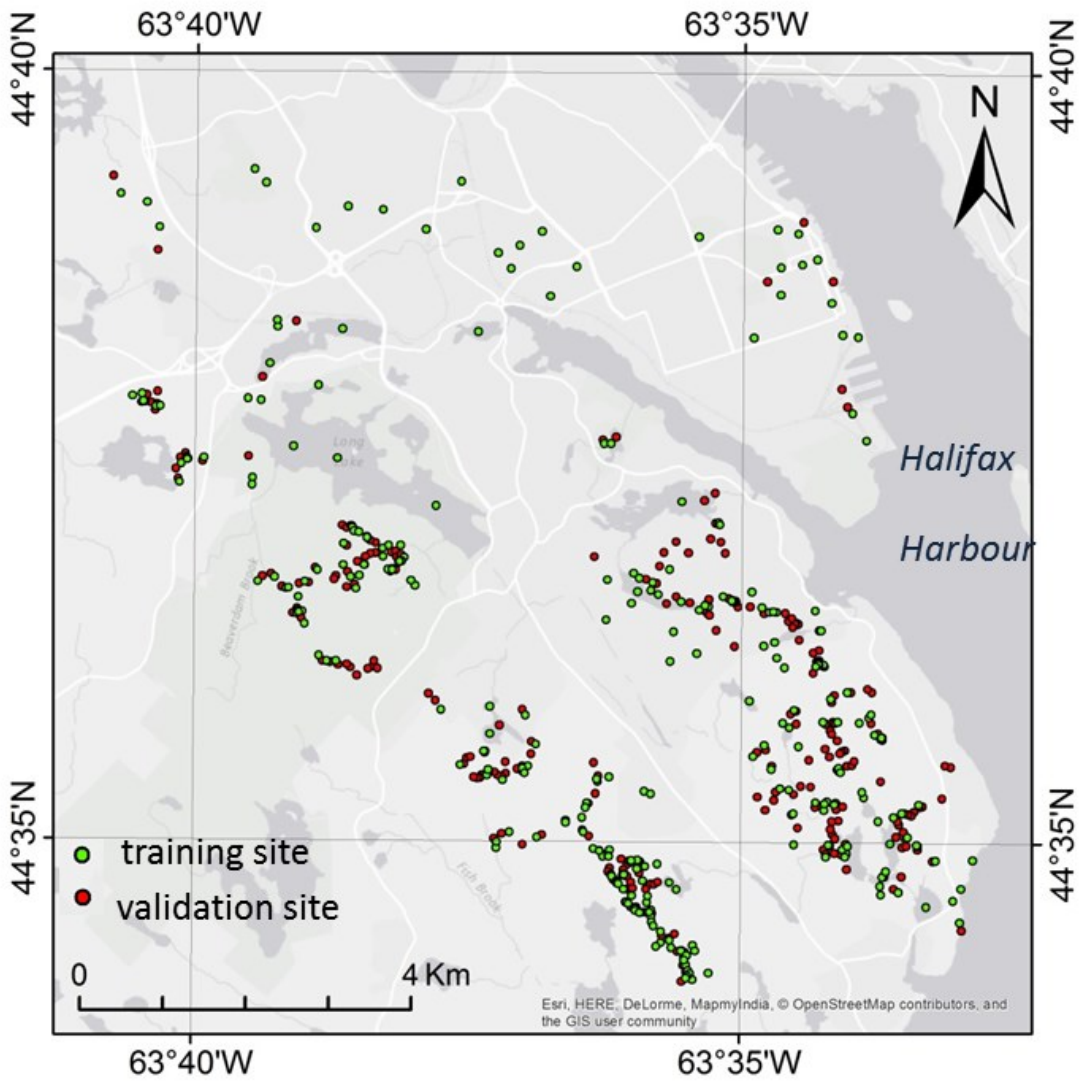
Figure 5.3: Training sites and validation sites of the twelve classes used.

Table 5.3: Number of training sites and validation sites for each class.

Class name	Training Sites	Validation Sites
barren	19	12
grass	16	3
industrial	10	4
lake	14	6
open-water/marsh complex	12	6
open bog	22	19
open fen	32	30
shrub/treed fen/bog	52	24
swamp	38	52
upland - sparse vegetation	63	34
upland forest	33	47
urban	7	3
Total	318	240

Among all the visited sites, 287 sites (170 training sites and 137 validation sites) were considered as being wetland (Table 5.3). Sites were defined as a wetland, such as in Tiner (1999), when the water table is close to (less than 10 cm) or at the surface, or when I found indicator plants, soil hydromorphy, or other evidence of an area that is often saturated with water. Several of the wetland sites were initially found by interpretation of aerial photographs and the slope model, or because they had been previously mapped as wetland on the DNR Map (Figure 5.2).

Planned wetland transects and routes between destinations were not always followed because of the rough terrain or dense vegetation. Custom maps showing trails and a low-slope mask (less than 2°) created from the lidar DEM were made in Mapwel (2012) software and uploaded to a Garmin 60cx GPS receiver. On arrival in the field a GPS fix was acquired and the time on the camera was synchronized with the GPS clock so that the photographs could be geocoded in the lab using GeoSetter (2012) software. A compass was used to identify bearing on photos if important and a 1:50,000 topographic paper map (NTS 011D12) was used to aid navigation. In the field, a special effort was made to visit the following sites: sites that represent the transition between upland and wetland, sites that did not match the low-slope mask, and sites along the route which confirmed the low-slope mask. On each site, the following

measurements were made: GPS location, elevation, class identification based on the descriptions in Table 5.1, and ground photographs.

5.2.5   NS DEM processing and comparison to the lidar DEM

NS DEM processing was performed in ArcGIS® (ESRI 2015) using a similar method to the one used for lidar in Chapter 4 of this thesis. Elevation values, based on the Nova Scotia Topographic Database contours, were used to interpolate a digital elevation model surface grid with the Topo to Raster algorithm. Topo to Raster was chosen as the interpolator because it was developed specifically for creating realistic landform that conforms to hydrologic application (Hutchinson et al. 2011). The following four derivative variables were calculated: (1) the Slope (SLP) that shows where the surface water runoff is slower (or faster); (2) the Compound Topographic Index (CTI) that shows wetter areas using slope combined with where flow is predicted to accumulate; (3) the Curvature (CRV) that shows deceleration (or acceleration) of water runoff; and (4) the Topographic Position Index (TPI) that gives the relative position in the landscape (hilltop to valley bottom).

In the case of elevation, absolute accuracy here refers to a value based on a vertical datum. The elevation points for the province are not particularly accurate in that absolute sense, plus the error is not consistent. However, concerning the creation of derivative products such as slope, it may still work fine at the scale necessary to aid wetland prediction. That scale is referred to as the *topo scale* by Wilson and Gallant where the surface morphology that affects catchment hydrology can be measured (Wilson and Gallant 2000). Both the NS DEM and lidar DEM are at a scale suitably characterized by the topo level. The lidar DEM is considered very accurate from an absolute sense (and therefore relative too), and though the NS DEM is less accurate absolutely, it is possible to have relative accuracy (i.e. relative to the topo scale needed for this application). The absolute accuracy of both the NS DEM and the lidar DEM will be measured by calculating a root mean squared error (RMSE) against survey markers recorded with a very accurate position and elevation value from the Nova Scotia Coordinate Referencing System (NSCRS). The RMSE will give an indication of the error of the predicted elevation data (the DEMs) by aggregating the magnitude of error made up of the difference in elevation at

each survey marker. This error, referred to in this thesis as *absolute error*, is compared to a precise vertical datum used for the survey markers (i.e. orthometric height).

Slope (as identified in chapter four of this thesis), is one of the more important derivatives in predicting modeled wetland. Errors in DEMs have been shown to be clearly correlated with terrain slope (Castrignano, Buttafuoco, Comolli, and Ballabio 2006). They have found that the most significant occurred in the steepest part of their study area (2006).

For comparison of relative accuracy, the NS DEM and the lidar DEM were both resampled to 8 m with equal origin specified so that pixel overlap was exactly matched. Slope was calculated for each DEM in ArcGIS® and one slope grid was converted using centroids to points retaining slope values. The corresponding value from the other slope grid was appended to the points so that there were two columns, each row identifying two slope values for each individual 8 m cell in the study area. Values were rounded to the nearest integer. These two columns were input to IBM SPSS Statistics (2015) and a cross tabulation was performed to identify the frequency of overlapping slope values for each slope grid.

The output matrix from the cross tabulation operation was graphed in Excel, with NS DEM slope values from 0 to 15 degrees graphed against each integer value of lidar slope from 0 to 10 degrees. The graph shows the amount (%), range, and distribution of NS DEM slope compared to each value of the lidar slope, with the purpose of showing the correlation between the two slope grids. The lidar DEM is considered the more accurate and the purpose of the correlation analysis is to provide insight into how the NS DEM can be used. In other words, the question to be addressed is if the NS DEM is relatively accurate at lower slopes where wetlands are more likely to occur.

5.2.6 Satellite Image processing

Most of the image processing was performed in PCI Geomatica 2014®. The Landsat 8 imagery digital numbers were converted to reflectance values using the top of atmosphere (TOA) reflectances procedure (United States Geological Survey 2015).

$$\rho\lambda' = M_p Q_{cal} + A_p \qquad\qquad (5)$$

where:

- $\rho\lambda'$ = TOA planetary reflectance, without correction for solar angle.
  M_ρ = Band-specific multiplicative rescaling factor from the metadata.
  A_ρ = Band-specific additive rescaling factor from the metadata.
  Q_{cal} = Quantized and calibrated standard product pixel values (DN)

TOA reflectance with a correction for the sun angle is then:

$$\rho\lambda = \frac{\rho\lambda'}{\sin(\theta_{SE})} \qquad\qquad (6)$$

where:

$\rho\lambda$ = TOA planetary reflectance
θ_{SE} = Local sun elevation angle provided in the metadata.
θ_{SZ} = Local solar zenith angle; $\theta_{SZ} = 90° - \theta_{SE}$

The RADARSAT-2 polarimetric SAR images were processed in the same way as the high resolution study except for the spatial resolution. They were filtered for removing speckle, as speckle can be considered noise and its intensity must be attenuated in order to resolve fine details on SAR images (Goodman 1976). First, the HH, HV, VV, and VH intensity images were filtered using a 7x7 Lee Adaptive filter with the FLE program of PCI Geomatica 2014® (PCI Geomatica 2014). The full polarimetric SAR images were filtered by applying a 5x5 polarimetric Lee speckle filter (Lee et al. 1999) with the PSPOLFIL program of PCI Geomatica 2014®. This filter preserves polarimetric properties by filtering each element of the covariance matrix independently, while maintaining spatial information. These filtered images were then used to compute the polarimetric variables that are listed in Table 5.4.

Both the intensity and polarimetric products were orthorectified with PCI Geomatica 2014® Orthoengine using the Radar Satellite Math Modelling method, with the Rational Function extracted from the image and a DEM. Fourteen check points were used to test the orthorectification of an image and resulted in a root mean square of 0.24 pixels in the x and

0.76 in the γ (see appendix C). This resulted in an output which corresponded very well with a corner reflector placed in field and other features in other high resolution imagery.

Table 5.4: List of polarimetric parameters used in the study.

Variable	Definition	Authors
Pedht	Pedestal height = minimum of Pr (copolarized signature)	van Zyl et al. 1987
Totpow	Total power = $\|S_{hh}\|^2 + 2\|S_{hv}\|^2 + \|S_{vv}\|^2$	Lopez-Martinez et al. 2005
γ	correlation coefficient $\gamma = S_{hh}S_{vv}/(\|S_{hh}\|^2\|S_{vv}\|^2)^{1/2}$	Rodriguez and Martin 1992
$\delta_{HH\text{-}VV}$	Phase difference	Lopez-Martinez et al. 2005
Pr_{max}	Maximum of the received power	Touzi et al. 1992
Pr_{min}	Minimum of the received power	Touzi et al. 1992
FP	Fractional polarisation = $Pr_{max} - Pr_{min}/Pr_{max} + Pr_{min}$	Zebker et al. 1987
CV	Coefficient of Variation = Pr_{min}/Pr_{max}	van Zyl et al. 1987
S_{max}	Maximum of the scattered intensity	Evans et al. 1988
S_{min}	Minimum of the scattered intensity	Evans et al. 1988
ND	Normalized Difference $ND_s = S_{max} - S_{min}/S_{max} + S_{min}$	Evans et al. 1988
d_{max}	Maximum of the degree of polarization	Touzi et al. 1992
d_{min}	Minimum of the degree of polarization	Touzi et al. 1992
Δd	$d_{max} - d_{min}$	Touzi et al. 1992
α_s	Magnitude of the symmetric scattering	Touzi 2007
$\Phi_{\alpha s}$	Phase of the symmetric scattering	Touzi 2007
ψ	Maximum polarization parameter for orientation	Touzi 2007
τ_m	Maximum polarization parameter for helicity	Touzi 2007
λ	Touzi dominant eigenvalue	Touzi 2007
FD dbl	Power related to double-bounce scattering	Freeman and Durden 1998
FD surf	Power related to surface scattering	Freeman and Durden 1998
FD vol	Power related to volume scattering	Freeman and Durden 1998
CP H	Entropy $(H) = \sum_{i=3}^{3} -p_i \, log_3(p_i)$	Cloude and Pottier 1997
CP A	Anistropy $(A) = \frac{\lambda_2 - \lambda_3}{\lambda_2 + \lambda_3}$	Cloude and Pottier 1997
CP α	Alpha angle $(\overline{\alpha}) = \sum_{i=3}^{3} \rho_i \, \alpha_i$	Cloude and Pottier 1997
CP β	Beta angle $(\beta) = 2 * $ orientation angle (ψ)	Cloude and Pottier 1997

5.2.7   Image classification

Representative training areas of each of the twelve land cover classes were delineated in ArcGIS® as polygon shapefiles, by using information collected in the field (from 318 GPS training sites), high resolution aerial photography and profiles of raw first and ground lidar points. The training areas were randomly located throughout the study area, but the number of training areas by class reflected the relative frequency of the different land covers inside the study area, as shown in Figure 5.4. These are the same training areas used for the high resolution study.
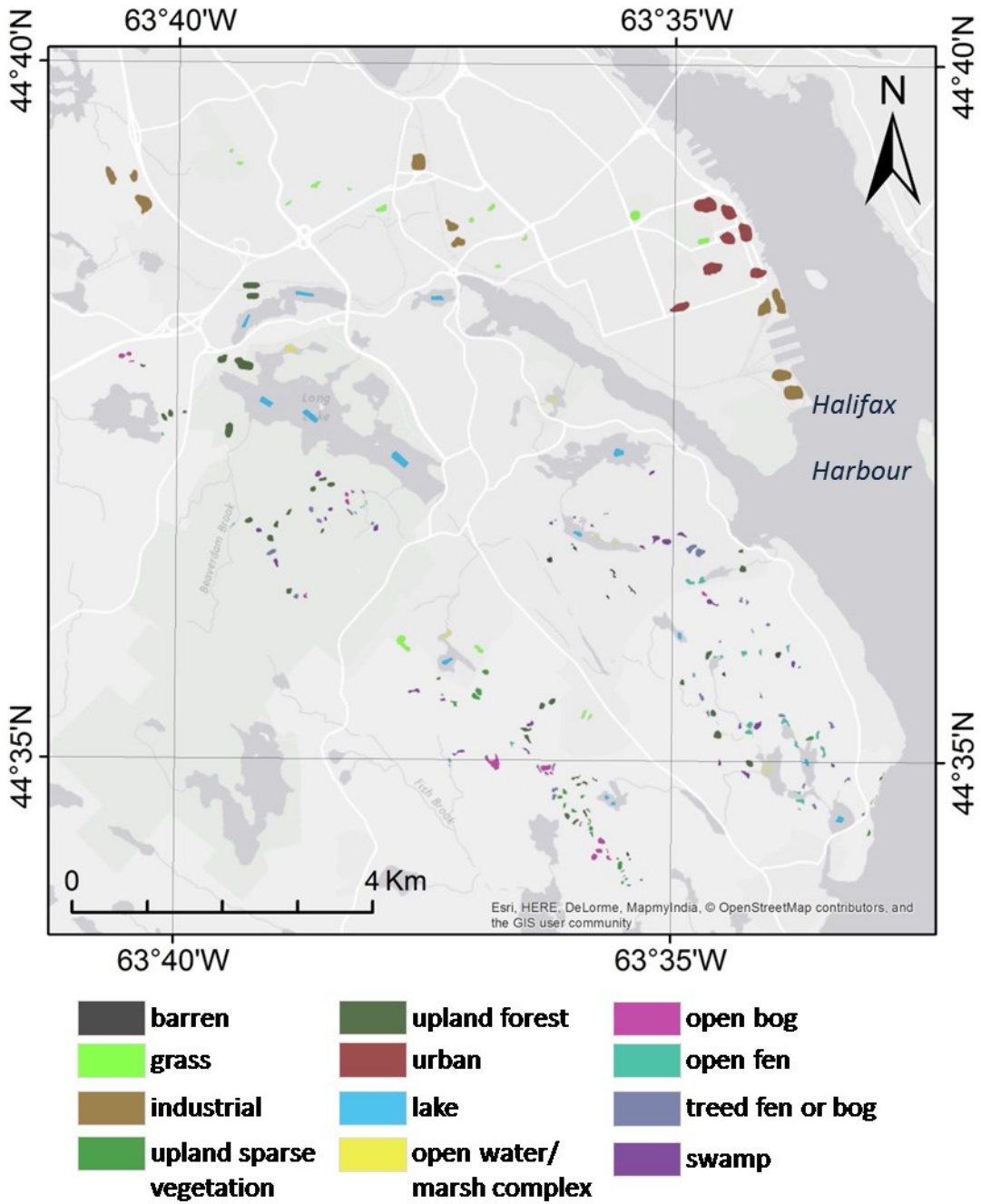
Figure 5.4: Location of the training areas for each class delineated using GPS points, aerial photography, and the raw lidar point cloud.

In this study a non-parametric decision tree type classifier, Random Forests (RF), was used because it does not assume normal distribution of the input data. It can therefore accommodate the data distribution differences between polarimetric SAR (Wishart) (Lee et al. 1994) and optical (Gaussian) data. RF was used to classify the following combinations of the NS DEM, Landsat 8 and RADARSAT-2 polarimetric SAR images:

1. Four NS DEM derivative variables

2. Landsat 8 coastal aerosol, blue, green, red, NIR images, SWIR 1, SWIR 2, and cirrus

3. RADARSAT-2 dual-polarized (HH and HV) intensity images

4. NS DEM derivatives and eight Landsat 8 images

5. NS DEM derivatives and RADARSAT-2 dual-polarized

6. NS DEM derivatives and RADARSAT-2 dual-polarized and Landsat 8 images

7. RADARSAT-2 HH, HV, VH, VV intensity and polarimetric variable images

8. NS DEM derivatives and RADARSAT-2 HH, HV, VH, VV intensity and polarimetric variable images

9. NS DEM derivatives and RADARSAT-2 HH, HV, VH, VV intensity and polarimetric variable images and Landsat 8 images

The RF algorithm was originally developed by Leo Breiman and Adele Cutler at the University of California, Berkeley (http://www.stat.berkeley.edu/~breiman/ RandomForests/) (Breiman 2001, 2003). The algorithm used for this study was developed in the R programming language (R Development Core Team 2012) and has been used successfully in recent studies on land cover mapping in the Hudson Bay Lowlands (Ou et al. 2014) as well as in other wetland mapping studies with ALOS-PALSAR L-band SAR and Landsat data in the Great Lakes Region (Bourgeau-Chavez et al. 2015a) and in New Brunswick (LaRocque et al. 2015). RF can be run with "sub-polygon" and "all-polygon" (http://www.amnh.org/our-research/center-for-biodiversity-conservation/biodiversity-informatics/open-source-software-and-scripts). The sub-polygon version randomly selects a user-determined number of training area pixels from each class. The all-polygon version, which I applied, uses all of the pixels in all of the training area polygons to define class training areas and has the advantage of using the actual class size. The RF classifier was set to a forest of 500 independent decision trees with the default number of

variables randomly sampled as candidates at the split of every node (i.e. mtry). The default values for mtry for a classification are calculated as the square root of p, where p is the number of variables in x, i.e., the matrix of predictors for the classification (https://cran.r-project.org/web/packages/randomForest/randomForest.pdf). Using the default value gives a setting which includes all of the input features, or in other words, all pixels will be randomly sampled as candidates at each split of every node.

The RF classifier is calibrated using two thirds of the training area data and is called "In Bag" data. "Out of Bag" data is the remaining third which is used to test the forest to validate the resulting classification. The 500 individual decision trees are created using "In Bag" data, and are applied to produce independent classifications which are subsequently combined into the final classification map (Waske and Braun 2009). RF will allow for bootstrap aggregating of "In Bag" data when there is relatively limited training data for some classes in order to increase the number of training pixels. However bootstrapping was not required in my study area as I had enough training sites. RF is an effective classifier because it is not sensitive to noise or over classifying, plus it can estimate the importance of individual input variables (Gislason et al. 2006; Waske and Braun 2009). The variable importance is ranked and presented in a plot of "Mean Decrease Accuracy", and shows the degree of usefulness of each input image to the final classification (see Appendix D). Values are ranked from low to high plotted on a Y axis so the higher the placement of an image, the more useful it was in performing the classification (Strobl et al. 2008; Louppe et al. 2013).

Classification accuracy was measured first using a confusion matrix (or error matrix), where training areas are compared to the equivalent land cover in the classified map. Each cell in the matrix shows the number of pixels classified compared to a particular class as defined by the training areas (Congalton 1991). The matrix computes individual class User's and Producer's accuracies and their related error of omission and commission as described in Congalton (1991). The User's accuracy identifies the probability that a pixel from the classification map is in the right class, plus the associated number of pixels misclassified to the wrong class (error of omission). The Producer's accuracy corresponds to the probability that a reference pixel is well

classified, and the associated number of misclassified pixels that actually belong to another class (error of commission).

The best combination of input images was selected based on the highest overall accuracy with a visual evaluation of each classified map produced. However, this method only gives an assessment of the classified image accuracy, which is different from the true mapping accuracy. An independent accuracy assessment is more robust and compares the resulting classified map with an independent set of field observation data acquired over the validation sites which are points recorded with GPS coordinates. Each validation site was compared to the classified map, and the map is considered to be correct. These comparisons were tabulated to produce the percentage of correct identifications computed as a function of the total number of wetland validation sites. A confusion matrix was not calculated because only wetland classes were used and some misidentification is due to confusion with non-wetland classes.

5.3   Results

5.3.1   Classified images

Before comparing to high resolution results, I had to establish the combination with the best result for accuracy. Table 5.5 shows an overall accuracy of the classifier that was applied to various combinations of input data. The lowest overall accuracy was when only the NS DEM variables (41.7%) are used. There is a notable increase in accuracy when the Landsat 8 images are used (78.5%) and a moderate increase when combined with the NS DEM variables (82.2%) which was the second highest overall accuracy. When either the RADARSAT-2 HH, HV, VH, VV intensity and polarimetric variables or the RADARSAT-2 dual-polarized images are combined with the NS DEM, the accuracy increases only to 65.9% and 67.5% respectively Higher accuracy is reached again with the combination of all three types of data, with the accuracy reaching 84.2% with the RADARSAT-2 HH and HV images and 81.0% with the RADARSAT-2 HH, HV, VH, VV intensity and polarimetric variables.

Table 5.5: Overall classification accuracy for the various data set combinations.

Data Combination	Overall accuracy (%)
Landsat 8	78.5
NS DEM	41.7
NS DEM & Landsat 8	82.2
NS DEM & RADARSAT-2 HH/HV	65.9
Landsat 8 & RADARSAT-2 HH/HV	81.8
NS DEM & RADARSAT-2 HH, HV, VH, VV intensity and polarimetric	67.5
Landsat 8 & RADARSAT-2 HH, HV, VH, VV intensity and polarimetric	78.7
NS DEM & RADARSAT-2 HH/HV & Landsat 8	84.2
NS DEM & RADARSAT-2 HH, HV, VH, VV intensity and polarimetric & Landsat 8	81.0

To substantiate the best combination from the overall accuracy I also made sure that the individual class accuracies were high too. Table 5.6 compares the User's accuracies of each individual class and their related average accuracies, when the classifier was applied to the following data combinations: 1) Landsat 8; 2) NS DEM & Landsat 8; 3) NS DEM & Landsat 8 & RADARSAT-2 HH/HV; and 4) NS DEM & Landsat 8 & RADARSAT-2 intensity (HH, HV, VH, VV) and polarimetric variable images. The addition of RADARSAT-2 HH/HV dual-polarized data has some positive effect on the class accuracies for the swamp and upland forest classes as well as for the "Industrial" and "Urban area" classes. However the benefit is not as clear as in the high resolution study and the addition of polarimetric variables reduces the accuracy.

Table 5.6: Classification accuracies using the RF Classifier.

Class	Landsat 8	NS DEM + Landsat 8	NS DEM + Landsat 8+ RADARSAT-2 HH & HV	NS DEM + Landsat 8 + RADARSAT-2 intensity & polarimetric variables
Barren	81.0	81.0	81.0	66.7
Grass	95.7	95.7	94.8	93.1
Industrial	86.4	89.3	93.2	94.7
Lake	98.2	98.2	98.8	98.8
Open-water/marsh complex	81.3	83.3	83.3	70.8
Open bog	75.5	78.7	81.9	79.8
Open fen	57.5	65.1	64.2	53.8
Shrub/treed fen/bog	50.5	55.0	51.4	42.2
Swamp	64.0	65.3	68.7	50.7
Upland sparse vegetation	65.4	69.2	66.7	61.5
Upland forest	87.3	89.8	92.6	94.7
Urban	70.5	81.1	87.0	87.4
Overall accuracy	78.5	82.2	84.2	81.0

Figure 5.5 and Figure 5.6 shows the resulting classified maps. Like Table 5.6, it shows some improvement when using additional datasets. While Landsat alone appears good, the addition of the NS DEM and RADARSAT-2 HH/HV dual-polarized provide a noticeable refinement.

a) Landsat 8

barren
grass
industrial
lake
open water/marsh complex
open bog
open fen
shrub/treed fen/bog
swamp
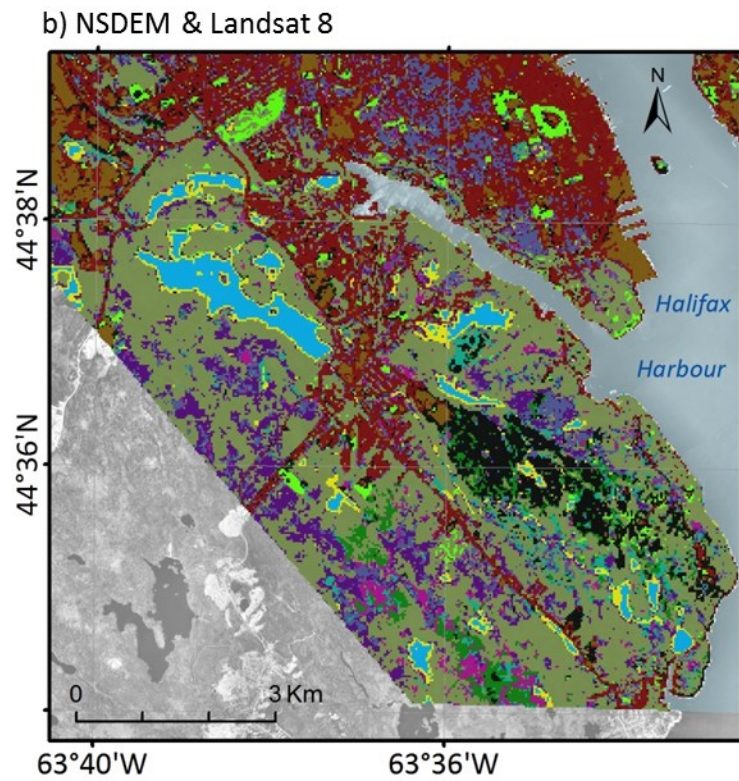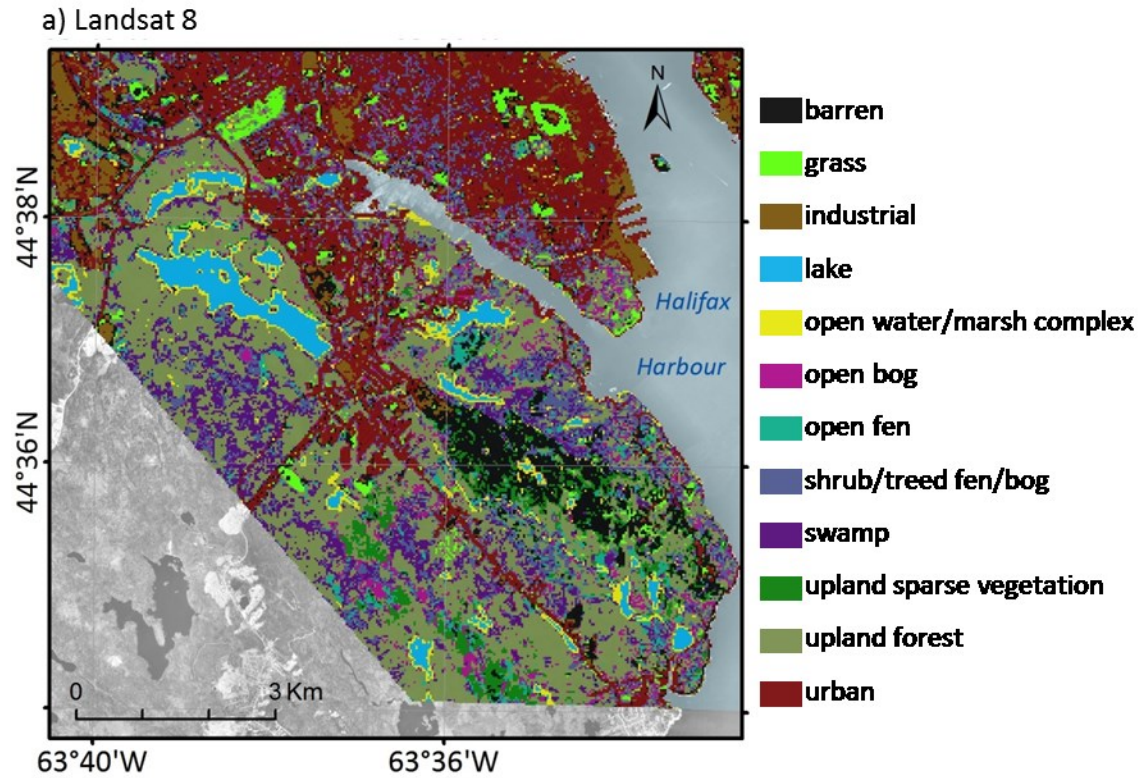upland sparse vegetation
upland forest
urban

b) NSDEM & Landsat 8

Figure 5.5: Classified images using the RF classifier applied to: a) Landsat 8; and b) NSDEM & Landsat 8 images.
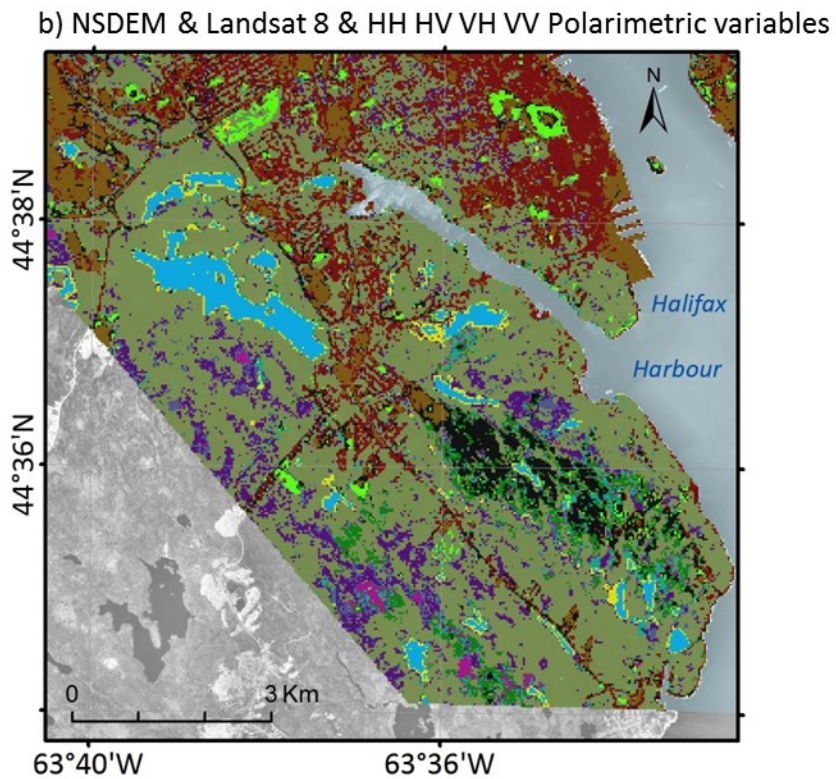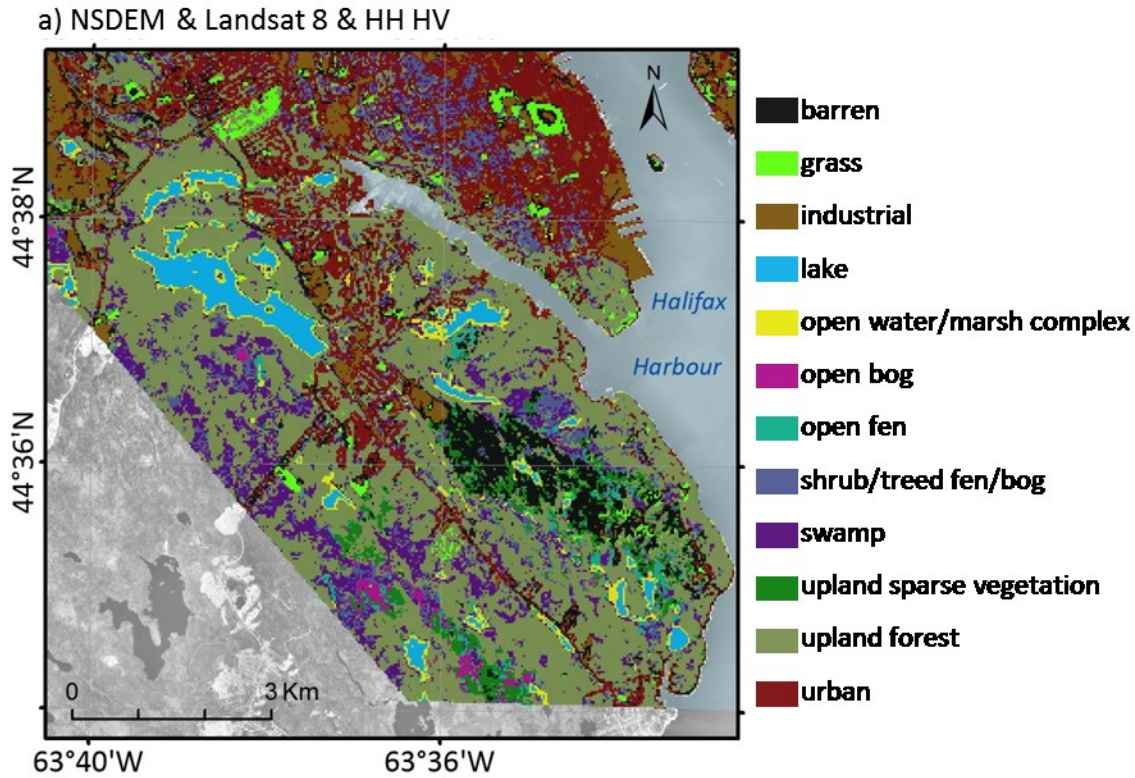
Figure 5.6: Classified images using RF classifier applied to: a) NS DEM & Landsat 8 & RADARSAT-2 dual-polarized; and b) NS DEM & Landsat 8 & RADARSAT-2 intensity and polarimetric variable images.

Table 5.6, Figure 5.5, and Figure 5.6 only give a general idea about the classification accuracy so it is necessary to identify where confusion between classes occurs. This is shown in Table 5.7 in the confusion matrix which also gives the User's and Producer's accuracies and the related omission and commission errors. Table 5.7 corresponds to the classification of NS DEM and Landsat 8 and RADARSAT-2 HH/HV dual-polarized variable combination, which had the highest overall classification accuracy (84.2%).

Most of the off-diagonal cells have a lower value, indicating that most of the pixels are reasonably well classified though there are some exceptions. Of the wetland classes only *lakes*, *open-water/marsh complex*, and *open bog* have a Producer's and User's accuracy over 80%. Open fen and the treed wetlands (*shrub/treed fen/bog* and *swamp*) have the lowest accuracies. This may be attributed to the lack of a canopy height model showing where treed areas are, plus a difficulty that this set of imagery has in separating the vegetation in open fen and treed areas. As expected, because of the outcome of treed areas in the high resolution study, tree canopy also interferes with accuracy for the medium resolution image inputs. This shows the value of having a lidar DEM which is much more accurate than the NS DEM. Barren has a higher User's accuracy here than it did for the high resolution study, meaning that the Landsat 8 optical imagery was better than the QuickBird for this class. Lastly, there is still a discrepancy between *open bog* and *upland sparse vegetation* but is not as pronounced as the high resolution study.

Table 5.7: Classification accuracies using the RF Classifier for the best case scenario (NS DEM derivatives plus dual-polarized RADARSAT 2 plus Landsat 8)

Classified Data					Reference Data										
	1 - barren	2 - grass	3 - industrial	4 - lake	5 – open-water / marsh complex	6 - open bog	7 - open fen	8 - shrub/treed fen/bog	9 - swamp	10 - upland sparse vegetation	11 - upland forest	12 - urban	row total	User's accuracy (%)	Error of commission (%)
1 - barren	47	0	2	0	0	0	1	0	0	5	1	2	58	81.0	19.0
2 - grass	2	110	0	0	0	1	0	0	0	0	2	1	116	94.8	5.2
3 - industrial	1	0	314	0	0	0	0	0	0	0	0	22	337	93.2	6.8
4 - lake	0	0	0	169	2	0	0	0	0	0	0	0	171	98.8	1.2
5 – open-water/marsh complex	1	0	0	4	40	0	1	1	1	0	0	0	48	83.3	16.7
6 - open bog	0	0	0	0	0	77	2	7	2	4	2	0	94	81.9	18.1
7 - open fen	0	1	0	0	2	5	68	7	11	4	8	0	106	64.2	35.8
8 – shrub/treed fen/bog	0	0	0	0	0	3	17	56	27	2	4	0	109	51.4	48.6
9 - swamp	0	0	0	0	0	0	3	16	103	2	26	0	150	68.7	31.3
10 - upland sparse vegetation	7	0	0	0	0	5	4	1	0	52	9	0	78	66.7	33.3
11 - upland forest	1	0	0	0	0	3	1	1	13	2	263	0	284	92.6	7.4
12 - urban	1	0	32	0	0	0	0	0	0	0	0	221	254	87.0	13.0
Column total	60	111	348	173	44	94	97	89	157	71	315	246			
Producer's accuracy (%)	78.3	99.1	90.2	97.7	90.9	81.9	70.1	62.9	65.6	73.2	83.5	89.8	Overall accuracy = 84.2%		
Error of omission (%)	21.7	0.9	9.8	2.3	9.1	18.1	29.9	37.1	34.4	26.8	16.5	10.2	Kappa coefficient = 82.2%		

Landsat 8's near infrared and two shortwave infrared bands are found in the top five most important variables in the classification with Radar at third and Slope at fifth. The DEM variables were more important in the previous study which used the more precise and accurate lidar. This shortfall in the variables from the NS DEM meant that the satellite data was more influential in the classification process. Near-infrared wavelengths are very sensitive to the vegetation of each class and vegetation seems thereby to be a determinant for classifying various land covers. Amongst all the RADARSAT-2 products, the HV and HH intensity spring images are the most important variables. HV is sensitive to volume scattering that again depends mainly on the vegetative component of each class.

5.3.2   Validation with the independent in-situ field sites

Analysing the performance of the image combination based solely on classification accuracies is not enough and it is necessary to compare the classified images with independent validation data sets in order to assess how accurate the map produced from each classification is. The classified maps were compared against the 137 wetland validation sites. Out of the 137 wetland sites, 69.3% and 56.2% were correctly identified when only Landsat 8 or the NS DEM were used individually (Table 5.8). The accuracy increased to 77.4% when Landsat 8 was added, and 71.5 when RADARSAT-2 dual-polarized HH and HV images were added in the classification, but when RADARSAT-2 HH, HV, VH, VV and polarimetric variables are used the accuracy dropped to 59.1%. The accuracy decreased when all three types of images were used but the percentage for the combination with the RADARSAT-2 HH, HV, VH, VV and polarimetric variable images (66.4%) is lower than for the combination with the RADARSAT-2 dual-polarized HH and HV images (73.7%). In all cases, the percentage of sites that are correctly identified as wetland are well above the one obtained with the DNR map that is currently used for wetland mapping by the government of Nova Scotia (46.7%). This map was produced mainly by photo-interpretation and field survey. The accuracy of mapping wetlands is still significantly better when using the best combination of high resolution imagery.

Table 5.8: Overall statistics of the identification of the 137 wetland ground truth sites on the classified maps or the DNR maps.

Source of data	Correctly identified as wetland		Correctly identified wetland class	
	N	%	N	%
Lidar+ RADARSAT-2 intensity & polarimetric + QuickBird	118	86.1	88	64.2
NS DNR map	64	46.7	13	9.5
Landsat 8	95	69.3	52	38.0
NS DEM	77	56.2	31	22.6
NS DEM + Landsat 8	106	77.4	64	46.7
NS DEM + RADARSAT-2 dual-polarized (HH/HV)	98	71.5	59	43.1
NS DEM + RADARSAT-2 dual-polarized (HH/HV) + Landsat 8	101	73.7	72	52.6
NS DEM + RADARSAT-2 intensity & polarimetric images	81	59.1	46	33.6
NS DEM + RADARSAT-2 intensity & polarimetric + Landsat 8	91	66.4	61	44.5

Identifying the GPS wetland sites in their proper wetland class is a more challenging task, and the related percentages are well below the correct identifications of the wetland/non-wetland classes. Again, the lowest accuracy is with the DNR map, on which only 9.5% of the GPS wetland validation sites are mapped in the right wetland class (Table 5.8). Like the high resolution study, the highest rate in identifying the proper wetland class was achieved when the triple combinations were used; i.e. 52.6% with the RADARSAT-2 dual-polarized HH and HV. It seems that both from the classification accuracy point of view (Table 5.5) and from the mapping accuracy point of view (Table 5.8) that the combination of NS DEM, Landsat 8 and the RADARSAT-2 HH and HV dual-polarized images gave the best accuracies. It is why that only this case will be considered further. In each of the following analyses it will be compared to accuracy obtained with the high resolution map in the previous study.

With the classified image, 21.9% of the misidentifications are due to wetland sites not being classified in the correct wetland class, but 26.3% are wetland sites being classified into a non-wetland class (Table 5.9). With the high resolution map, the same amount of 21.9% of the misidentifications are due to confusion among wetland classes and only 13.9% is due to confusion with a non-wetland class (Table 5.9).

Table 5.9: Distribution of the incorrectly identified wetland GPS observations as a function of the identification error source for the medium resolution and high resolution classified maps.

source of errors	NS DEM + RADARSAT-2 dual-polarized (HH/HV) + Landsat 8		Lidar & QuickBird & RADARSAT-2 intensity & polarimetric variables	
	N	%	N	%
non-wetland class	36	26.3	19	13.9
not the right wetland class	30	21.9	30	21.9
Total	66	48.2	49	35.8

In order to determine which wetland class the medium resolution classified map or the high resolution map gives the poorest identification results (by comparison with the GPS wetland validation sites), I have calculated the number and the percentage of correctly identified wetland validation sites for each wetland class (Table 5.10). There are some classes that are identified equally as well on the medium classified image and the high resolution, such as *lake*, *open-water/marsh complex*, and *shrub/treed fen/bog*. In both cases, the lakes and the open-water/marsh complex gave the highest mapping accuracy. The lowest accuracy in both (36.8% for medium resolution and 42.1% for high resolution) is for the "open bog" class. Open fen and swamp were mid-range for both medium and high resolution maps, though 16% to 19% lower accuracy for medium resolution.

Table 5.10: Number and percentage of the correctly identified wetland GPS observations as a function of the class.

class	total count	NS DEM + RADARSAT-2 dual-polarized (HH/HV) + Landsat 8		Lidar & QuickBird & RADARSAT-2 intensity & polarimetric variables	
		N (correct class)	%	N (correct class)	%
lake	6	6	100.0	6	100
open-water/marsh complex	6	5	83.3	5	83.3
open bog	19	7	36.8	8	42.1
open fen	30	17	56.7	22	73.3
shrub/treed fen/bog	24	11	45.8	11	45.8
swamp	52	26	50.0	36	69.2

On the medium resolution classified map, except for the swamp, misidentifications are mainly due to wetlands being identified as another wetland class (Table 5.11), instead of having wetlands being identified as a non-wetland (Table 5.12). Overall error was equal where the confusion mainly occurred with other wetland classes (Table 5.11) rather than with non-wetland classes (Table 5.12). However the medium resolution classification is significantly more likely to incorrectly misclassify a wetland as upland.

Table 5.11: Number and percentage of the wetland GPS observations that were not identified in the right wetland class for the medium and high resolution maps.

class	total count	NS DEM + RADARSAT-2 dual-polarimetric (HH/HV) + Landsat 8		Lidar & QuickBird & RADARSAT-2 intensity & polarimetric variables	
		N	%	N	%
lake	6	0	0.0	0	0
open-water/marsh complex	6	1	16.7	0	0
open bog	19	8	42.1	9	47.4
open fen	30	7	23.3	7	23.3
shrub/treed fen/bog	24	8	33.3	12	50.0
swamp	52	5	9.6	2	3.9
total	137	29	21.2	30	21.9

Table 5.12: Number and percentage of the wetland GPS observations that were identified as a non-wetland (i.e. upland) class for the medium and high resolution classified maps.

class	total count	NS DEM + Radarsat-2 dual pol (HH/HV) + Landsat 8		Lidar & QuickBird & RADARSAT-2 intensity & polarimetric variables	
		N	%	N	%
lake	6	0	0.0	0	0
open-water/marsh complex	6	0	0.0	1	16.7
open bog	19	4	21.1	2	10.5
open fen	30	6	20.0	1	3.3
shrub/treed fen/bog	24	5	20.8	1	4.2
swamp	52	21	40.4	14	26.9
total	137	36	26.3	19	13.9

5.3.3 Differences in the DEMs

The DEMs from the high resolution study and the medium resolution study were of different resolutions, but because of questions to the accuracy of the NS DEM, discrepancies were analysed to quantify the error and possible effect on wetland mapping. First, the RMSE was calculated using the NSCRS survey markers for the lidar DEM (1.062 m) and the NS DEM (2.107). These values showed that the lidar DEM was more accurate *overall*. To see if elevation differences were dispersed or clustered the difference in elevation values between the two datasets, differences in elevation were shown as seen in Figure 5.7. On the map systematic errors which may have resulted from miscalibrated equipment or other operator error are evident. However, aside from some mixed areas, the distribution of elevation errors generally seems to be clustered together. For this reason, the assumption that relative accuracy (i.e. elevation accuracy of a point compared to surrounding points in close proximity) is good will be adopted for the analysis in Chapter 4. In other words, though the model would not be expected to work if it does not show where water can accumulate (e.g. flat areas or base of hills), it is likely that the coarser NS DEM can still predict wetland location to some degree because the *local* terrain morphology is accurate.
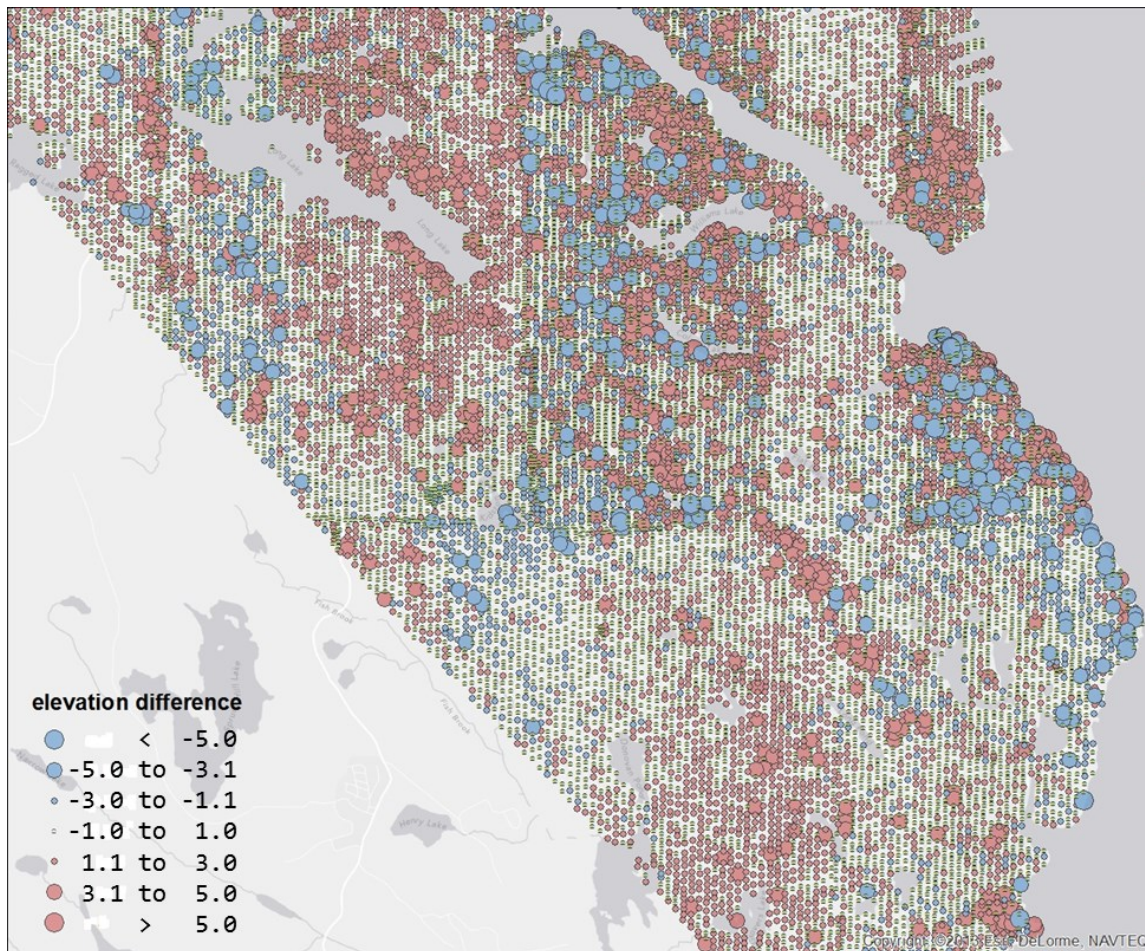
Figure 5.7: Elevation difference between Nova Scotia Topographic Database elevation points and the lidar DEM.

Slope was the fifth most important variable overall to the medium resolution classification and the top from the NS DEM variables. The NS DEM has less influence than the lidar DEM but still contributes to the successful classification. One of the concerns previously identified, was the accuracy in the relative sense. To analyze the difference two comparisons were made (Table 5.13). The first is a simple summary statistic of minimum and maximum slopes in each class. In all wetland cases except open bog (possibly due to sloped areas of raised bogs) the slopes are under two degrees for the lidar DEM, but maximum slope for open bog, open fen, shrub/treed fen/bog, and swamp all exceed two degrees. This indicates that the NS DEM does not always guide the wetland classifications.

Table 5.13: Slope comparison derived from the lidar DEM and NS DEM both resampled to an 8 m resolution.

Class	lidar slope (8 m)		NS DEM slope (8 m)	
	min	max	min	max
barren	2.8	16.9	0.2	11.9
grass	0.5	10.3	0.3	9.3
industrial	0.4	3.8	0.3	2.8
lake	0.1	0.2	0.0	0.0
open-water/marsh complex	0.2	0.7	0.0	1.2
open bog	0.4	3.1	0.3	3.8
open fen	0.5	1.5	0.4	3.8
shrub/treed fen/bog	0.4	1.9	0.1	2.7
swamp	0.4	1.6	0.2	5.2
upland sparse vegetation	2.8	10.1	0.5	7.3
upland forest	1.0	23.7	0.2	21.9
urban	2.3	6.9	2.0	5.7

Additional information to quantify the difference was done by comparing the slope value of the NS DEM against the slope value of the lidar DEM using a cross tabulation analysis in SPSS Statistics software (IBM 2015). Figure 5.8 is a graph of a cross tabulation analysis on the overlay of the NS DEM slope and the lidar slope. The graph shows that slopes agree better at low values. For example, a zero-degree slope for the provincial DEM matches 54% of the zero-degree lidar DEM slope (red line); and a one-degree provincial DEM slope matches 18% of the zero-degree lidar DEM slope. However, only 25% of the one-degree provincial slope matches the one-degree lidar slope (green line); and a two-degree provincial DEM slope matches 16% of the one-degree lidar DEM slope. This shows that the slopes are more likely to agree at low slopes, and that the provincial DEM slope becomes increasingly unreliable as slope increases (seen by the flattening of the graphs).
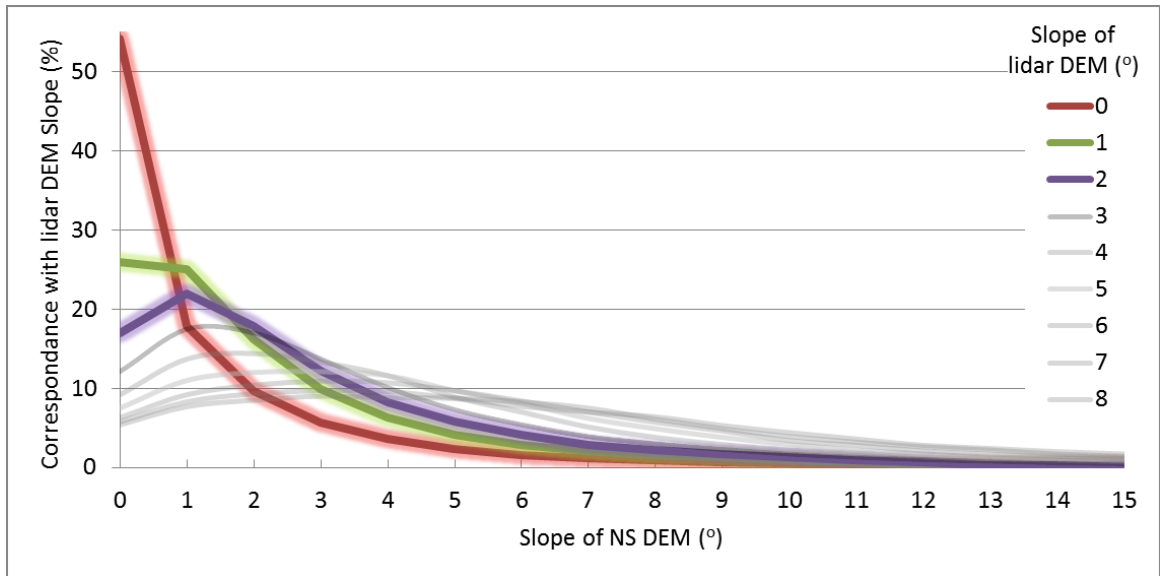
Figure 5.8: Graph showing cross tabulation of the provincial DEM slope and the lidar DEM slope. Values agree better at low slopes and the provincial DEM slope is less reliable as slope increases which is apparent in the flatter and broad graph lines.

The graph in Figure 5.9 shows the proportion of treed versus non-treed wetlands clipped to show the areas within the McIntosh Run Basin. More of the basin is mapped as wetland overall using the medium resolution imagery for both treed and non-treed wetlands. The high resolution imagery combinations were more consistent as well in mapping treed wetlands, and the proportion of treed wetland varied by 2.5% depending on the type of RADARSAT-2 variables used.
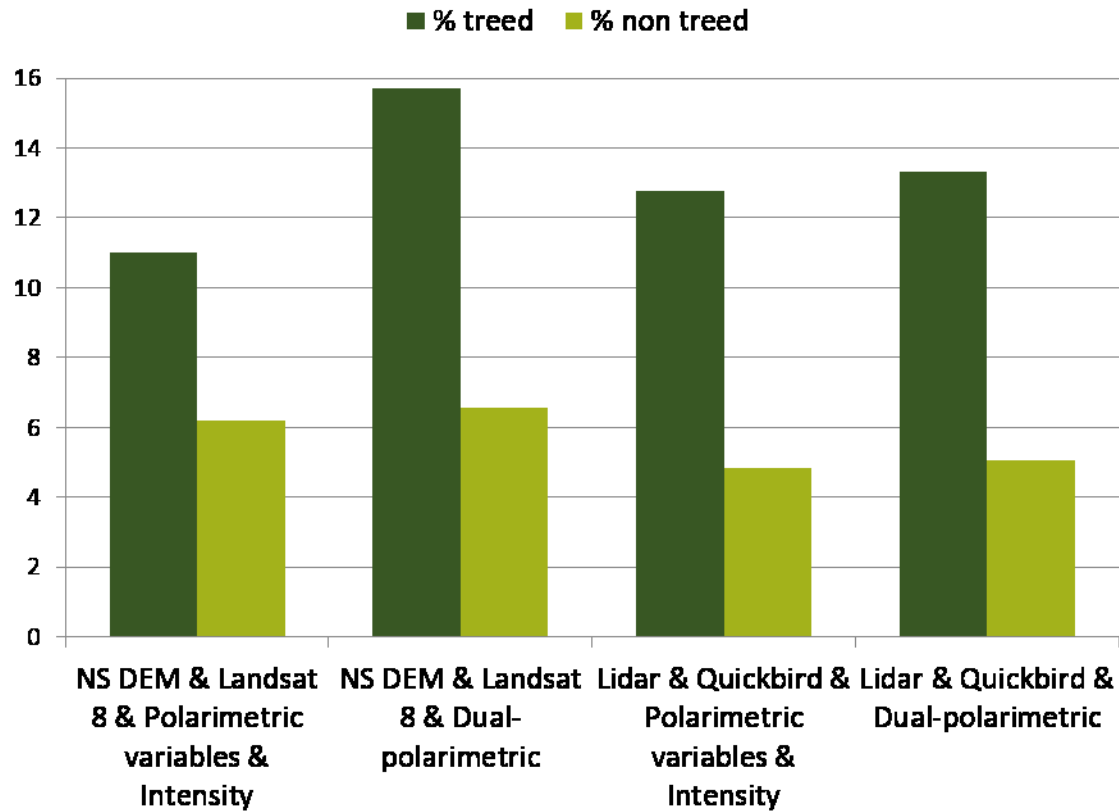
Figure 5.9: Proportion of treed and non-treed wetlands in the McIntosh Run Basin for two combinations of medium resolution imagery and two combinations of high resolution imagery.

5.4   Discussion

The present study tested various combinations of RADARSAT-2, NS DEM variables and Landsat 8 imagery used in land cover classifications with the RF Classifier. My study showed that a combined use of NS DEM variables and Landsat 8 imagery improved the accuracy the most (Table 5.8). RADARSAT-2 did not perform as well as other studies such as Whitcomb et al. 2009; Bourgeau-Chavez et al. 2001; and Fournier et al. 2007. This could be a result of the coarser scale of the resampled imagery as compared to the small size of many of the wetlands.

Landsat 8 is the most important input data in the classification. Optical imagery was already found to be suitable for mapping wetlands and surface hydrology, particularly open wetlands with low vegetation (Pietroniro and Leconte 2005; Harris et al. 2005, 2006; Meingast et al. 2014). Though topography relates to the way water flows across or into a wetland, the NS

DEM was likely not accurate enough to help too much with the location of wetlands. The slope did have some importance but not as much as the optical imagery. However, LaRocque et al. (2015) found that elevation derivatives were the most important input data for their classification. This was also the case for the high resolution analysis using the lidar DEM. The study by LaRocque also achieved better levels of accuracy because they used images of flooding conditions, plus an L-band radar system. L-band radar, because of its longer wavelength, is able to penetrate the vegetation canopy better than the C-band that I used.

Amongst all the RADARSAT-2 products, the spring HV intensity images are the most important variables. HV images are sensitive to volume scattering that again depends mainly on the vegetative component of each class. This plus the other important variables show that vegetation and terrain are the main determinants for classifying wetlands.

Brisco et al. (2011) found that C-band imagery can be used to clearly separate open water from deep marsh and shallow marsh, and that the Freeman-Durden parameters could potentially distinguish landcover at the vegetation species level. In addition, the Cloude-Pottier polarimetric decomposition could also provide for wetland species-level separation, and that with optical data should allow for an operational wetland mapping program. Corcoran et al. (2013) also recognized that multiple datasets would be valuable to map wetlands at the landscape scale, and analysed which data combinations would give the best classification accuracy. However, they did find that C-band polarimetric radar contributed to the third most accurate model, concluding that L-band is more appropriate for mapping wetlands in forested areas because of the longer wavelength.

My study also used a multi-temporal data approach, in addition to the multi-sensor, for the RADARSAT-2 acquisition. Combining these two approaches was successful in producing highly accurate wetland maps in Africa (Rebelo 2010), USA (Bourgeau-Chavez et al. 2008 2015a; Corcoran et al. 2011, 2013). The multi-temporal approach allows for capturing seasonal differences in the vegetation and water level conditions, which allow for better wetland type discrimination. RADARSAT-2 images acquired in the spring have a greater influence on the successful classification. This means that the presence of water in the wetlands as observed on the SAR images is critical for the classification. These images are also at a lower incidence angle

(which could normally be a problem compared to a steep angle) but they are leaf off (unlike the summer image) so are able to penetrate the canopy better.

Table 5.12 shows a problem with wetlands misclassified as upland for a number of points per class, especially for swamp. In this case, 40.4% of swamp is being misclassified as upland forest. The pattern is similar but not as severe for the high resolution study (chapter 3), which is likely attributable to the coarser DEM. The provinces wetland inventory also had more of a problem with treed wetlands misclassified as upland.

The obvious shortcoming of the lower spatial resolution is that it is impossible to resolve small or narrow features. The degree to which this had on the effect on the final classification accuracy is not as straightforward in the case of the data used in this study however. In other words, Landsat has higher spectral resolution than QuickBird in the sense that it has several more bands. Plus it has a slightly higher radiometric resolution at 12-bit. My QuickBird image displayed more variability than Landsat 8, probably due to shadow and other fine detail, and since I used a pixel based classification the extra features likely caused problems. To overcome this problem, high resolution imagery can be classified using an object based image analysis (OBIA) process which is the automated way of establishing context, but this was not done here.

As stated, the DNR map provides the most recent estimates for the number, location and class of wetlands in the province that are greater than or equal to ½ hectare (Nova Scotia Environment 2009). My study resulted in a better accuracy in part as a result of this area constraint of the larger minimum mappable unit (mmu) for the DNR map, plus the fact that no forested polygons on site class 3 or higher could be classified as wetland. The discrepancy due to these restrictions was not accounted for, however upon visual inspection there are still substantial areas of non-treed wetlands that have been omitted and areas that were incorrectly classified.

5.5 Summary and conclusions

My study showed that with RADARSAT-2 SAR polarimetric images acquired during high and low water levels, at steep and shallow incidence angles, with Landsat 8 optical and NS DEM derivative data, improves the mapping of wetland areas in the Long Lake Provincial Park/

Herring Cove Backlands area, over the current DNR map. However, RADARSAT-2 has limited benefit and Landsat 8 is the most significant type of input. The misidentification of the GPS wetland validation sites are mainly due to wetlands not being classified in the right wetland class but, unlike the high resolution study, a significant misclassification with upland. The DNR map that the government of Nova Scotia is currently using has a lot of misidentification of the GPS validation sites. Most of the error in non-treed wetlands are associated to not being in the right wetland class, and most of the error in treed wetlands are misclassified as upland. In each case, treed areas were the most challenging to classify properly.

There are several limitations in this study. The error found in the treed wetland classes might be reduced by using L-Band radar which is better able to penetrate the tree canopy (Touzi et al. 2009). Unlike LaRocque et al. (2015) I did not use an image that showed flooding conditions. Finally, it would have been preferable to have all images acquired within a shorter time span. Parts of my study area experienced significant change during the period for which my imagery was acquired (2005 to 2013).

editing, and format styling. Finally, I would like to express my gratitude to my family who was entirely supportive and patient.

5.7   References

Bourgeau-Chavez, L. L., Kasischke, E. S., Brunzell, S. M., Mudd, J. P, Smith, K. B. and Frick, A. L. 2001. "Analysis of spaceborne SAR data for wetland mapping in Virginia riparian ecosystems." *International Journal of Remote Sensing*, Vol. 22, No. 18, pp. 3665-3687.

Bourgeau-Chavez, L. L., Endres, S., Battaglia, M., Miller, M. E., Banda, E., Laubach, Z., Higman, P., Chaw-Fraser, P., and Marcaccio, J. 2015. "Development of a bi-national Great Lakes coastal wetland and land use map using three-season PALSAR and Landsat imagery." *Remote Sensing*, Vol. 7, No. 7, pp. 8655-8682.

Bourgeau-Chavez, L. L., Riordan, K., Miller, N., Nowels, M., and Powell, R. B. 2008. "Remotely monitoring Great Lakes coastal wetlands with multi-sensor, multi-temporal SAR and multi-spectral data." *Proceedings of the 2008 International Geoscience and Remote Sensing Symposium (IGARSS 2008)*: pp. I-428 - I-429.

Breiman, L. 2001. "Random Forest". *Machine Learning*, Vol. 45, No. 1, pp. 5-32.

Breiman, L. 2003. "Manual of Setting up, Using and Understanding Random Forest", V4.0, University of California Berkeley, Statistics Department, Berkeley.

Brisco, B., Kapfer, M., Hirose T., Tedford, B., and Liu, J. 2011. "Evaluation of C-band polarization diversity and polarimetry for wetland mapping." *Canadian Journal of Remote Sensing*, Vol. 37, pp. 82-92.

Brooks, K., Ffolliott, P., and Magner, J. 2013. *Hydrology and the management of watersheds (4th ed.)*. Ames, Iowa, USA: Wiley-Blackwell.

Canada Committee on Ecological (Biophysical) Land Classification. 1988. "Wetlands of Canada." Ottawa: Sustainable Development Branch, Canadian Wildlife Service, Conservation and Protection, Environment Canada. pp. 1-61.

Castrignano, A., Buttafuoco, G., Comolli, R., and Ballabio, C. 2006. "Accuracy assessment of digital elevation model using stochastic simulation." *Proceedings of the 7th International Symposium on Spatial Accuracy Assessment in Natural Resources and Environmental Sciences.* pp. 490–498.

Cloude, S., and Pottier, E. 1997. "An entropy based classification scheme for land applications of polarimetric SAR." *IEEE Transactions on Geoscience and Remote Sensing,* Vol. 35, No. 1, pp. 68-78.

Congalton, R. 1991. "A review of assessing the accuracy of classifications of remotely sensed data." *Remote Sensing of Environment*, Vol. 37, pp. 35–46.

Corcoran, J. M., Knight, J. F., Brisco, B., Kaya, S., Cull, A., and Murnagahn, K. 2011. "The integration of optical, topographic, and radar data for wetland mapping in Northern Minnesota." *Canadian Journal of Remote Sensing*, Vol. 37, No. 5, pp. 564-582.

Corcoran, J. M., Knight, J. F., and Gallant, A. L. 2013. "Influence of multi-source and multi-temporal remotely sensed and ancillary data on the accuracy of Random Forest classification of wetlands in Northern Minnesota." *Remote Sensing*, Vol. 5, No. 7, pp. 3212-3238.

ESRI [Computer software]. 2015. Retrieved from http://www.esri.com

Evans, D.L., Farr, T.G., van Zyl, J.J., and Zebker, H.A. 1988. "Radar polarimetry: Analysis tools and applications." *IEEE Transactions on Geoscience and Remote Sensing*, Vol. 26, No. 6, pp. 774-789.

Fournier, R., Grenier, A, M., Lavoie, A., and Hélie, R. 2007. "Towards a strategy to implement the Canadian Wetland Inventory using satellite remote sensing." *Canadian Journal of Remote Sensing*, Vol. 33, Supp. 1, pp. S1–S16.

Freeman, A., and Durden, S. 1998. "A three-component scattering model for polarimetric SAR data." *IEEE Transactions on Geoscience and Remote Sensing*, Vol. 36, No. 3, pp. 963-973.

Geosetter [Computer software]. 2012. Retrieved from http://www.geosetter.de/en/

Gislason, P., Benediktsson, J., and Sveinsson, J. 2006. "Random Forest for land cover classification." *Pattern Recognition Letters*, Vol. 27, pp. 294-300.

Goodman, J. W. 1976. "Some fundamental properties of speckles." *Journal of the Optical Society of America*, Vol. 66, No. 11, pp. 1145-1150.

Harris, A., Bryant, R. G., and Baird, A. J. 2005. "Detecting water stress in Sphagnum spp." *Remote Sensing of Environment*, Vol. 97, No. 3, pp. 371–381.

Harris, A., Bryant, R. G., and Baird, A. J. 2006. "Mapping the effects of water stress on Sphagnum: Preliminary observations using airborne remote sensing." *Remote Sensing of Environment*, Vol. 100, No. 3, pp. 363-378.

Hill, N, and Patriquin, D. 2014. "Ecological Assessment of the Plant Communities of the Williams Lake Backlands." Retrieved from Williams Lake Conservation Company: http://www.williamslakecc.org/documents/WLBFinalRep12Feb2014.pdf pp. 1-83.

Hutchinson, M., Xu, T., and Stein, J. 2011. "Recent Progress in the ANUDEM Elevation Gridding Procedure." Retrieved from http://geomorphometry.org/system/files/HutchinsonXu2011geomorphometry.pdf

IBM SPSS Statistics [Computer software]. 2015. Retrieved from http://www-01.ibm.com/software/analytics/spss/

LaRocque, A., Leblon, B., Bourgeau-Chavez, L., McCarty, J., French, N., and Woodward, R. 2015. "Evaluating wetland mapping techniques for New Brunswick using Landsat TM, ALOS-PALSAR and RADARSAT-2 dual-polarized images." *Canadian Journal of Remote Sensing* (submitted).

Lee, J.S., Grunes, M.R., Ainsworth, TL., Du, LJ., and Schuler, DL. 1999. "Unsupervised classification using polarimetric decomposition and the complex Wishart classifier." *IEEE Transactions on Geoscience and Remote Sensing*, Vol. 37, No. 5, pp. 2249-2258.

Lee J.S., Grunes, M.R., and Kwok R. 1994. "Classification of multi-look polarimetric SAR imagery based on the complex Wishart distribution." *International Journal of Remote Sensing*, Vol. 15, No. 11, pp. 2299-2311.

Lopez-Martinez, C., Pottier, E., and Cloude, S.R. 2005. "Statistical assessment of eigenvector-based target decomposition theorems in radar polarimetry." *IEEE Transactions on Geoscience and Remote Sensing*, Vol. 43, No. 9, pp. 2058-2074.

Louppe, G., Wehenkel, L., Sutera, A., and Geurts, P. 2013. "Understanding variable importances in forests of randomized trees." *Advances in Neural Information Processing Systems*, Vol. 26, pp. 431-439.

Mapwel [Computer software]. 2012. Retrieved from https://www.mapwel.net/

Meingast, K. M., Falkowski, M. J., Kane, E. S, Potvin, L. R., Benscoter, B. W., Smith, A. M. S., Bourgeau-Chavez, L. L., and Miller, M. E. 2014. "Spectral detection of near-surface moisture content and water-table position in northern peatland ecosystems." *Remote Sensing of Environment*, Vol. 152, pp. 536-546.

Neily, P. D., Quiget, E., Benjamin, L., Stewart, B., and Duke, T. 2003. "Ecological land classification for Nova Scotia: Volume I, mapping Nova Scotia's terrestrial ecosystems." Halifax, N.S.: Nova Scotia Department of Natural Resources, Renewable Resources Branch. pp. 1-77.

Nova Scotia Environment. 2009. "Nova Scotia Wetland Conservation Policy (Draft for Consultation)." pp. 1-24. Retrieved from http://www.gov.ns.ca/nse/wetland/docs/Nova.Scotia.Wetland.Conservation.Policy.pdf

Nova Scotia Geomatics Centre. 2015. "Digital Elevation Model Specifications." Retrieved from http://www.nsgc.gov.ns.ca/mappingspecs/Specifications/Compilation/Resource_NSTDB/default.htm

Nova Scotia Museum of Natural History. 1989. "Natural History of Nova Scotia, The Dynamics of Nova Scotia's Climate." pp. 94-103. Retrieved from https://ojs.library.dal.ca/NSM/article/download/3752/3438

Ou, C., Zhang, Y., LaRocque, A., Leblon, B., Webster, K., McLaughlin, J., and Barnett, P. 2014. "Model calibration for mapping permafrost using Landsat-5 TM and RADARSAT-2 images." *Proceedings of the 2014 IEEE International Geoscience and Remote Sensing Symposium (IGARSS 2014)*: pp. 4883-4886.

PCI Geomatica [Computer software]. 2014. Retrieved from http://www.pcigeomatics.com

Pietroniro, A., and Leconte, R. 2005. "A review of Canadian remote sensing and hydrology, 1999-2003." *Hydrological Processes*, Vol. 19, No. 1, pp. 285-301.

R Development Core Team 2012. "R: A language and environment for statistical computing." Vienna, R Foundation for Statistical Computing. Retrieved from https://www.r-project.org/

Rebelo, L. S. 2010. "Eco-hydrological characterization of inland wetlands in Africa using L-Band SAR." *IEEE Journal of Selected Topics in Applied Earth Observations and Remote Sensing*, Vol. 3, No. 4, pp. 554-559.

Rodriguez, E. and Martin, J.M. 1992. "Theory and design of interferometric synthetic aperture radars." *IEE Proceedings F Radar and Signal Processing*, Vol. 139, No. 2, pp. 147-159.

Schott, J.R. 2007. "*Remote Sensing: the image chain approach*." New York, NY, USA: Oxford University Press.

Strobl, C., Boulesteix, A.-L., Kneib, T., Augustin, T., and Zeileis, A. 2008. "Conditional variable importance for Random Forests." *BMC Bioinformatics*, Vol. 9, No. 1, pp. 307.

Telegraph Journal. February 21, 2011. "Profs defend wetlands mapping system." Retrieved from: http://telegraphjournal.canadaeast.com/front/article/1381

Tiner, R.W. 1999. *Wetlands indicators: a guide to wetland identification, delineation, classification, and mapping*. Lewis Publishers, Boca Raton (Florida, USA).

Touzi, R. 2007. "Target Scattering Decomposition in Terms of Roll-Invariant Target Parameters." *IEEE Transactions on Geoscience and Remote Sensing*, Vol. 45, No. 1, pp. 73-84.

Touzi, R., Deschamps, A., and Rother, G. 2009. "Phase of Target Scattering for Wetland Characterization Using Polarimetric C-Band SAR." *IEEE Transactions on Geoscience and Remote Sensing*, Vol. 47, No. 9, pp. 3241-3261.

Touzi, R., Goze, S., Le Toan, T., Lopes, A., and Mougin, E. 1992. "Polarimetric discriminators for SAR images." *IEEE Transactions on Geoscience and Remote Sensing*, Vol. 30, No. 5, pp. 973-980.

United States Geological Survey. 2015. "Using the USGS Landsat 8 Product." Retrieved from http://landsat.usgs.gov/Landsat8_Using_Product.php

van Zyl, J.J., Zebker, H.A., and Elachi, C. 1987. "Imaging radar polarization signatures: Theory and observation." *Radio science*, Vol. 22, No. 4, pp. 529-543.

Warner, B.G. and Rubec, C.D.A. (Eds.). 1997. "The Canadian Wetland Classification System. (2nd edition)." National Wetlands Working Group. Wetlands Research Centre. University of Waterloo. Ontario, pp. 1-68.

Waske, B., and Braun, B. 2009. "Classifier ensembles for land cover mapping using multi-temporal SAR Imagery." *ISPRS Journal of Photogrammetry and Remote Sensing*, Vol. 64, pp. 450-457.

Whitcomb, J., Moghaddam, M., McDonald, K., Kellndorfer, J., and Podest, E. 2009. "Mapping vegetated wetlands of Alaska Using L-band radar satellite imagery." *Canadian Journal of Remote Sensing*, Vol. 35, No. 1, pp. 54-72.

Wilson, J., and Gallant, J. C. 2000. *Terrain analysis: Principles and applications*. New York: Wiley.

Zebker, H.A., van Zyl, J.J., and Held, D.N. 1987. "Imaging radar polarimetry from wave synthesis." *Journal of Geophysical Research*, Vol. 92, No. B1, pp. 683-701.

Chapter 6.   Comparison and Discussion/Conclusion

6.1   Key Findings

The primary objective of my study was to investigate how remote sensing and GIS can be used to improve the Nova Scotia wetland inventory. My research was grounded in a theoretical framework for land cover mapping and applied various techniques in the processing of remotely sensed imagery. I also emphasize that, even though the objective of interpreting remotely sensed data (in this context) is to achieve a highly accurate representation of land cover, the processing and interpreting of geospatial data remain subject to personal conceptualisations (Comber 2005). For this reason, the user of the classification information must be aware of how it was created and for what purpose, so that they can use their best judgement for its suitability.

Finding 1: The use of any one source of imagery or dataset type (high-resolution or medium-resolution) resulted in higher accuracy than the current DNR map.

The classification process was first performed on the separate inputs of RADARSAT-2, high and medium resolution imagery, as well as high and medium resolution DEMs and DSM. For all single datasets, the accuracy of classification was superior to that of the currently used DNR map. Nonetheless, the accuracy of these new maps was compromised by a tendency for the classification technique to indiscriminately map obvious features whose classification would be recognizable if contextual cues from the surrounding landscape were considered (e.g. lines painted on a flat football field which would be interpreted as wetland from the slope).

I acquired four sets of RADARSAT-2 imagery, including images obtained from two different satellite incidence angles (high and low) and images with two different water levels (resulting from seasonal fluctuation and variations in precipitation). Initial assessments of individual acquisitions suggested that all four images should be included in further classification work using the following four configurations: steep/summer, shallow/summer, steep/spring, and shallow spring.

Finding 2: Using a combination of high resolution optical imagery, lidar, and PolSAR, improved identification of wetland location and class was possible, compared to the current DNR map.

As described in the preceding section, I performed individual image classifications to (1) determine how well each dataset performed on its own and (2) to determine the contribution of each dataset to the final classification. However, I found that using a combination of multiple datasets improved mapping accuracy compared to using a single type of input data alone. Indeed, optimal classification accuracy, mapping accuracy, and accuracy based on a visual assessment were obtained when all three types of input were used together. Moreover, higher accuracy was achieved both when identifying the presence or absence of wetlands and when mapping the individual wetland classes.

Finding 3: The lidar variables were most important when mapping wetlands using high-resolution data.

Lidar was used to measure elevation of the upper surface of the vegetation canopy (first return) to create the DSM, and elevation of the ground terrain (last return) to create the DEM. The Canopy Height Model (CHM) comprises the difference between these two surfaces. Lidar was very successful at mapping the terrain, even in treed areas, because of its high precision and ability to penetrate overstory vegetation canopy. Terrain has been used to facilitate other geomorphological and hydrological studies (Wilson and Gallant 2000), and similar concepts were applied in this thesis; topography was used to help predict relative landscape position (topographic position index), where runoff is slower (slope), where moisture is likely to accumulate (compound topographic index, derived from slope and flow accumulation), where runoff decelerates (curvature), and vegetation height (CHM). Variables derived from lidar were found to be most important in the high resolution classification. All five lidar derivatives were ranked in the top six positions of the list showing the importance of each input variable to the classification.

Finding 4: When mapping individual wetlands, medium-resolution data resulted in a lower accuracy than did high-resolution data.

The classification accuracy achieved for the various combinations of medium-resolution data was lower than that achieved with high-resolution data. However, medium-resolution data nonetheless yielded maps that were more accurate than the existing DNR map. This finding reveals that even the use of medium-resolution data can enhance the reliability of the current wetland inventory for the province.

Finding 5: The influence of medium-resolution inputs did not follow the same pattern as high-resolution inputs.

The Nova Scotia DEM was of limited benefit compared to lidar data, but the medium-resolution optical imagery (Landsat 8) performed better than did QuickBird imagery. Factors that may have contributed to this unexpected result include: the resampling of the QuickBird imagery from 2.4 m to 8 m; the use of only four bands for QuickBird compared to eight for Landsat 8; and the fact that QuickBird imagery may have been overly complex for a pixel-based image analysis and would have performed better in an object-based one.

6.2   Limitations

While this research has yielded significant findings, there are limitations which should be addressed before theoretical contributions are proposed. These include the limited generalizability of the study area (i.e. due to limited number of wetland types, etc.) as well as limitations imposed by experimental design (particularly the data collection phase), both of which are described in subsequent sections.

This study would have benefited from examining areas of Nova Scotia belonging to different ecological land classifications. For example, one conspicuous drawback of the study area is the lack of a shallow marsh class, and it would have been more informative if an area with this class could also have been selected. According to the DNR map, the study area appears to contain 51 marsh polygons (approximately 110 ha). However, shallow marshes had mostly been misclassified or were not accessed during field work. Field data were still collected for deep marshes; however, these typically transitioned into open-water wetlands or were too

small to resolve with the RADARSAT-2 imagery on their own. Furthermore, the deep marshes contained non-persistent emergent vegetation during the growing season and are therefore hard to distinguish from open-water wetlands in early spring imagery. For these reasons, I grouped deep marshes with the open-water wetland class in the final classification. Combining the open-water with deep marsh wetland classes created a sample size that was large enough to be resolved in the imagery.

Another important missing class is the vernal pool. At the beginning of the study, I decided to omit this wetland class because its small size and ephemeral nature would have required too many special considerations. Other studies (Van Meter et al. 2008) have included the vernal pool wetland class, but used more intensive interpretation of aerial photography than that associated with the DNR map.

Information from stream gauges was not available for the McIntosh Run, so it was not possible to obtain precise measurements of water levels. However, historical data provided by Environment Canada was used to estimate soil moisture conditions and degree of flooding. Additionally, due to the influence of urban development and fire, parts of my study area underwent significant changes during the time span covered by the image dates (2005 to 2013); therefore, it would have been preferable if all imagery used in this study had been captured over a shorter period of time.

Finally, RADARSAT-2 uses the C-band frequency when transmitting signals. While this is useful for observing changes in the soil moisture of wetlands (assuming negligible influence from forest canopy), L-band is better at penetrating tree cover and at delineating major environmental units (Slatton et al. 2008). An ideal study uses both frequencies of radar for comparative purposes, as was done in research by LaRocque et al. (2015).

6.3   Research Process Challenges

One challenge I faced during the collection of field data was that private property limited accessibility and thus restricted sampling efforts to certain areas. Initially, I planned to have transects cross specific wetlands; however, I worried that time constraints associated with this strategy would result in the collection of too few samples. Therefore, I instead opted to use

a purposive stratified sampling technique that considers the total area of each class (McCoy 2005). Compared with transects, this technique is more rapid and ensures that an adequate number of samples which are well distributed through the study area can be collected. Purposive stratified sampling can also be much more practical since it allows some flexibility in terms of route selection. Accessibility issues were addressed by creating maps which detailed property ownership and hiking trails to help plan routes. When impassible terrain was encountered in the field, an alternative route was located.

Compared to the method used to delineate wetlands in the DNR map, my automated classification procedure was more prone to indiscriminately misclassify obvious features. Indeed, this type of misclassification can be a significant problem for pixel-based supervised classifications. A benefit of data digitized from aerial imagery is that operators can interpret context. That is, they are not solely reliant on the feature itself for classification; they can also use cues from the surrounding landscape. For example, it is not possible for terrain data input to distinguish a level wetland from a level parking lot or recreational field, whereas this is a simple task for an air photo interpreter. This problem with the terrain data (i.e. excluding the canopy height model) is twofold: it cannot identify differences in vegetation, nor can it recognize proximal information such as dirt infields or peripheral information like cars. This illustrates why the use of multi-source and multi-temporal input data tends to be more successful in remote sensing classification applications.

Some decisions related to the preprocessing of data inputs were based on previously published literature (e.g. filtering for RADARSAT-2 and atmospheric correction for optical imagery). However, empirical evidence was used to determine suitable preparation techniques for terrain variables obtained from lidar. Specifically, parameters were chosen according to a visual assessment and results from previous experimentation.

6.4   Recommendations

It is important for wetlands to be understood from a regional perspective, such as a secondary basin level, because wetlands act as reservoirs, provide fire protection, attenuate flooding, reduce pollutants, and control the accumulation of sediment (Brooks et al. 2013).

Even when input data are of lower resolution, they can still provide a source of information which helps identify where development may conflict with sensitive areas. Thus, adopting a classification system which is standardized throughout a region is critically important. The cost of acquiring high resolution data may be prohibitive, but in the meantime it is important to continue to update mapping programs as they provide an ongoing baseline of information upon which to continually improve. Due to limited availability of high resolution data, I investigated the feasibility of mapping wetlands using a combination of radar, with terrain and optical imagery data that are easier to obtain and process for large areas (i.e. the provincial DEM and Landsat 8 imagery).

Processing remotely sensed images involves a statistical analysis of reflectance (in the case of optical imagery) or scattering characteristics (in the case of radar). However, understanding the characteristics of the land cover type can improve the accuracy of classification applications (King 2002), and this information can be provided by additional datasets. I opted to use terrain variables because wetlands are known to be influenced by hydrogeomorphic criteria. However, accurate soil characteristics would also be useful, but were not considered in my classifications.

Contextual information can increase the success of landcover classification derived from remotely sensed data. King (2002) highlighted this in a paper describing landcover mapping principles by citing the example of aerial photograph interpretation, where consideration of landscape pattern, landscape position, and other landscape associations is common and expected. Software designed to process and analyze remotely sensed imagery includes a large number of tools to facilitate this kind of classification process, such as object-based image analysis (OBIA). By grouping 'features', object-based classification becomes more efficient and provides the user with more options to analyse the data (Conchedda et al. 2008). This concept was first introduced in 1976 (Kettig and Landgrebe 1976); however, challenges related to hardware and software prevented a study from being published until 2002 (Knight et al. 2015). Today, this approach may provide more successful classification results, especially when using high-resolution optical imagery such as QuickBird.

Based on the results and lessons learned, I have identified other promising revisions to the method. The revisions could be applied to meet the same objectives specified in this thesis, but would test a different combination of input data. For example, in the best case scenario of the higher resolution inputs (i.e. lidar, RADARSAT-2 intensity and polarimetric variables, and QuickBird), QuickBird should be replaced by Landsat 8. While classifying Landsat 8 alone resulted in 69.3% of the 137 wetland ground truth sites being identified correctly, and the amount for QuickBird alone was 66.4%, the much larger footprint and cost-free option for Landsat 8 make it more attractive. Here, it would be good to account for that similarity and to explore if the better spectral and radiometric resolution of Landsat 8, outweighs the higher spatial resolution of QuickBird.

The ability of the RF classifier's capacity for non-parametric data rationalized the decision to combine various inputs together into one file for each classification. However, this meant that each input had to be resampled to the lowest spatial resolution (e.g. 8 m and 30 m). Given that the native spatial resolution of each data input varied (significantly for the recommendation above to use lidar and Landsat 8), it may be advantageous to classify each input separately and to combine those classification results using a multi-criteria approach. For example, the 2 m lidar DEM could be processed first to create a binary wetland/non-wetland mask. The 8 m RADARSAT-2 and the 30 m Landsat 8 could be used to classify only within the wetland mask portion, thus simplifying the information needed from these sources.

6.5   Research Topics Warranting Future Study

After efforts to improve wetland mapping accuracy, several new applications and research topics should be considered. For example, disturbances such as fire and anthropogenic development (both of which are of concern in the study area) are expected to affect land cover and may confuse the classification process, at least in the short-term. Therefore, future researchers should seek to continue improving classification methods, so that outputs are more robust.

Fire has been a major natural disturbance agent in the forests of Nova Scotia since the time of European settlement, more often occurring in late spring and throughout the summer.

However, fire frequency also depends on topography, soil, and climate, and more conducive conditions are found in the lowland districts and in the western ecoregion (Neily et al. 2008) where my study area is located. Fire is one natural event that can damage infrastructure, modify soil, affect the structure of the vegetation, and even change the hydrologic processes of a watershed (Brooks, Ffolliott and Magner 2013). On the other hand, work by Norton and De Lange (2003) in peat bogs of New Zealand suggested that fire is necessary to preserve diversity in plant communities as well as to sustain threatened bog species. Future studies should therefore seek to further elucidate the critical effects that fire has on wetlands. The study area has experienced frequent fires over time, including a large forest fire in 2009 and a smaller one in 2012. Beazley and Patriquin (2010) observed that much of the vegetation below ground had survived; therefore, regeneration was well underway a year later. During this particular fire, larger wetlands were not as damaged as smaller ones, and in fact helped limit the spread of fire; however, smaller wetlands were impacted by heat and have been one of the slowest features to re-vegetate (Beazley and Patriquin 2010).

Aside from the recovery period that immediately follows a fire, during which changes in hydrology and wetlands are the most severe, the effects of fire disturbance tend to be less extreme than those associated with urban development (Brooks, Ffolliott and Magner 2013). The current study area is also experiencing pressure from urban development, which is having a more or less permanent impact on the hydrology and wetlands of McIntosh Run. Striving to lower the harmful effects of development should be a goal of land-use management (Brooks, Ffolliott and Magner 2013). Nevertheless, even with a stringent impact mitigation program, a change in the area and function of wetlands is inevitable. Mapping and monitoring can help reduce issues such as flooding and reduced water quality.

Using the modeled wetlands produced in this study, future research could look at resilience of the watershed, that is, the ability of functioning wetlands to maintain ecological integrity, flood control, etc. and how changes to the watershed impede that ability.

6.6 Final Remarks

Wetlands are critically important ecological systems that are comparable to tropical rain forests in terms of biodiversity. They improve water quality by providing natural filtration mechanisms and by controlling the rate of runoff. Wetlands also provide social benefits for people and unique habitat for a multitude of plant and animal species. The economic value of wetlands may be obscure; however, when factors such as waterflow regulation, erosion control, and recreational benefits are considered, their substantial monetary value becomes more obvious. For these reasons, accurate assessment of wetland classification is essential for long-term monitoring, urban planning, and natural resource management applications. With proper stakeholder involvement, a watershed plan that provides clear and comprehensive strategies to address environmental and management issues can be created (Prince Edward Island Environment, Energy and Forestry nd).

One of the objectives of this thesis was to identify methods which are able to improve on the current wetland inventory used by the province of Nova Scotia. Remote sensing techniques present an affordable and practical solution, and were shown to dramatically improve accuracy compared to the current inventory. Though time constraints restricted this research to a single, representative pilot area, the methodology could feasibly be followed to begin the transition from research to production.

6.7 References

Beazley, R., and Patriquin, D. 2010. "Regeneration of Forest and Barrens after the Spryfield Fire." Retrieved from Halifax Field Naturalists: http://halifaxfieldnaturalists.ca/spryfieldfire/SpryfieldFire.html

Brooks, K., Ffolliott, P., and Magner, J. 2013. *Hydrology and the management of watersheds (4th ed.)*. Ames, Iowa, USA: Wiley-Blackwell.

Comber, A., Fisher, P., and Wadsworth, R. 2005. "What is land cover?" *Environment & Planning B: Planning & Design*, Vol. 32, No. 2, pp. 199-209.

Conchedda, G., Durieux, L., Mayaux, P. 2008. "An object-based method for mapping and change analysis in mangrove ecosystems." *ISPRS journal of photogrammetry and Remote Sensing*, Vol. 63, No. 5, pp. 578-589.

Kettig, R., and Landgrebe, D. 1976. "Classification of multispectral image data by extraction and classification of homogeneous objects." *IEEE Transactions on Geoscience Electronics*, Vol. 14, No. 1, pp. 19-26.

King, R.B. 2002. "Land cover mapping principles: a return to interpretation fundamentals." *International Journal of Remote Sensing.* Vol. 23, No. 18, pp. 3525-3545.

Knight, J., Corcoran, J., Rampi, L., and Pelletier, K. 2015. "Theory and Applications of Object-Based Image Analysis and Emerging Methods in Wetland Mapping." In: *Remote Sensing of Wetlands: Applications and Advances*. Boca Raton, FL, USA: CRC

LaRocque, A., Leblon, B., Bourgeau-Chavez, L., McCarty, J., French, N., and Woodward, R. 2015. "Evaluating wetland mapping techniques for New Brunswick using Landsat TM, ALOS-PALSAR and RADARSAT-2 dual-polarized images." *Canadian Journal of Remote Sensing* (2015).

McCoy, R. 2005. *Field methods in remote sensing*. New York, NY, USA: Guilford Press.

Neily, P., Quigley, E., and Stewart, B. 2008. "Mapping Nova Scotia's Natural Disturbance." Nova Scotia Department of Natural Resources. Retrieved from http://novascotia.ca/natr/library/forestry/reports/NDRreport3.pdf

Norton, D., and De Lange, P. 2003. "Fire and Vegetation in a Temperate Peat Bog: Implications for the Management of Threatened Species." *Conservation Biology.* Vol. 17, No. 1, pp. 138-148.

Prince Edward Island Environment, Energy and Forestry. nd. "A Guide to Watershed Planning on Prince Edward Island." Retrieved from http://www.gov.pe.ca/photos/original/eef_waterguide.pdf

Slatton, K., Crawford, M., and Chang, L. 2008. "Modeling temporal variations in multipolarized radar scattering from intertidal coastal wetlands." *ISPRS Journal of Photogrammetry and Remote Sensing*, Vol. 63, pp. 559-577.

van Meter, R., Bailey, L., Bailey, and Meter, R. 2008. "Methods for estimating the amount of vernal pool habitat in the Northeastern United States." *Wetlands.* Vol. 28, No. 3, pp. 585-593.

Wilson, J., and Gallant, J. C. 2000. *Terrain analysis: Principles and applications*. New York: Wiley.

Bibliography

Beazley, R., and Patriquin, D. 2010. "Regeneration of Forest & Barrens after the Spryfield Fire." Retrieved from Halifax Field Naturalists: http://halifaxfieldnaturalists.ca/spryfieldfire/SpryfieldFire.html

Bourgeau-Chavez, L. L., Kasischke, E. S., Brunzell, S. M., Mudd, J. P, Smith, K. B. and Frick, A. L. 2001. "Analysis of spaceborne SAR data for wetland mapping in Virginia riparian ecosystems." *International Journal of Remote Sensing*, Vol. 22, No. 18, pp. 3665-3687.

Bourgeau-Chavez, L. L., Endres, S., Battaglia, M., Miller, M. E., Banda, E., Laubach, Z., Higman, P., Chaw-Fraser, P., and Marcaccio, J. 2015. "Development of a bi-national Great Lakes coastal wetland and land use map using three-season PALSAR and Landsat imagery." *Remote Sensing*, Vol. 7, No. 7, pp. 8655-8682.

Bourgeau-Chavez, L. L., Riordan, K., Miller, N., Nowels, M., and Powell, R. B. 2008. "Remotely monitoring Great Lakes coastal wetlands with multi-sensor, multi-temporal SAR and multi-spectral data." *Proceedings of the 2008 International Geoscience and Remote Sensing Symposium (IGARSS 2008)*: pp. I-428 - I-429.

Breiman, L., 2001. "Random Forest". *Machine Learning*, Vol. 45, No. 1, pp. 5-32.

Breiman, L., 2003. "Manual of Setting up, Using and Understanding Random Forest", V4.0, University of California Berkeley, Statistics Department, Berkeley.

Breiman, L., and Cutler, A. nd. Random Forests. Retrieved from https://www.stat.berkeley.edu/~breiman/RandomForests/cc_home.htm

Brinson, M.M. 1993. "Changes in the Functioning of Wetlands Along Environmental Gradients." *Wetlands*. Vol. 13, No. 2, pp. 65-74.

Brisco, B. 2015. "Mapping and monitoring surface water and wetlands with synthetic aperture radar." In R. Tiner, M. Lang, and V. Klemas (Eds.), *Remote Sensing of Wetlands: Applications and Advances* (pp. 119-136). Boca Raton, FL, USA: CRC Press.

Brisco, B., Kapfer, M., Hirose T., Tedford, B., and Liu, J. 2011. "Evaluation of C-band polarization diversity and polarimetry for wetland mapping." *Canadian Journal of Remote Sensing*, Vol. 37, pp. 82-92.

Brisco, B., Touzi, R., van der Sanden, J. J., Charbonneau, F., Pultz, T. J. and D'Iorio, M. 2008. "Water resource applications with RADARSAT-2 – a preview." *International Journal of Digital Earth*, Vol. 1, No. 1, pp. 130-147.

Brooks, K., Ffolliott, P., and Magner, J. 2013. *Hydrology and the management of watersheds* (4th ed.). Ames, Iowa, USA: Wiley-Blackwell.

Canada Centre for Remote Sensing. nd. "Fundamentals of Remote Sensing: A Canada Centre for Remote Sensing Remote Sensing Tutorial." Retrieved from http://www.nrcan.gc.ca/sites/www.nrcan.gc.ca/files/earthsciences/pdf/resource/tutor/fundam/pdf/fundamentals_e.pdf.

Canada Committee on Ecological (Biophysical) Land Classification. 1988. "Wetlands of Canada." Ottawa: Sustainable Development Branch, Canadian Wildlife Service, Conservation and Protection, Environment Canada. pp. 1-61.

Castrignano, A., Buttafuoco, G., Comolli, R., and Ballabio, C. 2006. "Accuracy assessment of digital elevation model using stochastic simulation." *Proceedings of the 7th International Symposium on Spatial Accuracy Assessment in Natural Resources and Environmental Sciences*. pp. 490–498.

Cloude, S., and Pottier, E. 1997. "An entropy based classification scheme for land applications of polarimetric SAR." *IEEE Transactions on Geoscience and Remote Sensing*, Vol. 35, No. 1, pp. 68-78.

Comber, A., Fisher, P., and Wadsworth, R. 2005. "What is land cover?" *Environment and Planning B: Planning and Design*, Vol. 32, No. 2, pp. 199-209.

Conchedda, G., Durieux, L., Mayaux, P. 2008. "An object-based method for mapping and change analysis in mangrove ecosystems." *ISPRS journal of photogrammetry and Remote Sensing*, Vol. 63, No. 5, pp. 578-589.

Congalton, R. 1991. "A review of assessing the accuracy of classifications of remotely sensed data." *Remote Sensing of Environment*, Vol. 37, pp. 35–46.

Congalton, R.G., and Green, K. 1999. "Sample Design. In Assessing the accuracy of remotely sensed data: principles and practices." New York, NY, USA: CRC Press Inc. pp. 17-25.

Congalton, R. G., and Green, K. 2009. "Assessing the accuracy of remotely sensed data: Principles and practices." Boca Raton, FL, USA: CRC Press/Taylor & Francis.

Cooley, S. 2015. "Terrain Roughness." Retrieved July 5, 2014 from http://gis4geomorphology.com/roughness-topographic-position/

Corcoran, J. M., Knight, J. F., Brisco, B., Kaya, S., Cull, A., and Murnagahn, K. 2011. "The integration of optical, topographic, and radar data for wetland mapping in Northern Minnesota." *Canadian Journal of Remote Sensing*, Vol. 37, No. 5, pp. 564-582.

Corcoran, J. M., Knight, J. F., and Gallant, A. L. 2013. "Influence of multi-source and multi-temporal remotely sensed and ancillary data on the accuracy of Random Forest classification of wetlands in Northern Minnesota." Remote Sensing, Vol. 5, No. 7, pp. 3212-3238.

Ehlers, J., and Gibbard, P. L. 2004. "Quaternary glaciations: Extent and chronology." Amsterdam, Netherlands: Elsevier. GIS data retrieved from http://booksite.elsevier.com/9780444534477/digital_maps.php

Environment Canada. 2011. "Glossary". Retrieved from http://www.ec.gc.ca/default.asp?lang=En&n=7EBE5C5A-1#glossaryw

Environmental Laboratory. 1987. "Corps of Engineers wetlands delineation manual" Technical Report Y-87-1. U.S. Army Engineer Waterways Experiment Station, Vicksburg, MS.

ESRI [Computer software]. 2015. Retrieved from http://www.esri.com

Evans, D.L., Farr, T.G., van Zyl, J.J., and Zebker, H.A. 1988. "Radar polarimetry: Analysis tools and applications." *IEEE Transactions on Geoscience and Remote Sensing*, Vol. 26, No. 6, pp. 774-789.

Fournier, R., Grenier, A, M., Lavoie, A., and Hélie, R. 2007. "Towards a strategy to implement the Canadian Wetland Inventory using satellite remote sensing." *Canadian Journal of Remote Sensing*, Vol. 33, Supp. 1, pp. S1–S16.

Freeman, A., and Durden, S. 1998. "A three-component scattering model for polarimetric SAR data." *IEEE Transactions on Geoscience and Remote Sensing*, Vol. 36, No. 3, pp. 963-973.

Geosetter [Computer software]. 2012. Retrieved from http://www.geosetter.de/en/

Gislason, P., Benediktsson, J., and Sveinsson, J. 2006. "Random Forest for land cover classification." Pattern Recognition Letters, Vol. 27, pp. 294-300.

Goodman, J. W. 1976. "Some fundamental properties of speckles." Journal of the Optical Society of America, Vol. 66, No. 11, pp. 1145-1150.

Government of Canada. 2015. "Climate Data. Shearwater RCS, Environment Canada." Retrieved from http://climate.weather.gc.ca/index_e.html

GRASS-Wiki. 2015. "QuickBird." Retrieved from https://grasswiki.osgeo.org/wiki/QuickBird

Grenier, M., Demers, A.-M., Labrecque, S., Benoit, M., Fournier, R. A., and Drolet, B. 2007. "An object-based method to map wetland using RADARSAT-1 and Landsat ETM images: Test case on two sites in Quebec, Canada." *Canadian Journal of Remote Sensing*, Vol. 33, Supp. 1, pp. S2-S45.

Harris, A., Bryant, R. G., and Baird, A. J. 2005. "Detecting water stress in Sphagnum spp." *Remote Sensing of Environment*, Vol. 97, No. 3, pp. 371–381.

Harris, A., Bryant, R. G., and Baird, A. J. 2006. "Mapping the effects of water stress on Sphagnum: Preliminary observations using airborne remote sensing." *Remote Sensing of Environment*, Vol. 100, No. 3, pp. 363-378.

Hill, N, and Patriquin, D. 2014. "Ecological Assessment of the Plant Communities of the Williams Lake Backlands." Retrieved from Williams Lake Conservation Company: http://www.williamslakecc.org/documents/WLBFinalRep12Feb2014.pdf pp. 1-83.

Hogg, A., and Todd, K. 2007. "Automated discrimination of upland and wetland using terrain derivatives." *Canadian Journal of Remote Sensing*, Vol. 33, pp. S68-S83.

Hutchinson, M., Xu, T., and Stein, J. 2011. "Recent Progress in the ANUDEM Elevation Gridding Procedure." Retrieved from http://geomorphometry.org/system/files/HutchinsonXu2011geomorphometry.pdf

IBM SPSS Statistics [Computer software]. 2015. Retrieved from http://www-01.ibm.com/software/analytics/spss/

Illinois Department of Natural Resources. 2011. "Hydrophytic Vegetation." Retrieved from http://dnr.state.il.us/wetlands/ch1e.htm

Jacobson, J. E., Ritter, R. A. and Koeln, G. T. 1987. "Accuracy of Thematic Mapper derived wetlands as based on National Wetland Inventory data." American Society Photogrammetry and Remote Sensing Technical Papers, 1987 ASPRS-ACSM Fall Convention, Reno, NV. pp. 109-118.

Jennes, J. 2002. "Topographic Position Index." Retrieved May 1, 2014 from http://www.jennessent.com/downloads/tpi_documentation_online.pdf/

Kandus, P., Karszenbaum, H., Pultz, T., Parmuchi, G., and Bava, J. 2001. "Influence of flood conditions and vegetation status on the radar backscatter of wetland ecosystems", *Canadian Journal of Remote Sensing*, Vol. 27, No. 6, pp. 651-662.

Kasischke, E.S. and Bourgeau-Chavez, L.L. 1997. "Monitoring South Florida Wetlands Using ERS-1 SAR Imagery." Photogrammetric Engineering & Remote Sensing. Vol. 63, No. 3, pp. 281-291.

Kettig, R., and Landgrebe, D. 1976. "Classification of multispectral image data by extraction and classification of homogeneous objects." IEEE Transactions on Geoscience Electronics, Vol. 14, No. 1, pp. 19-26.

King, R.B. 2002. "Land cover mapping principles: a return to interpretation fundamentals." International Journal of Remote Sensing. Vol. 23, No. 18, pp. 3525-3545.

Knight, J., Corcoran, J., Rampi, L., and Pelletier, K., 2015. "Theory and Applications of Object-Based Image Analysis and Emerging Methods in Wetland Mapping." In: *Remote Sensing of Wetlands: Applications and Advances*. Boca Raton, FL, USA: CRC

Krause, K. 2003. "Radiance Conversion of QuickBird Data – Technical Note." Retrieved from: https://apollomapping.com/wp-content/ user_uploads/2011/09/Radiance_Conversion_of_QuickBird_Data.pdf

LaRocque, A., Leblon, B., Bourgeau-Chavez, L., McCarty, J., French, N., and Woodward, R. 2015. "Evaluating wetland mapping techniques for New Brunswick using Landsat TM, ALOS-PALSAR and RADARSAT-2 dual-polarized images." *Canadian Journal of Remote Sensing* (submitted).

Lee, J.S., Grunes, M.R., Ainsworth, TL., Du, LJ., and Schuler, DL. 1999. "Unsupervised classification using polarimetric decomposition and the complex Wishart classifier." *IEEE Transactions on Geoscience and Remote Sensing*, Vol. 37, No. 5, pp. 2249-2258.

Lee J.S., Grunes, M.R., and Kwok R. 1994. "Classification of multi-look polarimetric SAR imagery based on the complex Wishart distribution." International Journal of Remote Sensing, Vol. 15, No. 11, pp. 2299-2311.

Lee, J.S., Pottier, G., and Ferro-Famil, L. 2004. "Unsupervised terrain classification preserving polarimetric scattering characteristics." *IEEE Transactions on Geoscience and Remote Sensing*, Vol. 42, No. 4, pp. 722-731.

Li, J., and Chen, W. 2005. "A rule-based method for mapping Canada's wetlands using optical, radar and DEM data." International Journal of Remote Sensing, Vol. 26, No. 22, pp. 5051-5069.

Lillesand, T.M. and Kiefer, R.W. 1994. Remote Sensing and Image Interpretation. New York, NY, USA: John Wiley and Sons Inc.

Lopez-Martinez, C., Pottier, E., and Cloude, S.R. 2005. "Statistical assessment of eigenvector-based target decomposition theorems in radar polarimetry." *IEEE Transactions on Geoscience and Remote Sensing*, Vol. 43, No. 9, pp. 2058-2074.

Louppe, G., Wehenkel, L., Sutera, A., and Geurts, P, 2013. "Understanding variable importances in forests of randomized trees." Advances in Neural Information Processing Systems, Vol. 26, pp. 431-439.

Lynch-Stewart, P., Neice, P., Rubec, C. and Kessel-Taylor, I. 1996. "The Federal Policy on Wetland Conservation – Implementation Guide for Federal Land Managers." Ottawa, Environment Canada. pp. 1-20. Retrieved from http://nawcc.wetlandnetwork.ca/Fed%20Policy%20Wetland%20Conserv_Implement%20Guide%20for%20Fed%20Land%20Mgrs.pdf

Maclin, R., and Opitz, D. 2011. "Popular Ensemble Methods: An Empirical Study." Journal Of Artificial Intelligence Research, Vol. 11, pp. 169-198.

Mapwel [Computer software]. 2012. Retrieved from https://www.mapwel.net/

McCoy, R. 2005. Field methods in remote sensing. New York, NY, USA: Guilford Press.

Meingast, K. M., Falkowski, M. J., Kane, E. S, Potvin, L. R., Benscoter, B. W., Smith, A. M. S., Bourgeau-Chavez, L. L., and Miller, M. E. 2014. "Spectral detection of near-surface moisture content and water-table position in northern peatland ecosystems." *Remote Sensing of Environment*, Vol. 152, pp. 536-546.

Millard, K. and Richardson, M. 2013 "Wetland mapping with LiDAR derivatives, SAR polarimetric decompositions, and LiDAR–SAR fusion using a random forest classifier." *Canadian Journal of Remote Sensing*, Vol. 39, No. 4, pp. 290-307.

Millard, K., and Richardson, M. 2015. "On the importance of training data sample selection in random forest image classification: A case study in peatland ecosystem mapping." Remote sensing, Vol. 7, No. 7, pp. 8489-8515.

Mitsch, W. J., and Gosselink, J. G. 2007. Wetlands. Hoboken, New Jersey, USA: John Wiley & Sons, Inc.

Monette, S. and Hopkinson, C. 2010. "Development of an Urban Forest Canopy Model for input into a Lidar-based Storm Water Runoff Model for Halifax Harbour Watersheds." Retrieved from http://atlanticadaptation.ca/sites/discoveryspace.upei.ca.acasa/files/HRM%20Forest%20Canopy%20Final%20Report_0.pdf

Moore, Grayson, and Ladson. 1991. "Digital terrain modelling: A review of hydrological, geomorphological, and biological applications." Hydrological processes, Vol. 5, No. 1, pp. 3-30.

Neily, P. D., Quiget, E., Benjamin, L., Stewart, B., and Duke, T. 2003. "Ecological land classification for Nova Scotia: Volume I, mapping Nova Scotia's terrestrial ecosystems." Halifax, N.S.: Nova Scotia Department of Natural Resources, Renewable Resources Branch. pp. 1-77.

Neily, P. D., Quigley, E., Benjamin, L., Stewart, B., and Duke, T. 2005. "Ecological land classification for Nova Scotia." Halifax, N.S.: Nova Scotia Department of Natural Resources, Renewable Resources Branch. pp. 1-70.

Neily, P., Quigley, E., and Stewart, B. 2008. "Mapping Nova Scotia's Natural Disturbance." Nova Scotia Department of Natural Resources. Retrieved from http://novascotia.ca/natr/library/forestry/reports/NDRreport3.pdf

Newmaster, S.G., Harris, A.G. and Kershaw, L.J. 1997. Wetland Plants of Ontario. Edmonton, AB, Canada: Lone Pine Publishing.

Norton, D., and De Lange, P. 2003. "Fire and Vegetation in a Temperate Peat Bog: Implications for the Management of Threatened Species." Conservation Biology. Vol. 17, No. 1, pp. 138-148.

Nova Scotia Department of Natural Resources. 2011. "Ecosystems and Habitats Program Overview." Retrieved from http://novascotia.ca/natr/wildlife/habitats/wetlands.asp

Nova Scotia Environment. 2009. "Nova Scotia Wetland Conservation Policy (Draft for Consultation)." pp. 1-24. Retrieved from http://www.gov.ns.ca/nse/wetland/docs/Nova.Scotia.Wetland.Conservation.Policy.pdf

Nova Scotia Geomatics Centre. 2015. "Digital Elevation Model Specifications." Retrieved from http://www.nsgc.gov.ns.ca/mappingspecs/Specifications/Compilation/Resource_NSTDB/default.htm

Nova Scotia Legislature. 2007. "Environmental Goals and Sustainable Prosperity Act, Bill No. 146." Retrieved from http://nslegislature.ca/legc/PDFs/annual%20statutes/2007%20Spring/c007.pdf

Nova Scotia Museum of Natural History. 1989. "Natural History of Nova Scotia, The Dynamics of Nova Scotia's Climate." pp. 94-103. Retrieved from https://ojs.library.dal.ca/NSM/article/download/3752/3438

Ontario Ministry of Natural Resources. 2007. "Evaluation of Lidar Elevation Derivatives." Unpublished Internal Document.

Ontario Ministry of Natural Resources. 2014. "Ontario Wetland Evaluation System Southern Manual 3rd edition, version 3.3." pp. 1-284. Queen's Printer for Ontario. Retrieved from http://files.ontario.ca/environment-and-energy/parks-and-protected-areas/ontario-wetland-evaluation-system-southen-manual-2014.pdf

Ou, C., Zhang, Y., LaRocque, A., Leblon, B., Webster, K., McLaughlin, J., and Barnett, P. 2014. "Model calibration for mapping permafrost using Landsat-5 TM and RADARSAT-2 images." *Proceedings of the 2014 IEEE International Geoscience and Remote Sensing Symposium (IGARSS 2014)*: pp. 4883-4886.
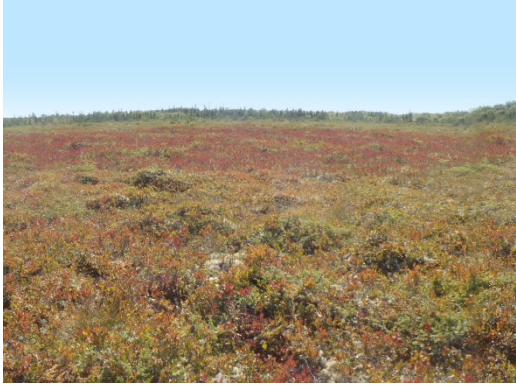
Ozdarici-Ok, A., Akar, O., and Gungor, O. 2012. "Evaluation of Random Forest method for agricultural crop classification." European Journal of Remote Sensing, Vol. 45, No. 3, pp. 421-432.

Ozesmi, S. L., and Bauer, M. E. 2002. "Satellite remote sensing of wetlands." Wetland Ecology and Management, Vol. 10, pp. 381-402.

PCI Geomatica. 2014. "PCI Geomatica Help File." Retrieved from PCI Geomatica software.

Pennock, D., Zebarth, B., and DeJong, E. 1987. "Landform classification and soil distribution in hummocky terrain, Saskatchewan, Canada." Geoderma, Vol. 40, No. 3-4, pp. 297-315.

Pielou, E. 1991. "After the Ice Age the return of life to glaciated North America." Chicago, IL, USA: University of Chicago Press.

Pietroniro, A., and Leconte, R. 2005. "A review of Canadian remote sensing and hydrology, 1999-2003." Hydrological Processes, Vol. 19, No. 1, pp. 285-301.

Poff, N.L. 1996. "A hydrogeography of unregulated streams in the United States and an examination of scale-dependence in some hydrological descriptors." Freshwater Biology. Vol. 36, pp. 71-91.

Pope, K.O., Rejmankova E., Paris J.F., and Woodruff, R. 1997. "Detecting Seasonal Flooding Cycles in Marshes of the Yucatan Peninsula with SIR-C Polarimetric Radar Imagery." Remote Sensing of Environment, Vol. 59, No. 2, pp. 157-166.

Prince Edward Island Environment, Energy and Forestry. nd. "A Guide to Watershed Planning on Prince Edward Island." Retrieved from http://www.gov.pe.ca/photos/original/eef_waterguide.pdf

R Development Core Team, 2012. "R: A language and environment for statistical computing." Vienna, R Foundation for Statistical Computing. Retrieved from https://www.r-project.org/

Rao, B., Dwivedi, R., Kushwaha, S., Bhattacharya, S., Anand, J., and Dasgupta, S. (1999). Monitoring the spatial extent of coastal wetlands using ERS-1 SAR data. International Journal of Remote Sensing, Vol. 20, No. 13, pp. 2509-2517.

Rebelo, L. S., 2010. "Eco-hydrological characterization of inland wetlands in Africa using L-Band SAR." IEEE Journal of Selected Topics in Applied Earth Observations and Remote Sensing, Vol. 3, No. 4, pp. 554-559.

Rodriguez, E. and Martin, J.M. 1992. "Theory and design of interferometric synthetic aperture radars." IEE Proceedings F Radar and Signal Processing, Vol. 139, No. 2, pp. 147-159.

Sader, A., Ahl, D., and Liou, W. 1995. "Accuracy of Landsat-TM and GIS rule-based methods for forest wetland classification in Maine." Remote Sensing of Environment, Vol. 53, pp. 133-144.

Schoewe, W.H. 1951. "The Geography of Kansas: PART III. Hydrogeography." Transactions of the Kansas Academy of Science. Vol. 54, No. 3 , pp. 263-329.

Schott, J.R. 2007. "Remote Sensing: the image chain approach." New York, NY, USA: Oxford University Press.

Slatton, K., Crawford, M., and Chang, L. 2008. "Modeling temporal variations in multipolarized radar scattering from intertidal coastal wetlands." *ISPRS journal of photogrammetry and Remote Sensing*, Vol. 63, pp. 559-577.

Sokol, J., McNairn, H., and Pultz, T. 2004. "Case studies demonstrating the hydrological applications of C-band multipolarized and polarimetric SAR." *Canadian Journal of Remote Sensing*, Vol. 30, No. 3, pp. 470-483.

Strobl, C., Boulesteix, A.-L., Kneib, T., Augustin, T., and Zeileis, A. 2008. "Conditional variable importance for Random Forests." *BMC Bioinformatics*, Vol. 9, No. 1, pp. 307.

Telegraph Journal. February 21, 2011. "Profs defend wetlands mapping system." Retrieved from: http://telegraphjournal.canadaeast.com/front/article/1381

Tiner, R.W. 1999. *Wetlands indicators: a guide to wetland identification, delineation, classification, and mapping*. Lewis Publishers, Boca Raton (Florida, USA).

Touzi, R. 2007. "Target Scattering Decomposition in Terms of Roll-Invariant Target Parameters." *IEEE Transactions on Geoscience and Remote Sensing*, Vol. 45, No. 1, pp. 73-84.

Touzi, R., Deschamps, A., and Rother, G. 2009. "Phase of Target Scattering for Wetland Characterization Using Polarimetric C-Band SAR." *IEEE Transactions on Geoscience and Remote Sensing*, Vol. 47, No. 9, pp. 3241-3261.

Touzi, R., Deschamps, A., and Rother, G. 2007. "Wetland Characterization using Polarimetric RADARSAT-2 Capability." *Canadian Journal of Remote Sensing*, Vol. 33, Supp. 1, pp. 56-67.

Touzi, R., Goze, S., Le Toan, T., Lopes, A., and Mougin, E. 1992. "Polarimetric discriminators for SAR images." *IEEE Transactions on Geoscience and Remote Sensing*, Vol. 30, No. 5, pp. 973-980.

United States Geological Survey. 2015. "Using the USGS Landsat 8 Product." Retrieved from http://landsat.usgs.gov/Landsat8_Using_Product.php

United States Natural Resources Conservation Service. (2012). Hydric Soils Technical Note 8. Retrieved from http://www.nrcs.usda.gov/wps/portal/nrcs/detail/soils/use/hydric/?cid=nrcs142p2_053983

van Beijma, S., Comber, A., and Lamb, A. 2014. "Random Forest classification of salt marsh vegetation habitats using quad-polarimetric airborne SAR, elevation and optical RS data." *Remote Sensing of Environment*, Vol. 149, pp. 118-129.

van Meter, R., Bailey, L., Bailey, and Meter, R. 2008. "Methods for estimating the amount of vernal pool habitat in the Northeastern United States." *Wetlands*. Vol. 28, No. 3, pp. 585-593.

van Zyl, J.J., Zebker, H.A., and Elachi, C. 1987. "Imaging radar polarization signatures: Theory and observation." *Radio science*, Vol. 22, No. 4, pp. 529-543.

Vitt, D.H. 1994. "An Overview of Factors that Influence the Development of Canadian Peatlands." *Memoirs of the Entomological Society of Canada*. Vol. 126, No. 169, pp. 7-20.

Wang, J., Shang J., Brisco, B., and Brown, R. 1998. "Evaluation of multi-date ERS-1 and multispectral Landsat imagery for wetland detection in Southern Ontario." *Canadian Journal of Remote Sensing*, Vol. 31, pp. 214-224.

Warner, B.G. and Rubec, C.D.A. (Eds.). 1997. "The Canadian Wetland Classification System. (2nd edition)." National Wetlands Working Group. Wetlands Research Centre. University of Waterloo. Ontario, pp. 1-68.

Waske, B., Heinzel, V., Braun, M., and Menz, G. 2007. "Random Forests for classifying multi-temporal SAR data." In *Proceedings Envisat Symposium*, Montreux, Switzerland. April 23-27, 2007.

Waske, B. and Braun, B. 2009. "Classifier ensembles for land cover mapping using multi-temporal SAR Imagery." *ISPRS journal of photogrammetry and Remote Sensing*, Vol. 64, pp. 450-457.

Whitcomb, J., Moghaddam, M., McDonald, K., Kellndorfer, J., and Podest, E. 2009. "Mapping vegetated wetlands of Alaska Using L-band radar satellite imagery." *Canadian Journal of Remote Sensing*, Vol. 35, No. 1, pp. 54-72.

Wilson, J., and Gallant, J. C. 2000. *Terrain analysis: Principles and applications*. New York: Wiley.

Woodhouse, I. 2006. *Introduction to microwave remote sensing.* Boca Raton, FL, USA: Taylor & Francis.

Zebker, H.A., van Zyl, J.J., and Held, D.N. 1987. "Imaging radar polarimetry from wave synthesis." *Journal of Geophysical Research*, Vol. 92, No. B1, pp. 683-701.

Appendix A

Class		Description
barren		Area with more than 50% exposed rock outcrop and less than 25% vegetation.
grass		Area of manicured grass such as recreation fields and golf courses.
industrial		built-up areas consisting of large, low-rise industrial buildings and parking lots.

lake		Deeper water with no apparent vegetation.
open-water / marsh complex		Combination of open-water wetland and shallow marsh. Marshes have shallow water levels that can fluctuate daily and expose the soil. Shallow or open-water wetlands have water depths up to 2m that are typically stable, but soil may occasionally become exposed.
open bog		Ombrotrophic peatland area with primarily ericaceous plants and sphagnum, and less than 25% tree coverage. They have a raised or level surface and are not affected by runoff or ground water.
open fen		Minerotrophic peatland with ericaceous plants, sedges and brown mosses and less than 25% tree coverage. The ground and surface water movement is more stable, and exposed water in channels can form characteristic patterns.

shrub/treed fen/ bog		Peatland with more than 25% tree coverage. Treed fens and bogs are not easily differentiated and so are combined for this research.
swamp		wetlands dominated by trees (typically > 30% cover) that are influenced by minerotrophic groundwater. They can be found on either mineral or peat soils and are typically considered the driest wetland type.
upland sparse vegetation		area with less than 50% exposed rock outcrop. vegetation primarily low and ericaceous.
upland forest		forested stand containing trees at least 3m in height.

urban		built-up areas consisting of high-rise urban core buildings, streets and sidewalks.

Appendix B

Author and classification method	Platform	Input variable	Classification accuracy (%)	
Brisco et al. 2011 (Maximum-likelihood Classifier)	Airborne Convair-580 (C-band) polSAR	Cloude-Pottier Decomposition	Overall Whitetop Sedge Phragmites Grasses Cattail Bulrush Open water	64.65 83.64 69.55 54.46 27.44 62.28 58.33 96.84
Corcoran et al. 2011 (Random Forests Classifier)	RADARSAT-2 (C-band) polSAR	HH, HV, VH, VV Cloude-Pottier Decomposition Freeman-Durden Decomposition Van Zyl Decomposition	Overall Water Emergent wetlands Forested wetlands Scrub/shrub Wetlands Upland	63 84 56 46 46 74
	Aerial Orthophoto	Blue Green Red Near Infrared		
	National Elevation Dataset	Slope Curvature		
Corcoran et al. 2013 (Random Forests Classifier)	RADARSAT-2 (C-band) polSAR	Cloude-Pottier Decomposition Freeman-Durden Decomposition Van Zyl Decomposition	Overall Water Emergent Wetland Forested Wetland Scrub/Shrub Wetland Upland	69 95 56 71 60 72
	ALOS PALSAR (L-band) dualPol	HH and HV		
	Aerial Orthophoto-NAIP	Blue Green Red Near infrared NDVI		
	National Elevation Dataset	Slope Aspect Curvature Flow Accumulation		

	Landsat 5 TM	Blue Green Red Near Infrared SWIR1 SWIR2 TIR NDVI Tasseled Cap		
	USDA Soil Survey Geographic Database	Soil type Drainage class Hydric class		
LaRocque et al. 2015 (Random Forests Classifier)	RADARSAT-2 (C-band) polSAR	HH and HV	Overall	94.3
	ALOS-PALSAR (L band) dualPol	HH and HV	Urban (dense) Urban (sparse) Cultivated Pasture Grass Softwood forest Hardwood forest	97.5 95.5 98.2 97.2 94.4 91.5 83.8
	Landsat 5 TM	Blue Green Red Near Infrared SWIR1 SWIR2	Mixed forest Scrub Shrub Bare land Peatland Marsh Shrub wetland Forested wetland Aquatic bed	91.7 96.1 92.5 98.5 89.2 88.5 94.2 95.0
	DEM (1:50,000)	Slope	Water	100.0
Millard and Richardson 2013 (Random Forests Classifier)	RADARSAT-2 (C-band) polSAR	Touzi Decomposition Cloude-Pottier Decomposition Freeman-Durden Decomposition	Overall Open bog Treed bog Fen Marsh Upland shrub	88.0 75.2 78.7 57.5 69.5 30.3

	Lidar	SAGA wetness index Topographic wetness Terrain ruggedness indices Various texture measures of both the DEM and DSM (mean, contrast, homogeneity, dissimilarity, etc.) Slope, Aspect Channel Network Base Level Altitude above channel network Slope length Profile curvature Planimetric curvature Catchment area	Upland mixed forest Roads Fields Buildings Water	90.2 24.6 75.7 9.7 82.2
van Beijma et al. 2014 (Random Forests Classifier)	Astrium Airborne Demonstrator (S- and X-Band) polSAR	Channel Intensity Cloude-Pottier Decomposition Freeman-Durden Decomposition Van Zyl Decomposition	Overall Bare sand/mud wet Bare sand/mud dry Pioneer Salicornia Pioneer Spartina Salt Marsh Meadow Juncus maritimus	78.20 90.44 82.87 50.47 41.52 88.43 72.82
	Aerial Orthophoto (Astrium Geostore)	Blue Green Red Near Infrared		
	Landsat	Normalized Difference Vegetation Index		
	Lidar	Digital Surface Model		

Appendix C

Residual Error Report

Residual Units: Image pixels

Residual Summary for 1 Images

GCPs: 0 X RMS Y RMS

Check points: 14 X RMS 0.24 Y RMS 0.76

Listing: GCPs only All images

PointID	Res	Res X	Res Y	Type	Image ID	Image X	Image Y	Comp X	Comp Y
G0003	1.72	-0.33	1.69	Check	product	339.9	1030.8	339.6	1032.5
G0001	1.25	0.03	1.25	Check	product	531.6	1685.6	531.7	1686.8
G0005	1.02	0.07	1.01	Check	product	862.4	490.7	862.5	491.7
G0004	0.86	0.43	0.75	Check	product	629.1	990.7	629.5	991.5
G0013	0.72	-0.09	0.71	Check	product	851.4	2442.6	851.3	2443.3
G0011	0.56	0.29	0.48	Check	product	984.1	1617.7	984.4	1618.1
G0012	0.55	0.20	0.51	Check	product	1120.2	2069.8	1120.4	2070.3
G0002	0.48	-0.30	-0.37	Check	product	98.8	1083.9	98.5	1083.5
G0010	0.40	-0.39	0.09	Check	product	695.2	2024.8	694.8	2024.9
G0006	0.39	0.03	0.39	Check	product	1061.1	555.4	1061.1	555.8
G0009	0.35	0.01	0.35	Check	product	1168.0	1137.1	1168.0	1137.4
G0014	0.26	0.20	-0.16	Check	product	1175.2	2397.4	1175.4	2397.3
G0007	0.22	0.04	-0.21	Check	product	1004.3	943.7	1004.3	943.4
G0008	0.20	0.19	0.06	Check	product	851.1	1332.5	851.3	1332.5

Appendix D
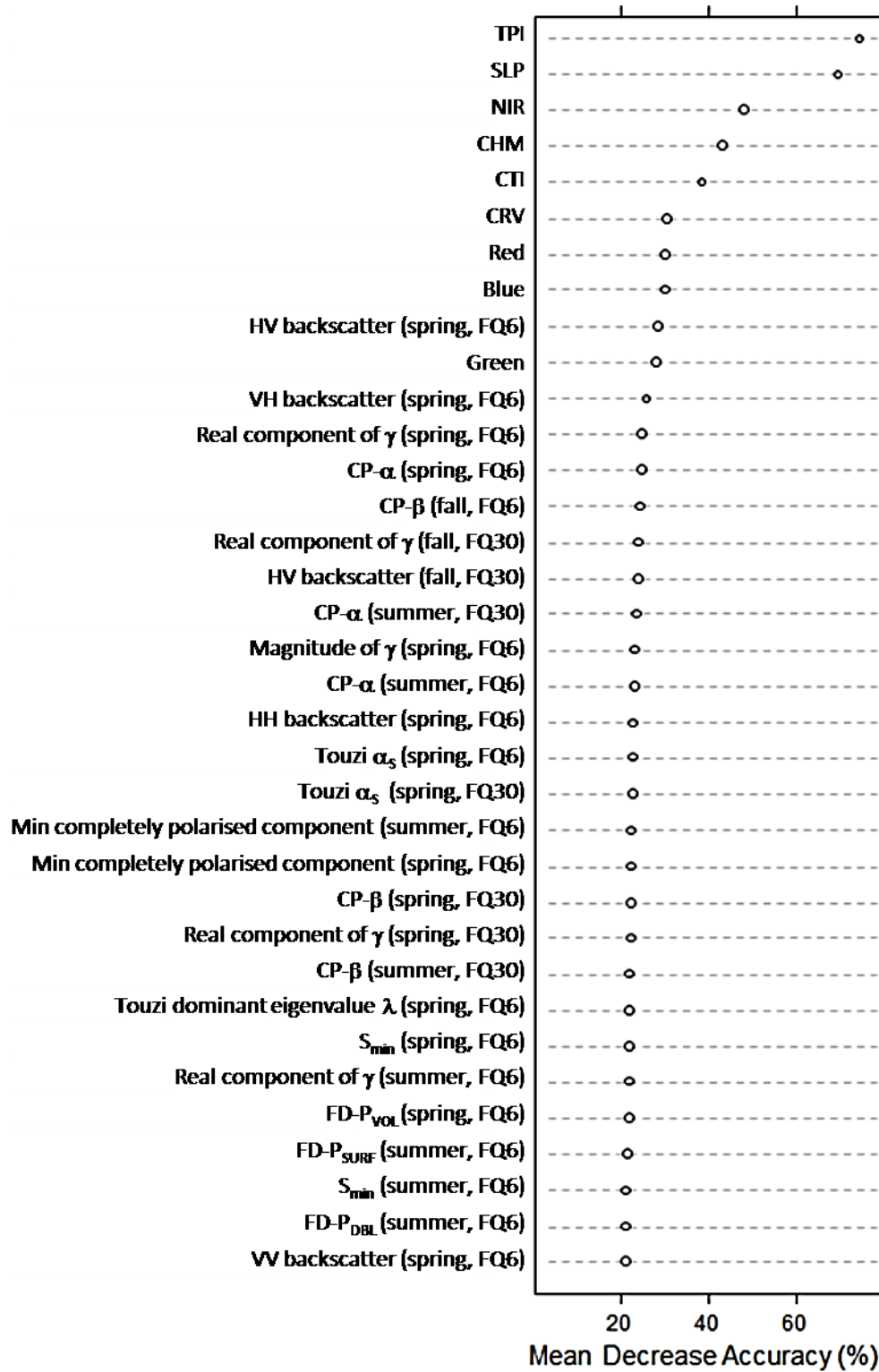
Variables of importance for the best case scenario of lidar derivatives with RADARSAT-2 HH, HV, VH, VV intensity images and polarimetric variables and the five QuickBird images.
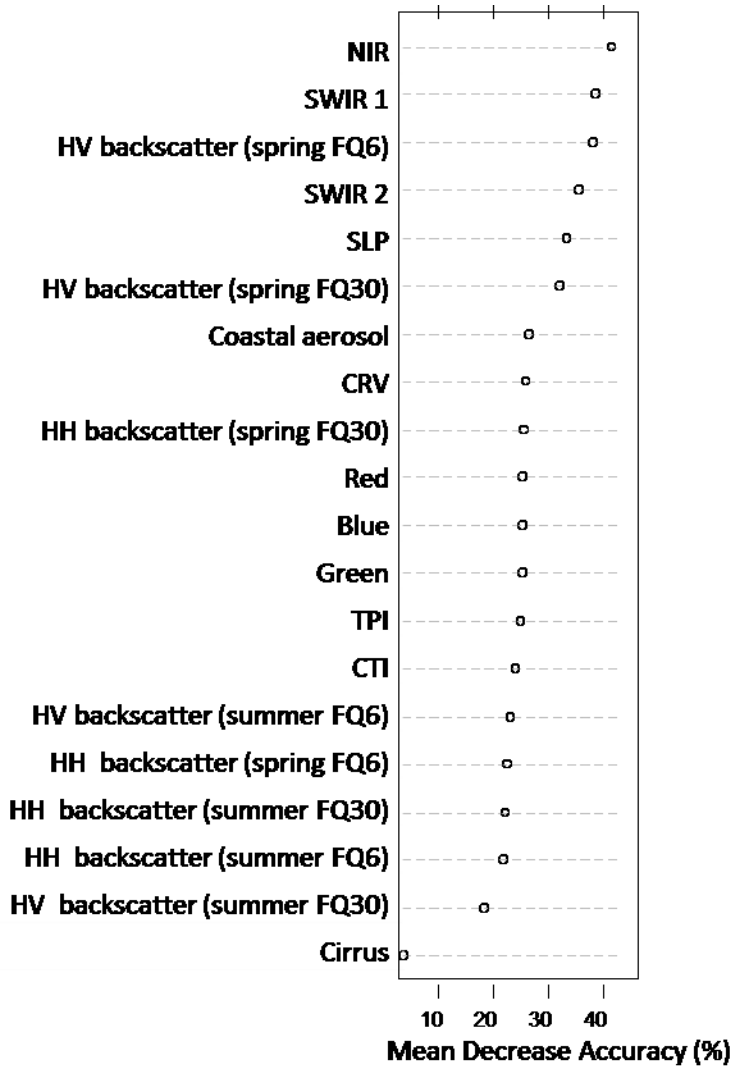
List of the importances for datasets from the best case scenario of four NS DEM derivatives plus RADARSAT-2 HH/HV dual-polarized images plus nine Landsat 8 images.